

**POWER ALLOCATION AND RELAY
SELECTION STRATEGIES FOR COGNITIVE
BUFFER-AIDED RELAY NETWORKS**

BY

YASSER F. ALERYANI

A Thesis Presented to the
DEANSHIP OF GRADUATE STUDIES

KING FAHD UNIVERSITY OF PETROLEUM & MINERALS

DHAHRAN, SAUDI ARABIA

In Partial Fulfillment of the
Requirements for the Degree of

MASTER OF SCIENCE

In

TELECOMMUNICATION ENGINEERING

DECEMBER 2015

KING FAHD UNIVERSITY OF PETROLEUM & MINERALS
DHAHRAN 31261, SAUDI ARABIA

DEANSHIP OF GRADUATE STUDIES

This thesis, written by **YASSER F. AL-ERYANI** under the direction of his thesis adviser and approved by his thesis committee, has been presented to and accepted by the Dean of Graduate Studies, in partial fulfillment of the requirements for the degree of **MASTER OF SCIENCE IN TELECOMMUNICATION ENGINEERING**.

Thesis Committee



Prof. Salam A. Zummo (Adviser)

Dr. Saad Al-Ahmadi (Member)

Dr. Wessam Mesbah (Member)

Dr. Ali A. Al-Shaikh
Department Chairman

Dr. Salam A. Zummo
Dean of Graduate Studies

3/1/16

Date

© Yasser F. Al-Eryani
2015

Dedication

*To my parents, sisters, and brothers for their endless support and
love.*

ACKNOWLEDGMENTS

All praise and thanks be to Almighty Allah, the one and only who helps us in every aspect of our lives.

Acknowledgement is due to King Fahd University of Petroleum and Minerals for giving me this precious opportunity to resume my Master degree.

I would like to express deep gratefulness and appreciation to my Thesis advisor Prof. Salam Zummo for his continuous help, guidance, and encouragement throughout the course of this work. He spent a lot of his precious time helping me and advising me at each step.

Beside my advisor, I would like to express my deep appreciation and gratefulness to Dr. Anas Salhab for his continuous help and endless support for making this work in the way it is now.

Additionally, I would like also to thank my Thesis committee members: Dr. Saad Al-Ahmadi and Dr. Wessam Mesbah for their great help and cooperation, which contributed significantly to the improvement of this work. Finally, my heartfelt gratitude goes to my parents, my sisters, and brothers for their encouragement, prayers, and moral support.

TABLE OF CONTENTS

LIST OF TABLES	ix
LIST OF FIGURES	x
ABSTRACT (ENGLISH)	xiv
ABSTRACT (ARABIC)	xvi
CHAPTER 1 INTRODUCTION	1
1.1 Background	5
1.1.1 Physical Layer Buffering	5
1.1.2 Cognitive Radio Networks	8
1.1.3 Multiple-Input Multiple-Output Schemes	9
1.1.4 Convex Optimization	10
1.1.5 Genetic Algorithm	12
1.1.6 Performance Measures in Cooperative Networks	14
1.2 Literature Review	15
1.2.1 Relay Selection and Bidirectional Relaying	16
1.2.2 Transmission Power Allocation for Cooperative Relaying Schemes	20
1.3 Thesis Motivation	22
1.4 Thesis Contributions	24
1.4.1 Outage Behaviour of Cooperative Networks	24
1.4.2 Design and Optimization of Single-Antenna Schemes	25

1.4.3	Design and Optimization of Multi-Antenna Schemes	26
1.5	Thesis Organization	26
CHAPTER 2 OUTAGE BEHAVIOR OF COGNITIVE DF UNI-		
DIRECTIONAL RELAY NETWORKS		28
2.1	Introduction	28
2.2	Conventional Unbuffered Relay Networks	29
2.2.1	System and Channel Models	30
2.2.2	Outage Probability	31
2.3	Buffer-Aided Relaying	38
2.3.1	System and Channel Models	39
2.3.2	Max-Link Relay Selection Protocol	40
2.3.3	Outage Probability	42
2.4	Simulation Results	52
2.4.1	Conventional Unbuffered Relaying	53
2.4.2	Buffer-Aided Relaying	55
2.4.3	Conventional versus Buffer-Aided Relaying	59
2.5	Conclusions	61
CHAPTER 3 DESIGN AND ANALYSIS OF SINGLE-ANTENNA		
COGNITIVE DF RELAYING SCHEMES		63
3.1	Introduction	63
3.2	Unidirectional Transmission Relaying	65
3.2.1	System and Channel Models	65
3.2.2	Transmission Power Allocation	67
3.3	Bidirectional Transmission Relaying	72
3.3.1	System and Channel Models	73
3.3.2	Problem Formulation	75
3.3.3	A New Bidirectional Relaying Protocol for Buffer-Aided DF Relay Network	78
3.3.4	Transmission Power Allocation Scheme	81

3.3.5	Complexity Analysis	83
3.4	Effect of Delay in Buffer-Aided DF Relaying	85
3.4.1	Average Packet Delay at the Source	87
3.4.2	Average Packet Delay at the Relay	88
3.5	Simulation Results	89
3.5.1	Unidirectional Transmission	90
3.5.2	Bidirectional Transmission	93
3.5.3	Delay Effect in Buffer-Aided Relaying	97
3.6	Conclusions	99
 CHAPTER 4 DESIGN AND ANALYSIS OF MULTIPLE- ANTENNA SCHEMES		 101
4.1	Introduction	101
4.2	Unidirectional Relaying	102
4.2.1	System Model	103
4.2.2	Problem Formulation	105
4.2.3	New MIMO-based Relay Selection Scheme	109
4.2.4	Antenna Transmission Power Allocation Scheme	111
4.2.5	Complexity Analysis	114
4.3	Bidirectional Relaying	115
4.3.1	System Model	115
4.3.2	Problem Formulation	118
4.3.3	Bidirectional Relaying Protocol	121
4.3.4	Transmission power allocation	124
4.4	Simulation Results	128
4.4.1	Unidirectional Relaying	129
4.4.2	Bidirectional	132
4.5	Conclusions	134
 CHAPTER 5 CONCLUSION AND FUTURE WORK		 136
5.1	Introduction	136

5.2	Outage Behavior of Cognitive Relay Networks	137
5.3	Single-Antenna Relaying Scheme	138
5.4	Multiple-Antenna Relaying Scheme	138
5.5	Future Work	139
REFERENCES		140
VITAE		148

LIST OF TABLES

2.1	Possible States	51
3.1	Central processing unit times (seconds) for 100 channel realization . .	84
4.1	Central processing unit times (seconds), for 100 channel realization.	115

LIST OF FIGURES

1.1	Simple buffer-aided relaying scheme.	6
1.2	Building blocks of buffer-aided DF relay node: (a) unidirectional, (b) bidirectional.	7
2.1	Cognitive radio DF relay network (solid lines: desired signals, dotted lines: interfering signals).	31
2.2	Cognitive radio network with buffer-aided DF relays (solid lines: desired signals, dotted lines: interfering signals).	39
2.3	An illustrative example of max-link unidirectional relaying protocol.	41
2.4	Outage probability of the SN with equal-power interferers and different number of relays N with $\gamma_{th} = 5$ dB.	53
2.5	Outage probability of the SN with different PN interference power with $\gamma_{th} = 5$ dB.	54
2.6	Outage probability of the PN with different interference powers $\gamma_{th} = 5$ dB.	55
2.7	Outage probability of the PN with equal-power interferers $\gamma_{th} = 5$ dB.	56
2.8	Simulation and analytical results of outage probability of the SN that uses buffer-aided relaying scheme under different number of relays with $P_{S_p} = 8$ dB, $\gamma_{th} = 5$ dB.	57
2.9	Outage probability of the SN with different number of relays and different number of maximum buffer size L with $P_{S_p} = 8$ dB, $\gamma_{th} = 5$ dB.	57

2.10	Outage probability of the SN and PN $P_{Interference} = 8$ dB and $\gamma_{th} = 5$ dB.	58
2.11	outage probability of the SN for both conventional unbuffered and buffer-aided relaying schemes with different values of maximum buffer size L $P_{Sp} = 8$ dB, $\gamma_{th} = 5$ dB, and $N = 1$	59
2.12	outage probability of the SN for both conventional unbuffered and buffer-aided relaying schemes with different values of maximum buffer size L $P_{Sp} = 8$ dB, $\gamma_{th} = 5$ dB, and $N = 4$	60
3.1	Cognitive radio network with buffer-aided DF relays (solid lines: desired signals, dotted lines: interfering signals).	66
3.2	System model for cognitive radio network with buffer-aided DF half duplex bidirectional relays (solid lines: desired signal, dotted lines: interfering signal).	74
3.3	Possible bidirectional transmission modes of the secondary network.	75
3.4	Flowchart for the proposed bidirectional relaying protocol.	79
3.5	Illustrative example of different packet delay in the DF max-link scheme.	85
3.6	Simulation and analytical results of the achievable normalized PN, SN and sum rates with $N = 4$, $L = 50$, and $I_{th} = 10$ dB.	90
3.7	Achievable normalized rate of the PN, SN and their sum rate for both conventional and buffer-aided ($L = 20$) relaying schemes with $N = 4$ and $I_{th} = 10$ dB.	91
3.8	Achievable normalized rate of the PN, SN and their sum rate with $I_{th} = 10$ dB for conventional and buffer-aided relaying using different number of relays and buffer sizes.	92
3.9	Achievable normalized PN, SN, and sum rates per user versus maximum power budget for both unidirectional and bidirectional relaying schemes with $I_{th} = 10$ dB, $L = L_1 = L_2 = 50$, $\mu = 200$, and $N = 4$	94

3.10	Achievable normalized PN, SN, and sum rates per user versus maximum power budget P_T for both optimal and proposed schemes with $I_{th} = 10$ dB, $L = 50$, $\mu = 200$, and $N = 4$	95
3.11	Achievable PN, SN, and sum rates per user versus maximum power budget P_T for conventional and buffer-aided relaying with $I_{th} = 10$ dB, $\mu = 200$, and $N = 4$	96
3.12	Achievable PN, SN, and sum rates per user versus maximum allowable delay μ with $P_T = 10$ dB, $I_{th} = 10$ dB, $L = 50$, and $N = 4$	97
3.13	Packet average delay versus buffer size for bidirectional relaying with $L_1 = L_2 = L$, and unidirectional relaying with two different number of relays, $N = 1$ and $N = 4$	98
3.14	Packet average delay versus the number of relays for both bidirectional relaying with $(L_1 = L_2 = L)$, and unidirectional relaying with two different buffer sizes, $L = 1, L = 10$	99
4.1	Cognitive radio network with MIMO buffer-aided DF relays (solid lines: desired signals at any possible transmission, dotted lines: interfering signals at any possible transmission).	104
4.2	Proposed antenna transmission power allocation scheme applied for maximizing $R_{S,R_i} + R_{S_p,D_p}$ when the $S - R_i$ link is selected.	114
4.3	Cognitive radio network with MIMO buffer-aided DF relays (solid lines: desired signals, dotted lines: interfering signals).	116
4.4	Possible bidirectional transmission modes of the secondary network.	118
4.5	A flowchart for the proposed bidirectional relaying protocol.	122
4.6	Proposed antenna transmission power allocation scheme applied for maximizing $R_{U_1,R_i} + R_{S_p,D_p}$ when the \mathcal{M}_1 mode is selected.	128
4.7	Achievable primary and secondary average normalized rate for the optimal simulated solution, proposed sub-optimal solution, and separate optimal simulation with $I_{th} = 10$ dB, $M = 4$, $N = 4$, $L = 10$ and $k = 5$	129

4.8	Achievable normalized rate versus different values of maximum buffer size L with $I_{th} = 10$, $M = 4$, and $k = 5$	131
4.9	Achievable normalized rate versus different values of antennas M with $I_{th} = 10$, $L = 10$, $k = 5$, and $N = 4$	132
4.10	Achievable normalized rate versus different values of interference thresholds $I_{th} = 10$ dB and $I_{th} = 20$ with $L = 10$, $M = 4$, and $N = 4$.	133
4.11	Achievable normalized rate versus different values of antennas with $L = 50$, $I_{th} = 10$ dB, and $N = 4$	134

THESIS ABSTRACT

NAME: Yasser F. Al-Eryani

TITLE OF STUDY: Power Allocation and Relay Selection Strategies for Cognitive Buffer-Aided Relay Networks

MAJOR FIELD: Telecommunication Engineering

DATE OF DEGREE: December 2015

Cooperative wireless communications has been proposed as one of the smart solutions to extend overall cellular coverage area and support better quality of service (QoS) for terminals especially those located at cell edges. Along with cognitive radio (CR) techniques and multiple-input multiple-output (MIMO) schemes, cooperative relaying has represented an excellent area of research for the next generation of wireless communication techniques 5G to improve both power and spectrum efficiencies and enhance the reliability of wireless communication. Recently, the concept of buffering was exported from the media access control (MAC) to the physical layer to enhance the way relay works and add some sort of time diversity. In this thesis, first, the outage behavior of cognitive unidirectional decode-and-forward (DF) relay network of both conventional unbuffered and buffer-aided

relaying schemes was investigated. Outage behavior analysis is followed by performance comparison between the conventional and buffer-aided relaying schemes. Additionally, the single antenna scenario of buffer-aided DF relay network in both unidirectional and bidirectional schemes was investigated. Using convex optimization theory, an optimal expressions for the transmission power that allocates a maximum power budget between primary and secondary transmitters at each time slot were derived. At the same time, a low complexity bidirectional relaying protocol for buffer-aided relay network that is followed by transmission power allocation schemes for every possible transmission mode are proposed and investigated. For MIMO cooperative buffered relay networks, a low complexity relay selection scheme and bidirectional relaying protocol were proposed and evaluated. The designed schemes under MIMO scenario are followed by investigating an optimization methods that allocates a maximum power budget among all transmitting primary and secondary networks antennas at each time slot. Average packet delay that occurs due to physical layer buffering is also studied and investigated. Our work ends with final conclusions about the efficiency and effectiveness of using physical layer buffering on cooperative relaying regarding the delay constraints, diversity gain, and coding gain. It was found that the proposed bidirectional relaying protocol introduces a satisfactory performance with much lower complexity and controlled packet delay. Additionally, buffer-aided relays are found to be a good solution for cognitive network since they enhance the secondary network without the need to increase their transmission power.

CHAPTER 1

INTRODUCTION

Wireless communication witnesses a huge and continuous development to fulfil the growing demands for high speed multimedia transmission services with acceptable quality of service (QoS). Power and frequency are the most precious resources in wireless communication networks and are subjected to a strict laws that control their allocation and usage among service providers. Several techniques were proposed in literature to enhance the efficiency of power and frequency usage such as cognitive radio (CR), cooperative communication, power allocation schemes, buffer-aided relaying, and multiple-input multiple-output (MIMO) antenna schemes [1].

In cooperative wireless communication network, user terminals communicate through intermediate devices called relays. Relay node is used as a repeater that receive a message signal from source, process it, and then retransmits it to the destination. There are mainly two major types of relaying techniques; The first one is called decode-and-forward (DF) where the relay receives a certain noisy

signal from the source, decodes it, and generates a noise-free version of the signal to be transmitted to destination. The second relaying scheme is called amplify-and-forward (AF) at where the relay receives a noisy signal from the source, and then amplifies it by a certain gain factor, and then retransmits it to the destination. Generally, relaying techniques are used to increase the overall network throughput, extend the coverage area and decrease the power requirements of the system for network users, especially those located at cell edges.

Cooperative relaying schemes could be implemented in one direction between source-destination pair or in two directions between two transceiver nodes. For one-way relaying (OWR) or the so called unidirectional relaying, relay node receives a message signal from the source, and then applies some processing to it and in the second time slot, transmits it to the destination. On the other hand, for two-way relaying (TWR) which is referred as bidirectional relaying, both terminal nodes are transmitting and receiving during one transmission session.

CR is considered as one of the promising techniques that are used to increase the spectrum usage efficiency. There are two paradigms of CR that allow for simultaneous spectrum access of both licensed primary and unlicensed secondary (cognitive) users, namely, overlay and underlay techniques. In overlay CR, secondary user (SU) accesses the spectrum of the primary user (PU) when its not in use by PU. However, in underlay CR, SU accesses the licensed spectrum with PU simultaneously with a restriction that interference caused by SU on PU is below some threshold value [2].

To further enhance cooperative system performance, MIMO antenna schemes are used at both user terminals in addition to relay nodes. MIMO systems can be used either to achieve a diversity or multiplexing gain depending on the system requirements. In the case of multiplexing gain, different information signals are transmitted at each transmit antenna after multiplied by precoding matrix at the source side and then a decoding matrix at the destination side. These precoding and decoding matrices are chosen to guarantee a full utilization of MIMO channels. In the case of diversity gain, the same message signal is transmitted through all transmission antennas. At receiving antenna, a certain combining technique is used to combine received message signals at all receiving antennas to produce a better signal at the output of the receiver [3].

Conventional relaying uses a fixed established transmission protocols for both unidirectional and bidirectional schemes. These fixed protocols do not fully utilize the best channel conditions at a certain time slot. Recently, the concept of buffering was exported from the media access control (MAC) to the physical layer to enhance the way the relay works and achieve time diversity in cooperative network. Buffer-aided relaying is offered to overcome the limitations of conventional un-buffered relaying schemes at which the best link on the network may not be selected for transmission or reception due to fixed relaying scheduling. In buffer-aided relaying, data transmission is not restricted to a fixed number of time slots to accomplish a complete end-to-end (e2e) message signal transmission from source to destination. Instead, message signals could be stored in a buffer that is

attached at the relay node for an arbitrary number of time instances until the best channel conditions are met between that relay node and the destination [4, 5].

Buffering strategy on relay nodes differs depending on the utilized relaying scheme. In DF relaying, a message signal is stored at the buffer as a packet of bit sequence after being demodulated and decoded. On the other hand, in AF relaying, a message signal is stored at the relay buffer as quantized unmodulated signal [6, 7].

Buffer-aided relaying has been proven to achieve coding and diversity gains compared to that of conventional unbuffered relaying network. This advantage of physical layer buffering has made it an excellent solution for CR cooperative relay network due to the fact that performance enhancement is achieved without the need to increase the secondary network (SN) transmission power which may violate the primary network (PN) interference constraints.

Most of the previous work in the literature that has investigated transmission power allocation, cognitive relays, MIMO schemes, bidirectional relaying protocols was done on conventional unbuffered relaying network which could make them not applicable for buffer-aided relaying networks.

Our aim in this thesis is to investigate and analyze the network of cognitive buffer-aided DF relaying. Transmission power allocation schemes that allocate a maximum power budget between the PN and the SN is to be proposed and investigated for a variety of network layouts that use buffer-aided relays. Additionally, a low complexity bidirectional relaying protocols that achieve the end-to-end (e2e)

data transmission between transceiver nodes are to be proposed and evaluated in this thesis.

1.1 Background

In this section, the theoretical backgrounds necessary for the thesis work is briefly discussed. Firstly, a brief introduction to physical layer buffering is presented. The concept of underlay CR network as one of the efficient solution in cooperative communication technology that enhances spectrum efficiency is also discussed. A theoretical discussion on MIMO schemes is also given in some details as they are important in several scenarios in this thesis work. Additionally, convex optimization theory is introduced as a mathematical tool for finding closed-form expressions of constrained transmission power allocation problems for different network layouts. Another power allocation tool which includes heuristic algorithm that is called Genetic algorithm (GA) is also discussed. Finally, some different measures of network performance or the so called target or cost functions such as outage probability, normalized rate, and bit error rate are enumerated and briefly described.

1.1.1 Physical Layer Buffering

In wireless communication networks, nodes are usually equipped with buffers to control traffic and differentiate between home users and guest users. These buffering techniques are controlled by network and transportation layer protocols and

only affected by the e2e successful reception of the data packets[8].

Recently, the concept of buffering has been also used in the design and optimization of relaying protocols at the physical layer. Figure 1.1 shows a simple buffer-aided relaying scheme model consisting of a source, a half-duplex unidirectional relay R equipped with a buffer of maximum size L , and destination.

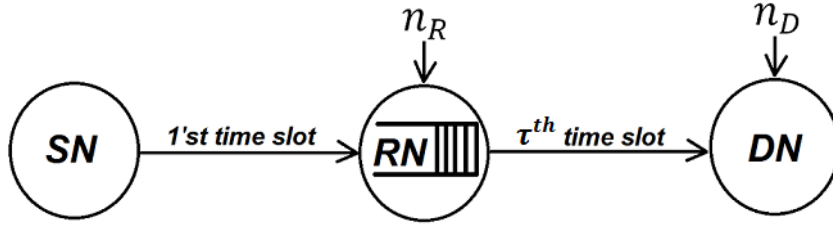


Figure 1.1: Simple buffer-aided relaying scheme.

Regarding the scenario of unidirectional buffer-aided DF relaying scheme, the number of time slots required to achieve one complete data transmission between source and destination is not restricted to two time slots (as was the case for conventional unbuffered relaying scheme), instead demodulated signal is stored at relay buffer B of maximum size L for some subsequent number of time slots until best channel conditions are met between the relay and the receiving node. L denotes maximum number of packet signals that could be stored in the buffer B before an overflow occurs.

On the other hand, in bidirectional buffer-aided relay network, each relay is equipped with two buffers, B_1 and B_2 of maximum size L_1 and L_2 , respectively. These buffers are used to store received signals from two communicating user terminals U_1 and U_2 , respectively. Figure 1.2 shows a block diagram for both unidirectional and bidirectional DF relay node. As can be seen from this figure,

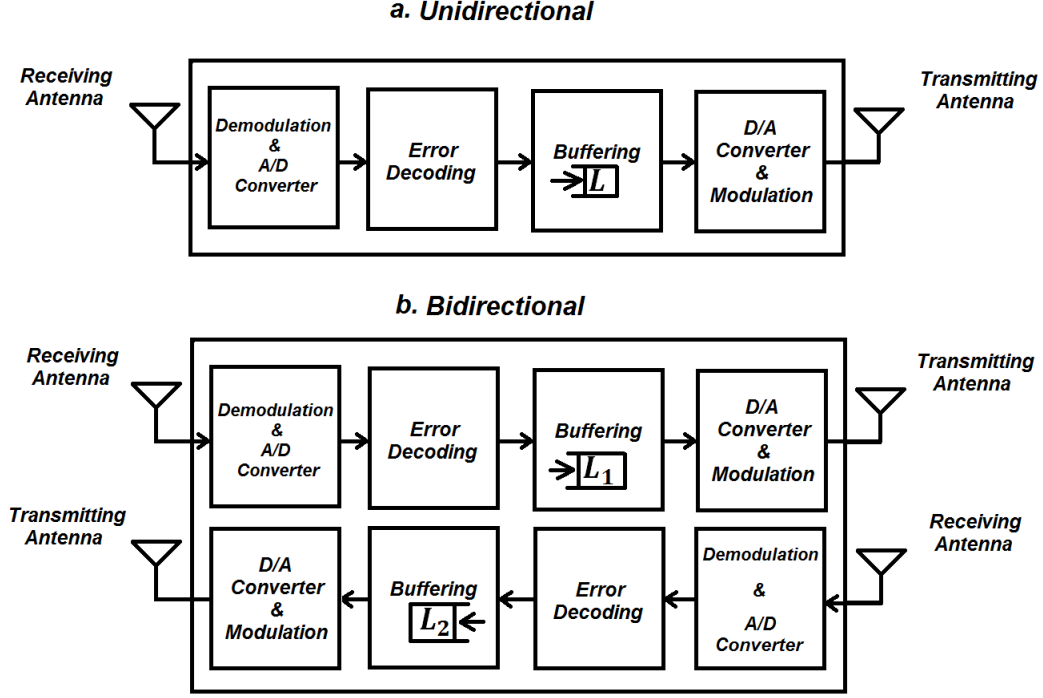


Figure 1.2: Building blocks of buffer-aided DF relay node: (a) unidirectional, (b) bidirectional.

the received message is first demodulated and then buffered as a digital noise-free signal waiting to be relayed to destination when some certain conditions are met.

Two main protocols are used in unidirectional buffer-aided relaying to control data flow from the transmitting node to the receiving node, namely, the max-max and max-link relaying protocols. In max-max relaying protocol, data transmission takes place in two time phases. During the first time slot, the best source-relay link to a relay, with a buffer that is not full, is chosen to receive a message signal from the source side. while, during the second time slot, the best relay-destination link that is related to a relay with a buffer that is not empty is chosen to receive its oldest buffered signal to destination. In max-link protocol, at any arbitrary time slot, the best source-relay link or relay-destination link is chosen either for

receiving or transmitting, respectively.

In bidirectional relaying with buffering, some adaptive mode selection schemes that select the best transmission mode among a set of all possible transmissions were investigated by researchers. Buffer-aided unidirectional/bidirectional protocols are discussed in details in Chapters 3 and 4.

Physical layer buffering introduces serious delay issues that may affect data transmission process, especially in real-time applications at which a significant delay may corrupt the quality of the received data such as online gaming and video conferencing.

1.1.2 Cognitive Radio Networks

CR is an intelligent and spectrally efficient wireless scheme that has the ability to sense its surrounding environments and modify its operating system parameters such as transmission powers, operating frequencies, and modulation schemes depending on changing constraints of the nearby wireless network [9]. Two types of users exist in CR networks namely, PU which has the authority to use the licensed spectrum, and SU which senses PU spectrum and uses it for transmission and reception depending on the type of the used CR scheme [10].

In CR, two main schemes of spectrum sharing are used, namely, overlay and underlay. The most practical of CR scheme which is used in this thesis work is the underlay spectrum sharing technique at which the SU is permitted to utilize the spectrum of the PU simultaneously conditioned that the interference caused

by the SU on the PU is not exceeding a predefined threshold value [10]. However, in overlay scheme, the SU participates in transmitting some data of the PU to keep its performance above some targeted level.

In wireless cognitive underlay relay networks, the interference on the PU at any time slot may be caused either by the SU terminal or by one or more relay nodes depending on the used relaying protocol. This leads to the need for power control strategy to control the power of SU, all active relays, and the PU as well. Transmission power allocation in CR systems should maximize the SU and PU sum rate and maintain interference threshold constraints. In this thesis work, underlay CR scheme is considered in the analysis of different buffer-aided relaying network layouts.

1.1.3 Multiple-Input Multiple-Output Schemes

MIMO is a wireless transmission scheme at which more than one antenna are used at both source and destination in order to enhance the link reliability (diversity gain), the spectral efficiency (multiplexing gain), or both. The link reliability is increased by using the MIMO scheme in transmitting the same signal through all antennas. In the receiver side, received signals are combined using some combining schemes such as equal gain combining (EGC) and maximum ratio combining (MRC).

In this thesis work, MIMO scheme is used to enhance multiplexing gain by increasing the network overall e2e bit rate. One of the most famous MIMO schemes

that enhances multiplexing gain of the network is called singular value decomposition (SVD) method. Using SVD method, channel gain matrix is decomposed into a multiplication of three unitary matrices one of them used as a precoding matrix at the transmitter and another one is used as a decoding matrix at the receiver. SVD changes MIMO channel into an equivalent parallel uncorrelated channels and their number depends on the rank of the channel gain matrix.

Despite their complexity, MIMO systems are used in cooperative relaying networks as a smart solution to enhance the relay node performance. A significant use for MIMO scheme is when the direct link between source and destination suffers from a deep fading and transmission power is bounded by some other constraints such as the PU interference.

1.1.4 Convex Optimization

In the field wireless communication, the problem of mathematical optimization is defined as the selection of a best element among a group of available elements [11]. In other words, an optimization problem consists of maximizing or minimizing a real function by systematically choosing input values from a range of an allowed set and computing the value of the function.

A mathematical problem of optimization has a standard form given by [12] :

$$\begin{aligned}
& \text{minimize } f_o(\mathbf{X}), \\
& \text{subject to } f_i(\mathbf{X}) \leq b_i, \ i = 1, \dots, m, \\
& h_j(x) = a_j, \ i = 1, \dots, n
\end{aligned} \tag{1.1}$$

where $f_o(\mathbf{X})$ is the objective function to be minimized, \mathbf{X} is a vector of variables to be optimized, $f_i(\mathbf{X})$ is the i^{th} inequality constraint function, and the constant b_i is the limit or bound of the i^{th} constraint function, $h_j(\mathbf{X})$ is the j^{th} equality constraint function, and the constant a_j is the limit or bound of the j^{th} constraint function. A vector \mathbf{X}^* is considered an optimal solution of the optimization problem if it has value among all possible vectors that produce the maximum or minimum value of the objective function and satisfy the constraints in the same time. This means that for any other vector \mathbf{Z} , with $f_i(\mathbf{Z}) \leq b_i \ i = 1, \dots, m$ we have $f_o(\mathbf{X}^*) \leq f_o(\mathbf{Z})$.

A problem is called convex if the objective function $f_o(\mathbf{X})$ and all constraint functions $f_i(\mathbf{X})$ and $h_j(\mathbf{X})$ are convex, i.e., satisfy the following condition [12]:

$$f_i(\alpha\mathbf{X} + \beta\mathbf{Y}) \leq \alpha f_i(\mathbf{X}) + \beta f_i(\mathbf{Y}), \tag{1.2}$$

for all $\mathbf{X}, \mathbf{Y} \in R^n$ and all $\alpha, \beta \in R$ with $\alpha + \beta = 1$, and $\alpha \geq 0, \beta \geq 0$.

1.1.5 Genetic Algorithm

For small networks with linear constraints and cost functions, direct and systematic methods of convex optimization are used in the derivation of closed-form expressions for transmission power allocation. However, for large networks with a huge number of nodes, several strategies were proposed in the literature, but none of them can not be considered as a general method [13]. This is due to the fact that in these kind of problems, the cost function is highly non-linear. Consequently, these problems are considered mathematically complicated and no closed-form solution is available. These problems are classified as non-programmable (NP) problems and their solution generally involves in the use of some iterative or heuristic algorithms. There is no general proof that GA is guaranteed to converge to the optimal solution, however, they are expected to produce near-optimal performance with reasonable processing times with lower complexity [14].

GA is considered as a heuristic search algorithm that is used in practical applications as an optimization tool for complex systems. Additionally, GA belongs to the larger class of evolutionary algorithms (EA), at which the natural evolution processes such as inheritance, mutation, selection, and crossover is considered as a direct inspiration for their performance and techniques. In GA, a population or a set of initial randomly selected optimization problem solutions is evolved toward a better solution at each evolution state or the so called iteration. Each population on each iteration step is called generation. Out of n_p possible solutions on a certain generation, only $n_{parents}$ population that produce the best possible solutions

are chosen to form a bases for generating $n_p - n_{parents}$ children. The process of generating children from parents is called crossover, and mutation [15].

- **Crossover**

In optimization problems that use GA, crossover is a method that is used to produce the next generation population values from the present iteration. There are many methods to perform crossover on best selected values. One practical method used is called, n -point crossover. In this method, vectors representing parents split into n smaller vectors and the new vectors are combined by combining the parts of the vectors from different parents together and generate a complete set of vectors representing the next generation values. Usually, in optimization methods that uses GA, vectors or populations are represented in binary form and crossover is performed among different binary vectors that represent each population value.

- **Mutation**

Mutation is a genetic operator used to maintain genetic diversity from one generation of a population of genetic algorithm chromosomes to the next. Similar to crossover, mutation is used to generate some of the next generation populations, however mutation guarantees that the iterative genetic algorithm diverge from the optimal solution due to crossover. Mutation tries to maintain some features of vector bits from the previous iteration. It could be performed by flipping two adjacent bits on parent vectors to generate some children vectors.

1.1.6 Performance Measures in Cooperative Networks

There are many performance measures used by researchers as cost or target functions to be optimized by assigning some optimal/sub-optimal transmission power values. Also, they can be used as a measure of merit when designing relaying protocols in cooperative wireless networks. Each of these measures are used to serve some performance target of the network such as diversity gain or multiplexing gain or both. The most important performance measures can be listed as follows:

- **Probability of Outage**

It is the most common performance measure used in implementing transmission power allocation and relay selection to enhance the diversity gain of the network. Outage probability is defined as the probability that the signal-to-interference plus noise ratio (SINR) of a received signal falls below a certain threshold value. This threshold value is the minimum SINR required by the receiver to be able to decode the received message signal. Generally, the outage probability of unidirectional wireless system is defined as [16]:

$$P_{out} = P(\gamma_{SD} \leq \gamma_{Th}), \quad (1.3)$$

where, γ_{SD} is the e2e SINR between the source and destination terminals. Closed-form expressions for probability of outage of conventional cooperative communication networks under different scenarios were extensively studied in literature [17, 18, 19].

- **Transmission Rate**

This measure is usually used by researchers as the cost function for cooperative network in optimizing transmission power and designing relay selection schemes. In this thesis work, transmission rate is changing according to the instantaneous channel quality. This means the desired enhancement is achieved on the network multiplexing gain [18, 19].

- **Bit Error Rate (BER)**

It is defined as the probability that a bit will be received incorrectly. This cost or target function is used as a performance measure in cooperative networks that focus on enhancing both diversity and multiplexing gain of the network. The derivation of a closed-form expression for the BER is usually achieved using some statistical and mathematical tools such as the characteristic function and the moment generating function of the e2e SINR. Well defined expressions of BER also exist in the literature for a variety of cooperative wireless relaying networks scenarios [20].

1.2 Literature Review

Relay nodes are the core of cooperative network and they are used in retransmitting message signals that were received from the transmitting node to the receiving node. Relay nodes are used to extend the network coverage and increase the overall network throughput for wireless terminals, especially for those located

at cell edges [21]. Research topics on cooperative relay networks are focused on outage performance, unidirectional/bidirectional relaying protocols, relay selection, and transmission power allocation [22, 23]. To fully utilize relaying schemes, researchers merged the concept of relaying with other supporting technologies such as CR and MIMO systems [24, 25]. However, most of MIMO cooperative network layouts considered the case at which all network relays participate in data transmission of a single source which makes it inefficient way, especially for multiple-user scenarios. Beside, cognitive relay network researches in the literature mainly considered the performance of the SN separately from that of the PN.

1.2.1 Relay Selection and Bidirectional Relaying

The topic of relay selection is considered as a major issue in enhancing the network performance and to fully utilize the spatial diversity added to the network by relay nodes. In conventional unbuffered relaying networks, max-min relay selection strategy which was proposed by Krikidis in [26] is considered as the most practical relay selection scheme that is called max-min relaying protocol. This protocol takes the minimum link related to each relay and then select the relay that is with maximum channel gain among those minima. It is considered as the optimal scheme for single-antenna scenarios, however its implementation in MIMO systems at which a set of channel gains affect the link capacity is limited.

The topic of relay selection in MIMO system with conventional relaying net-

work was investigated in [27]. Authors used iterative and GA techniques to select antennas and assign them the suitable power that maximizes the e2e normalized rate. The selected antennas may belong to different relays which means that a single user may reserve more than one active relay within the network. This strategy is considered inefficient for multi-user scenarios since it reduces the probability of existence of active relays to serve other users. Additionally, a set of relay selection algorithms which are based on discrete iterative stochastic optimization for the uplink of cooperative MIMO networks were proposed in [28]. These algorithms are complicated and time consuming since they mainly depended on iterative and search procedures which makes them unattractive for real-time applications with small transceiver devices that use small batteries. In [29], relay selection strategies for two-way cooperative relay with MIMO system were proposed and investigated. These methods depended on maximizing the minimum of the eigenvalues of the Wishart matrices from the selected relay to the two user nodes. However, this method considered AF relays and were significantly complicated and time consuming.

Regarding buffer-aided relaying systems, two main relay selection protocols were proposed in literature. The first scheme is called max-max relaying protocol and it divides the transmission process into two time phases. During the first phase, the link with the highest channel gain in source-relay possible links is chosen from the set of available relays with some empty storage spaces in their buffers. Whereas, during second phase, the best link in the relay-destination side

is chosen from the available relays that are loaded with some buffered data [30]. This protocol does not fully utilize the best link at a certain time slot because it restricts data transmission in two consecutive hops. To overcome the limitation of max-max relaying protocol, the second and more general relay selection protocol was proposed in [31], which is called max-link protocol. In this protocol, at any arbitrary time slot, based on the instantaneous channel gains of the overall source-relay and relay-destination links, a decision is made whether the transmitting node or the relay node is transmitting. One terminal could continue transmitting its data for some number of subsequent time slots as long as it has the best link. The main measure of link superiority is the single-link channel gain. However, with more complicated network layouts such as MIMO schemes or CR networks at which link superiority depends on channel gain matrix or PU interference power as well, no clear strategy is defined for the best link in the literature.

Bidirectional relaying is a practical solution for two-way wireless cooperative networks that use half-duplex relay node to exchange information between terminal users. For conventional unbuffered relaying schemes, the time division broadcast (TDBC) and the multiple access broadcast (MABC) protocols are the most famous bidirectional relaying protocols that use half-duplex relay nodes and control data flow between two transceiver nodes [4]. Both are considered as fixed predefined data flow protocols.

In TDBC protocol, data transmission takes place in three subsequent time slots. During the first time slot, user one sends its message signal to relay. During

the second time slot, user 2 sends its message signal to relay. While during the third time slot, the relay combines the received decoded signals, modulates the resultant, and then broadcasts the signal to both users [32]. On the other hand, the MABC protocol reduces the number of time slots to two only. During the first time slot, user 1 and user 2 use some multiple-access scheme and send their messages to relay node. While During the second time slot, the relay node combines the received decoded signals, modulates the resultant, and then broadcasts the signal to both users [33]. These fixed pre-established relaying protocols do not fully utilize the best channel conditions at a certain time slot as the selected link is not necessarily the best link in the network.

For unidirectional buffer-aided relaying scheme, the max-link relay selection is the most common protocol used to decide which relay to transmit or receive data at a certain time slot [34]. In such networks, it is possible to select the best link for transmission either on user 1-relay or user 2-relay link. Transmission link and data transmission direction are selected from a set of all possible transmissions such that a certain performance measure is maximized [35].

In buffer-aided relaying, bidirectional protocols are designed to have an adaptive mode selection scheme that is changing with respect to channel qualities on different links. Bidirectional buffer-aided relaying protocols have been investigated recently for some variety of network layouts that use buffered DF relay nodes. These protocols divide data transmission between any two terminals that communicate through a relay node into six possible modes. Each bidirectional

relaying protocol tries at each time slot to select the best transmission mode that enhances a certain performance measure [36].

The first buffer-aided bidirectional relaying protocol was introduced by Zlatnov *et al* in [37]. Authors derived the decision function that conducts adaptive link selection according to instantaneous channel knowledge. This protocol was mainly derived with unlimited buffer size which increases the average message delay. To overcome delay issues, Jamali *et al* derived an optimal adaptive mode selection with fixed transmission power and limited buffer size in [38]. To further enhance the system performance, Jamali proposed a new bidirectional relaying scheme that combines the problem of adaptive link selection with power optimization problem that is depending on instantaneous channel state information (CSI) [39, 40]. Generally, all the previously proposed bidirectional relaying protocols of buffer-aided relaying do not consider the average packet delay which is mainly investigated for the scenario of single-relay network.

1.2.2 Transmission Power Allocation for Cooperative Relaying Schemes

In [41], Madsen *et al* derived asymptotic bound for outage probability and ergodic capacity of cooperative system that uses a single conventional relay. Authors used the derived measures as cost functions in the derivation of optimal expressions for the transmitted power levels of both the source and the relay. Power allocation showed that a much better performance can be achieved when power values are

optimized compared to that with uniform pre-assigned power allocation methods. TO further enhances the analysis, in [42], authors extended the work in [41] and proposed a new transmission power allocation scheme that assumes only partial CSI instead of full CSI in the analysis. As the previous researches in [41, 42], focused on unidirectional relaying, in [?], Authors showed network coding with physical layer broadcast property is used to enhance the performance of mutual independent data exchange among two wireless nodes. The significance behind the proposed approach is that the single-way transmission of both node is achieved separately.

The concept of MIMO in cooperative communication was firstly considered by in [43]. In that paper, all transmitting and receiving nodes were equipped with multiple antennas. Also, an optimal expression was derived for the terminal powers that maximizes the network capacity and minimizes the probability of outage. However, the relay transmission power per antenna was assigned using semi-blind gain amplification due to the complexity of deriving of closed-form expressions to allocate the optimal transmission power values. As an extension to the work done in [43], an efficient MIMO cooperative CR antenna selection and antenna transmission power allocation algorithms were developed in [6]. This antenna-relay selection and power allocation algorithm depends on iterative and heuristic techniques. This method searches for the best set of antennas and then assigns them the near-optimal power values. One disadvantage of this method is that each user may use more than one active relay at a certain time slot which

makes this method inefficient for multiple-user scenarios.

The performance of single antenna buffer-aided relay network with optimal transmission power allocation was illustrated in [44]. Also, the effect of buffer size on the maximum achievable rate of single-antenna buffer-aided relay network was investigated [4]. Additionally, in [34] authors derived a closed-form expression for the probability of outage of buffer-aided relay network under max-link unidirectional relaying protocol and analyzed average packet delay of the network. This work is considered as one of the few sophisticated works which investigate buffer-aided relaying networks.

1.3 Thesis Motivation

In this section, the main motivations behind this thesis work and the importance of the investigated topics are introduced. The research methodology which was followed to achieve the objectives of this thesis is also presented.

As can be noticed from the literature, transmission power allocation schemes were extensively discussed and evaluated by researchers for different scenarios of cooperative unbuffered relaying networks with and without CR interference constraints. Some researchers also considered the addition of MIMO system on each secondary user and relay nodes. The optimization problems in the literature have mainly depended on optimizing the normalized rate of the SN irrespective of that of the PN.

It can also be noticed from the literature that buffer-aided relaying was not

given the same attention as conventional relaying, only few publications derived optimal/sub-optimal power allocation for buffer-aided relaying networks with single antenna. The combination of MIMO system with buffer-aided relaying CR networks has not been investigated yet.

In the area of relay selection schemes, all the previous works on buffer-aided relaying considered the link with maximum point-to-point channel gain as the best link. Such assumption is not practical, especially for more complicated channel layouts such as cognitive networks and MIMO-based relays. This is due to the fact that the best link depends on other factors such as the interference power caused by the PN and the MIMO channel quality.

Regarding bidirectional buffer-aided relaying, researchers only considered the scenario of a single relay and derived a complicated protocol that selects the optimal transmission mode among a set of all possible transmission modes. This means that no one has considered the case of bidirectional multiple-relay scheme with or without the concept of MIMO. Additionally, in all the previous works in the literature on buffer-aided relaying, the packet delay was not bound and the message signal was assumed to be buffered to infinite number of time slots when best channel conditions are not met. It is important to mention here that the uncontrolled message delay introduces a serious problem to the network operations, especially for real-time applications such as video gaming and online conferencing.

Motivated by the previous literature, we can notice that there are some topics of research in buffer-aided relaying that has not been investigated yet. For exam-

ple, deriving optimal/sub-optimal buffer-aided relaying protocols for more complex networks such as MIMO and cognitive networks. Additionally, enhancing the network performance by investigating and proposing variety of power allocation methods.

Also, it has been noticed that the relay selection of bidirectional relaying with multiple-relay has not been considered yet and this shows the need for an efficient and low complexity protocols for relay selection.

Another possible area of research lies in the message signal delay control. The optimal buffer-aided relaying protocol presented in the literature introduces unbounded delay. Additionally, an optimal delay-limited buffer-aided protocol even for the simplest networks is not known. Currently, bounding the delay is done by heuristically modifying the optimal buffer-aided relaying protocol for unbounded delay.

1.4 Thesis Contributions

This section briefly discusses the main contributions of this thesis work.

1.4.1 Outage Behaviour of Cooperative Networks

In this part of the thesis work, the outage behavior of conventional unbuffered relay network is studied and a closed-form expression for the probability of outage is derived. Additionally, a closed-form expression for the outage probability of unidirectional buffer-aided multiple-relay network is derived and evaluated.

Finally, a performance comparison for outage behavior of conventional unbuffered and buffer-aided relaying networks is studied. The end of this part of the thesis work, a conclusive discussion supported by some solid facts that motivated further investigation and analysis of buffer-aided relaying schemes due to their superiority over conventional unbuffered relaying networks is presented.

1.4.2 Design and Optimization of Single-Antenna Schemes

In this part of the thesis work, max-link unidirectional relaying protocol is used in the derivation of closed-form optimal transmission power allocation expressions. The problem mainly allocates a maximum power budget among both the PN and SN for each possible time slot such that their sum rate is maximized. This technique could be used by a single wireless operator company that splits its terminal users into cognitive and non-cognitive users in and schedule the power budget optimally among them.

In the case of bidirectional buffer-aided relaying, a low complexity bidirectional relaying protocol that controls half-duplex data flow between two user terminals is proposed and evaluated. The aim of the proposed protocol is to maximize the SN rate, decrease system complexity, and bound the message delay of the network. The bidirectional relaying protocol is followed by a transmission power allocation scheme for each possible transmission mode.

Finally, a theoretical analysis of the average packet delay of the unidirectional buffer-aided relaying scheme that uses max-link relay selection strategy is ana-

lyzed.

1.4.3 Design and Optimization of Multi-Antenna Schemes

In this part of the thesis work, the same procedure of single-antenna protocol design and power optimization schemes is repeated but with the addition of MIMO transceivers at all transmitting and receiving nodes of the network. An efficient and low complexity MIMO-based relay selection scheme that select the best link among all available links is proposed and analyzed. Additionally, a sub-optimal algorithm that allocates a maximum power budget among all transmitting primary and secondary user antennas is proposed and evaluated and compared with that of the optimal solution.

1.5 Thesis Organization

The rest of this thesis is organized as follows. Chapter Two investigates the outage behavior of both conventional unbuffered and buffer-aided relaying networks. The chapter also introduces the concept of physical layer buffering in DF relaying schemes. Chapter Three presents the design and optimization of single antenna schemes of unidirectional-bidirectional cognitive buffer-aided relay network. Chapter Four presents the design and analysis of multiple antenna schemes of unidirectional-bidirectional cognitive buffer-aided relay network. Finally, Chapter Five concludes the thesis work by highlighting the main contributions and conclusions of the thesis. It also suggests some future works in the field of buffer-aided

relaying networks.

CHAPTER 2

OUTAGE BEHAVIOR OF COGNITIVE DF UNIDIRECTIONAL RELAY NETWORKS

2.1 Introduction

This chapter investigates the outage behavior of cognitive DF relay networks for both conventional unbuffered and buffer-aided relaying schemes. Closed form expressions are derived for the probability of outage of cognitive unbuffered multiple-relay networks of the SN and PN. Additionally, closed-form expressions are derived for outage probability of cognitive buffer-aided multiple-relay networks of the SN and PN. Outage performance comparison between conventional relaying

and buffer-aided relaying revealed that a significant coding gain is achieved when relays are equipped with buffer of maximum length equals to one. Beside, as the size of buffer increases, diversity gain increases significantly as well.

The remaining of this chapter is organized as follows: Section 2.2 studies the outage performance of cognitive DF relay networks with conventional relaying. The outage performance of cognitive buffer-aided DF relay networks is investigated in Section 2.3. Section 2.4.3 presents simulation results and compares the outage behavior of cognitive DF relay networks for conventional and buffer-aided relaying schemes. Section 2.5 concludes the chapter and briefly describes the important results.

2.2 Conventional Unbuffered Relay Networks

In this section, the outage behavior of unidirectional opportunistic DF relay network is investigated [45]. DF relay is the most practical relaying scheme in cooperative networks due to its ability to remove channel effect at each hope and produce a noise-free signals to be relayed to destination. In conventional unidirectional DF relaying scheme, data transmission is achieved based on a constant pre-assigned schedule that takes place in two consecutive time slots. During the first time slot, relay node receives a noisy signal from transmitting node, demodulates it, and then uses some error correction technique (after changing it to digital form) to remove channel effect. While, during the second time slot, the noise-free decoded signal is modulated again and then retransmitted to destination.

In DF relaying, outage occurs when the SINR at the input of relay node or at the input of user terminals falls below a certain threshold value γ_{th} . In that case, relay node or destination will fail to decode the received signal and hence, an automatic repeat request (ARQ) packet is sent to transmitter asking for signal retransmission.

2.2.1 System and Channel Models

In this section, we consider a CR network that consists of a PN with one PU source (S_p) and one PU destination (D_p), and SN with one SU source (S), one SU destination (D), and N cognitive DF relays $[R_i]_{i=1}^N$ as shown in Figure 2.1. In this figure, solid and dotted lines represent the desired and interfering signal signals at any possible transmission, respectively.

Without loss of generality, the direct $S - D$ link is not considered in this model as it is assumed to be suffering from severe fading and shadowing effects. In addition, PUs and SUs are assumed to access the spectrum simultaneously (underlay CR). In order to maintain a certain QoS level to the PU, the average interfering power caused by SUs should not exceed a certain interference threshold denoted by I_{th} [46].

We define h_{S,R_i} , h_{S,D_p} , $h_{R_i,D}$, h_{R_i,D_p} , h_{S_p,D_p} , h_{S_p,R_i} , and $h_{S_p,D}$ as the complex channel gains between S and R_i , S and D_p , R_i and D , R_i and D_p , S_p and D_p , S_p and R_i , and S_p and D , respectively. We assume that all channel coefficients are independent but not identically distributed (i.n.d.) slowly varying Rayleigh

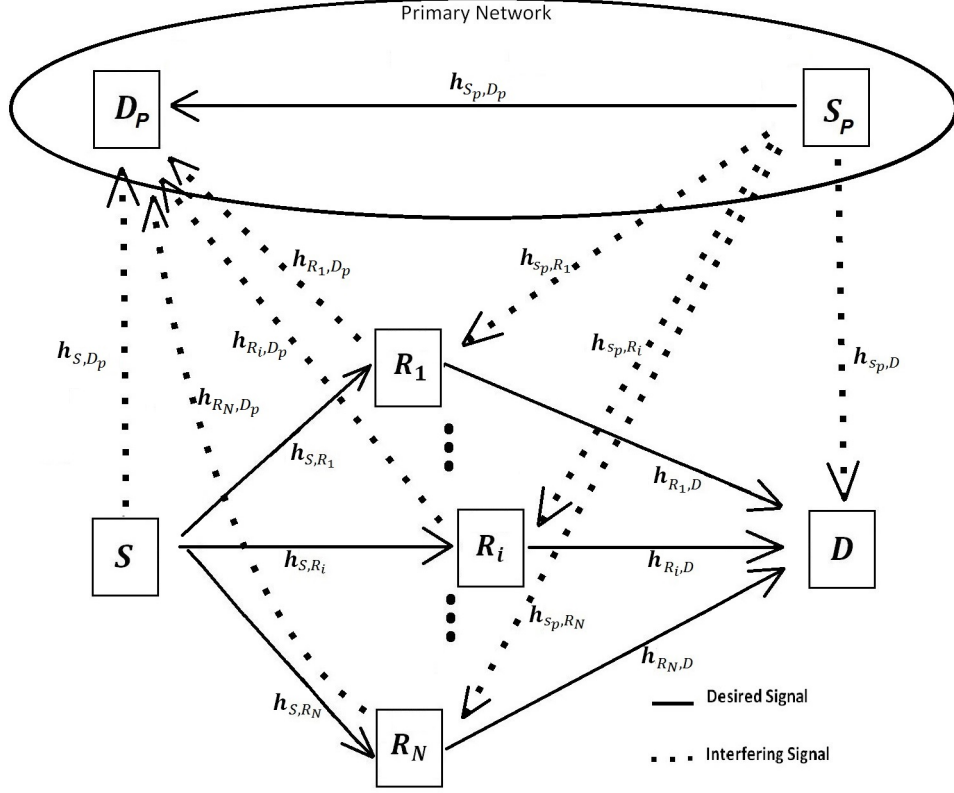


Figure 2.1: Cognitive radio DF relay network (solid lines: desired signals, dotted lines: interfering signals).

fading random variables (RVs) such that they remain unchanged during one time slot. The PN transmitter is assumed to be transmitting at every time slot during network operation time.

2.2.2 Outage Probability

For unidirectional opportunistic DF relaying network, a complete data transmission takes place in two subsequent time slots. During the first time slot, the S transmits its signal to the N relays and a decoded set is formed to contain the set of all relays who have succeeded to decode the received signal conditioned in a minimum transmission rate. While, during the second time slot, only the best

relay from the decoding set is chosen to forward the signal to the D . The received signal at the i^{th} best relay is given by

$$y_{R_i} = \underbrace{h_{S,R_i}x_s}_{\text{Desired Signal}} + \underbrace{h_{S_p,R_i}x_{s_p}}_{\text{Interference Signal}} + \underbrace{n_{R_i}}_{\text{AWGN}}, \quad (2.1)$$

where h_{S,R_i} and h_{S_p,R_i} are the channel gains of $S-R_i$ and S_p-R_i links, respectively, x_s and x_{s_p} denotes the transmitted symbols of the S and the S_p , respectively and $\mathbb{E}[|x_s|^2] = P_s$ and $\mathbb{E}[|x_{s_p}|^2] = P_{s_p}$, and n_{R_i} is the AWGN at the input of the i^{th} relay with constant power spectral density equals to N_o . During the second time slot, the best relay forwards a noise-free signal to the D . The received signal at the D is given by

$$y_D = \underbrace{h_{R_i,D}x_{R_i}}_{\text{Desired Signal}} + \underbrace{h_{S_p,D}x_{s_p}}_{\text{Interference Signal}} + \underbrace{n_D}_{\text{AWGN}}, \quad (2.2)$$

where x_{R_i} is the transmitted symbol of the R_i and with $\mathbb{E}[|x_{R_i}|^2] = P_{R_i}$, and n_D is the AWGN at the input of the D with constant power spectral density equals to N_o .

When $S-R$ link is selected for transmission, the received signal at D_p in any arbitrary time slot is given by

$$y_{D_p} = \underbrace{h_{S_p,D_p}x_{s_p}}_{\text{Desired Signal}} + \underbrace{h_{S,D_p}x_s}_{\text{Interference Signal}} + \underbrace{n_{D_p}}_{\text{AWGN}}, \quad (2.3)$$

where h_{S_p,D_p} and h_{S,D_p} are the channel gains of S_p-D_p and $S-D_p$ links, re-

spectively, x_s and x_{s_p} is the transmitted symbol of S and S_p , respectively with $\mathbb{E}[|x_s|^2] = P_s$ and $\mathbb{E}[|x_{s_p}|^2] = P_{s_p}$, and n_{D_p} is the AWGN at the input of D_p with constant power spectral density equals to N_o . Using (2.1) and (2.3), the SINRs at the input of i^{th} relay and D_p are respectively given as

$$\gamma_{S,R_i} = \frac{\frac{P_s}{N_o} |h_{S,R_i}|^2}{\frac{P_{s_p}}{N_o} |h_{S_p,R_i}|^2 + 1}, \quad (2.4)$$

$$\gamma_{S_p,D_p} = \frac{\frac{P_{s_p}}{N_o} |h_{S_p,D_p}|^2}{\frac{P_s}{N_o} |h_{S,D_p}|^2 + 1}. \quad (2.5)$$

To find the probability of outage of the SN, let us define C_J to be the set of active relays who have succeeded in the process of decoding the received message signal that was transmitted from the S . C_J is known as the decoding set at any arbitrary time slot and is given by [45]

$$\begin{aligned} C_J &\triangleq \left\{ k \in O_R : \frac{1}{2} \log_2 (1 + \gamma_{S,R_k}) \geq R_0 \right\} \\ &= \left\{ k \in O_R : \gamma_{S,R_k} \geq 2^{2R_0} - 1 \right\}, \end{aligned} \quad (2.6)$$

where O_R is a set of J relays and R_0 denotes a fixed normalized rate threshold of the SN. During the second time slot, after decoding the received signal, only the best relay in C_J forwards the re-encoded signal to the D . The selection of the best relay is done using the following criterion

$$R_{i^*} = \underset{l \in C_J}{argmax} \{ \gamma_{R_l,D} \}, \quad (2.7)$$

where $\gamma_{R_l,D}$ is the SINR at the input of the destination D of the signal received from the l^{th} relay that belongs to the decoding set. It can be written as

$$\gamma_{R_l,D} = \frac{\frac{P_{R_l}}{N_o} |h_{R_l,D}|^2}{\frac{P_{S_p}}{N_o} |h_{S,D_p}|^2 + 1}. \quad (2.8)$$

The probability of outage of the SN under opportunistic relaying scheme is defined as [47]

$$\begin{aligned} P_{out}^{SN} &\triangleq P_r \left[\frac{1}{2} \log_2 (1 + \gamma_D) < R_0 \right] \\ &= \sum_{J=0}^N \sum_{C_J} P_r [\gamma_{R_{i^*},D} < u | C_J] P_r [C_J], \end{aligned} \quad (2.9)$$

where the internal summation is taken over all possible $\binom{N}{J}$ subsets of size J from the overall available relays in the network. The probability $P_r [C_J]$ is the probability of the occurrence of the certain decoding set C_J which can be written as

$$P_r [C_J] = \prod_{R_l \in C_J} P_r [\gamma_{S,R_l} \geq u] \prod_{m \notin C_J} P_r [\gamma_{S,R_m} < u]. \quad (2.10)$$

To find $P_r [\gamma_{S,R_l} < u]$, we first write

$$\gamma_{S,R_l} = \frac{P_S \frac{|h_{S,R_l}|^2}{N_o}}{P_{S_p} \frac{|h_{S_p,R_l}|^2}{N_o} + 1} = \frac{Y_1}{X_1 + 1} = \frac{Y_1}{Z_1} \quad (2.11)$$

The CDF of γ_{S,R_l} is found using the following criterion [48]

$$P_r [\gamma_{S,R_l} < u] = \int_1^\infty f_{Z_1}(z_1) \int_0^{uz_1} f_{Y_1}(y_1) dy_1 dz_1, \quad (2.12)$$

where $f_{Z_1}(z_1)$ is the probability density function (PDF) of the denominator which

can be found using a simple random variable transformation and written as

$$f_{Z_1}(z_1) = \lambda_{S_p, D} \exp(-\lambda_{S_p, R_l}(z_1 - 1)),$$

where

$$\lambda_{S_p, R_l} = \left[\frac{P_{s_p}}{N_o} \sigma_{S_p, R_l}^2 \right]^{-1}. \quad (2.13)$$

while

$$f_{Y_1}(y_1) = \lambda_{S, R_l} \exp(-\lambda_{S, R_l} y_1). \quad (2.14)$$

substitute f_{Z_1} and f_{y_1} on 2.12 and integrating, yields

$$P_r[\gamma_{S, R_l} < u] = 1 - \frac{\lambda_{S_p, R_l} \exp(-\lambda_{S, R_l} u)}{\lambda_{S_p, R_l} + \lambda_{S, R_l} u} \quad (2.15)$$

To find the second phase probability of outage that is conditioned in the decoding set which is denoted by $P_r[\gamma_{R_{i^*}, D} < u | C_J]$, we first rewrite the e2e SINR of the best relay as follows

$$\gamma_{R_{i^*}, D} = \frac{\frac{P_{R_{i^*}}}{N_o} |h_{R_{i^*}, D}|^2}{\frac{P_{s_p}}{N_o} |h_{S_p, D}|^2 + 1} = \frac{Y_2}{X_2 + 1} = \frac{Y_2}{Z_2}. \quad (2.16)$$

The CDF of the SINR of the best selected relay can be found using [48]

$$P_r[\gamma_{R_{i^*}, D} < u | C_J] = \int_1^\infty f_{Z_2}(z_2) \int_0^{uz_2} f_{Y_2}(y_2) dy_2 dz_2, \quad (2.17)$$

where $f_Z(z)$ is the probability density function (PDF) of the denominator which

can be found using a simple random variable transformation and written as

$$f_{Z_2}(z_2) = \lambda_{S_p,D} \exp(-\lambda_{S_p,D}(z_2 - 1)),$$

where

$$\lambda_{S_p,D} = \left[\frac{P_{s_p}}{N_o} \sigma_{S_p,D}^2 \right]^{-1}.$$

The PDF $f_{Y_2}(y_2)$ of the signal to noise ration (SNR) $\gamma_{Y_2} = \frac{P_{R_i^*}}{N_o} |h_{R_i^*,D}|^2$ of the desired signal between the best selected relay i^* and the D given a certain decoding set C_J can be written as

$$\begin{aligned} f_{Y_2}(y_2) &= \sum_{l=1}^J f_{\lambda_{R_l,D}}(y_2) \prod_{m=1, m \neq l}^J F_{\lambda_{R_m,D}}(y_2), \\ &= \sum_{l=1}^J \lambda_{R_l,D} \exp(-y_2 \lambda_{R_l,D}) \prod_{m=1, m \neq l}^J (1 - \exp(-\lambda_{R_m,D} y_2)), \end{aligned} \quad (2.19)$$

where

$$\lambda_{R_x,D} = \left[\frac{P_{R_x}}{N_o} \sigma_{R_x,D}^2 \right]^{-1}.$$

Using binomial formula, (2.19) can be rewritten as

$$\begin{aligned} f_{Y_2}(y_2) &= \sum_{l=1}^J (-\lambda_{R_l,D}) \sum_{n=0}^{J-1} \left[(-1)^n \right. \\ &\quad \times \left. \sum_{j_1 < \dots < j_n, j_{(\cdot)} \neq l} \exp(-y_2 (\lambda_{R_{j_1},D} + \dots + \lambda_{R_{j_n},D} + \lambda_{R_l,D})) \right], \end{aligned} \quad (2.20)$$

where the summation $\sum_{j_1 < \dots < j_n, j_{(\cdot)} \neq l}$ is taken over all $\binom{J-1}{n}$ possible subsets of n from the set $C = C_J - l = \{1, \dots, l-1, l+1, \dots, J\}$ and $j_{(\cdot)}$ denotes the index of relay selected from C_J .

Substituting (2.18) and (2.20) in (2.17) and simplifying yields

$$\begin{aligned}
P_r [\gamma_{R_{i^*},D} < u | C_J] &= \sum_{l=1}^J (-\lambda_{R_l,D}) \sum_{n=0}^{J-1} \left[(-1)^n \right. \\
&\times \sum_{j_1 < \dots < j_n, j_{(.)} \neq l} \frac{1}{\lambda_{R_{j_1},D} + \dots + \lambda_{R_{j_n},D} + \lambda_{R_l,D}} \\
&\times \left. \left(1 - \frac{\lambda_{s_p,D} \exp(-(\lambda_{R_{j_1},D} + \dots + \lambda_{R_{j_n},D} + \lambda_{R_l,D}) u)}{\lambda_{s_p,D} + (\lambda_{R_{j_1},D} + \dots + \lambda_{R_{j_n},D} + \lambda_{R_l,D}) u} \right) \right]. \tag{2.21}
\end{aligned}$$

Substituting (2.10) and (2.21) in (2.9), the exact outage probability of the SN can be written as

$$\begin{aligned}
P_{out}^{SN} &= \sum_{J=0}^N \sum_{C_J} \left\{ \sum_{l=1}^J (-\lambda_{R_l,D}) \sum_{n=0}^{J-1} \left[(-1)^n \right. \right. \\
&\times \sum_{j_1 < \dots < j_n, j_{(.)} \neq l} \frac{1}{\lambda_{R_{j_1},D} + \dots + \lambda_{R_{j_n},D} + \lambda_{R_l,D}} \\
&\times \left. \left(1 - \frac{\lambda_{s_p,D} \exp(-(\lambda_{R_{j_1},D} + \dots + \lambda_{R_{j_n},D} + \lambda_{R_l,D}) u)}{\lambda_{s_p,D} + (\lambda_{R_{j_1},D} + \dots + \lambda_{R_{j_n},D} + \lambda_{R_l,D}) u} \right) \right] \Big\} \\
&\times \left\{ \prod_{R_k \in C_J} \left(\frac{\lambda_{S_p,R_k} \exp(-\lambda_{S_p,R_k} u)}{\lambda_{S_p,R_k} + \lambda_{S_p,R_k} u} \right) \prod_{m \notin C_J} \left(1 - \frac{\lambda_{S_p,R_m} \exp(-\lambda_{S_p,R_m} u)}{\lambda_{S_p,R_m} + \lambda_{S_p,R_m} u} \right) \right\}. \tag{2.22}
\end{aligned}$$

For the PN, relay selection on the SN does not affect the interference signal on the PN. With the assumption of equal variance for all SN channel gains that interfere on the PN, and also the assumption of equal transmission power for all interfering transmission nodes, the probability of outage of the PN is defined as

$$P_{out}^{PN} = P(\gamma_{S_p,D_p} < u). \tag{2.23}$$

where $\gamma_{S_p,D_p} = \frac{|h_{S_p,D_p}|^2 P_{S_p}}{|h|^2 P_{SN} + N_o}$, where h is the channel gain of the interfering link from

any transmitting node at the SN. By solving (2.23) in a similar procedure to that of (2.8), the probability of outage of the PN is then given by

$$P_{out}^{PN} = 1 - \frac{\lambda \exp(-u\lambda_{s_p, D_p})}{\lambda + u\lambda_{s_p, D_p}}, \quad (2.24)$$

where

$$\lambda_{s_p, D_p} = \left[\frac{P_{s_p}}{N_o} \sigma_{s_p, D_p}^2 \right]^{-1},$$

also, λ is the average SNR between any SN transmitting node and the PN receiving node at any arbitrary time slot and is defined by $\lambda = \left[\frac{P}{N_o} \sigma_{x, D_p}^2 \right]^{-1}$, where x denotes any transmitting node of the SN that causes an interference on the PN receiving node.

It is important to mention that outage probability expressions were derived under the assumption that the the interference caused by the SN on the PN is always below a predefined threshold value I_{th} which indicate that the effect of I_{th} is trivial in this chapter. However, the effect of the PN interference threshold values is investigated in details in the subsequent chapters.

2.3 Buffer-Aided Relaying

This section investigates and analyzes the outage behavior of cognitive buffer-aided DF multiple-relay network.

2.3.1 System and Channel Models

In this section, we consider a CR network that consists of a PN with one PU source (S_p) and one PU destination (D_p), and a SN with one SU source (S), one SU destination (D), and N cognitive DF relays $[R_i]_{i=1}^N$ as shown in Figure 2.2. Each relay is assumed to be equipped with a buffer B of maximum size L , where L is the number of data packets that can be stored in the buffer before an overflow occurs. The instantaneous number of stored information packets at the buffer B_i of the i^{th} relay is denoted by $\Psi(R_i)$, where $0 \leq \Psi(R_i) \leq L$. As illustrated in Figure 2.2, the solid and dotted lines represent desired and interfering signals in each possible transmission mode, respectively.

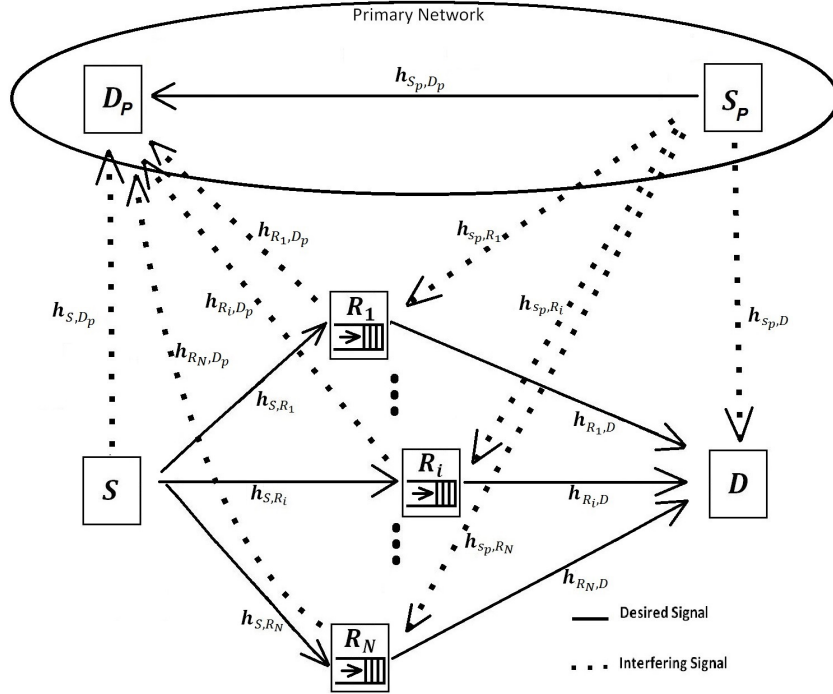


Figure 2.2: Cognitive radio network with buffer-aided DF relays (solid lines: desired signals, dotted lines: interfering signals).

Without loss of generality, the direct $S - D$ link is not considered in this model

as it is assumed to be suffering from severe fading and shadowing effects ¹. In addition, PUs and SUs are assumed to access the spectrum simultaneously. In order to maintain a certain QoS level at the PU, the average received interference power due to SUs should not exceed a certain interference threshold denoted by I_{th} [33]. All channel coefficients are assumed to be i.n.d. slowly varying Rayleigh fading RVs such that they remain unchanged during one time slot. We denote $h_{x,y}$ as the channel coefficient between terminals x and y . Each receiving terminal is assumed to experience an AWGN at its input with constant variance N_o . Transmitted signals from S , R_i , and S_p are denoted by x_S , x_{R_i} , and x_{S_p} respectively. To avoid the need for heavy and fast back-haul links, a central processing unit that performs relay selection and power allocation operations is assumed to exist in the network with a full CSI acknowledgement.

2.3.2 Max-Link Relay Selection Protocol

For the unidirectional buffer-aided relaying scheme, max-link selection is the most practical protocol that is used to control data flow from the S to the D . Max-link has three possible cases that control the information packet flow in buffer-aided relay networks as follows [26]

Case I: All relays buffers are empty, i.e., $\Psi(R_i) = 0, \forall i = 1, 2, \dots, N$. In this case, the best link is chosen from the $S - R$ available links and the buffer content of the selected relay is increased by one packet.

¹This assumption is more probable in cognitive radio networks at which the SN transmission power is relatively low to maintain a certain QoS at the PN.

Case II: Buffers of all relays are fully loaded, i.e., $\Psi(R_i) = L, \forall i = 1, 2, \dots, N$. In

this case, the relay related to the best $R_i - D$ link is selected to transmit its oldest stored packet to the destination.

Case III: There are some available buffers that are not full and some available buffers that are not empty. In this case, the relay related to the best $S - R_i$, or $R_i - D$ link is selected for reception or transmission of a data packet, respectively.

To illustrate the performance of max-link relaying protocol, Figure 2.3 shows an illustrative example of the way max-link protocol works. In this example, the

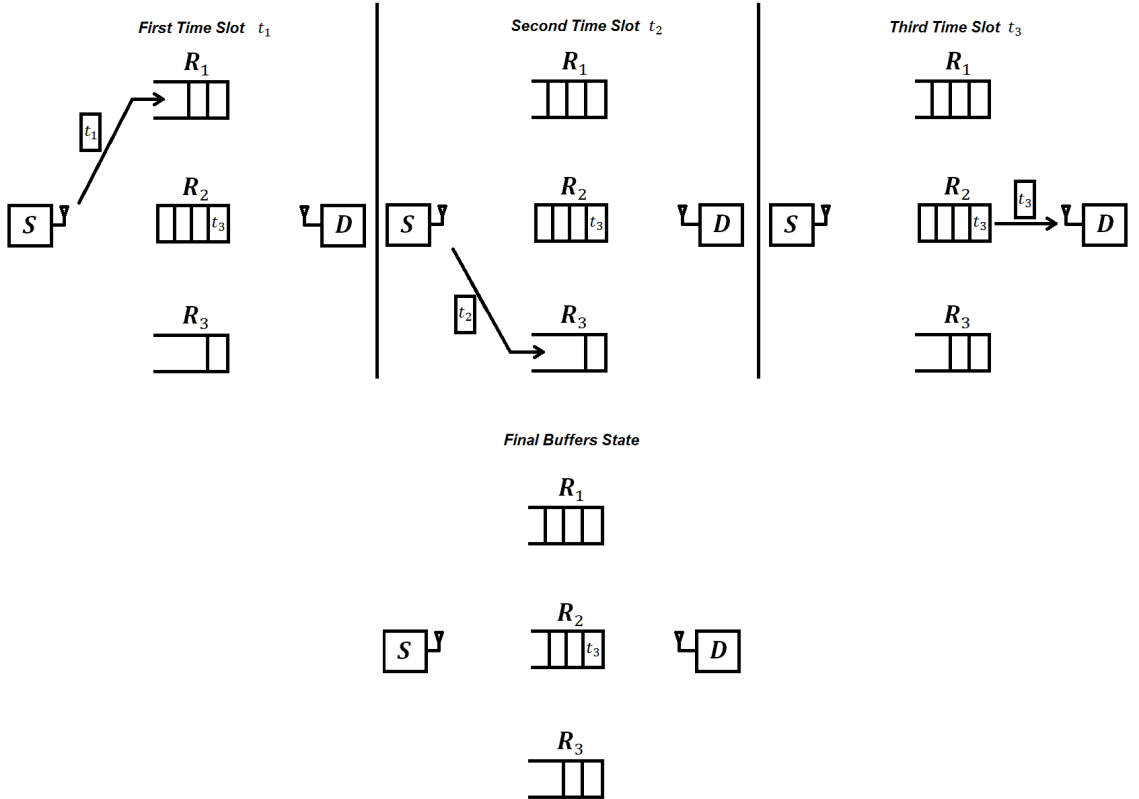


Figure 2.3: An illustrative example of max-link unidirectional relaying protocol.

cooperative network consist of three relays each with instantaneous buffer size

$\psi(R_1) = 2$, $\psi(R_2) = 4$, and $\psi(R_3) = 1$, respectively. The maximum buffer size of all relays is $L = 4$. During the network operation, at an arbitrary time slot t_1 , the $S - R_1$ link is happened to be the link with maximum channel gain and hence, S sends an information packet to be buffered at R_1 in the third position. During the second time slot t_2 the $S - R_3$ link is selected since it is containing the maximum channel gain, and hence S sends an information packet to be buffered at R_3 in the third position. Finally, during the third time slot t_3 , the $R_2 - D$ link contains the highest instantaneous channel gain and hence, R_2 sends the oldest buffered information packet to the destination. The final new instantaneous buffer sizes are then $\psi(R_1) = 3$, $\psi(R_2) = 3$, and $\psi(R_3) = 2$.

In general, for buffer-aided relay network that uses max-link relay selection scheme, the index of the best relay is found using the following criterion

$$R_{i^*} = \arg \max_{R_i \in \mathcal{C}} \left\{ \bigcup_{R_i \in \mathcal{C}: \Psi(R_i) \neq L} \{|h_{S,R_i}|^2\}, \bigcup_{R_i \in \mathcal{C}: \Psi(R_i) \neq 0} \{|h_{R_i,D}|^2\} \right\}, \quad (2.25)$$

where \mathcal{C} is the set of all active relays who have empty buffers to receive additional messages and the set of all relays who have available buffered messages to be relayed to the destination.

2.3.3 Outage Probability

In this section, outage behavior of CR buffer-aided DF multiple-relay network is investigated and analyzed. Max-link relay selection scheme that was presented in the last section is used in the analysis as it represents the most practical relaying

scheme for unidirectional buffer-aided relay networks.

If at a certain time slot t , the best relay R_{i^*} is selected to receive an information packet from the source node, the received signal at the relay is given by

$$y_{R_{i^*}} = \underbrace{h_{S,R_{i^*}}x_s}_{\text{Desired Signal}} + \underbrace{h_{S_p,R_{i^*}}x_{s_p}}_{\text{Interference Signal}} + \underbrace{n_{R_{i^*}}}_{\text{AWGN}}, \quad (2.26)$$

where $h_{S,R_{i^*}}$ and $h_{S_p,R_{i^*}}$ are the channel gains of $S - R_{i^*}$ and $S_p - R_{i^*}$ links, respectively, x_s and x_{s_p} are the transmitted symbols of the S and the S_p , respectively with $\mathbb{E}[|x_s|^2] = P_s$ and $\mathbb{E}[|x_{s_p}|^2] = P_{s_p}$, and $n_{R_{i^*}}$ is the AWGN at the input of the i^{th} relay with constant power spectral density equals to N_o . On the other hand, if the best relay R_{i^*} is selected to transmit its oldest stored information packet to destination, the received signal at the destination is given by

$$y_D = \underbrace{h_{R_{i^*},D}x_{R_{i^*}}}_{\text{Desired Signal}} + \underbrace{h_{S_p,D}x_{s_p}}_{\text{Interference Signal}} + \underbrace{n_D}_{\text{AWGN}}. \quad (2.27)$$

Similarly, the received signal at D_p at any arbitrary time slot is given by

$$y_{D_p} = \underbrace{h_{S_p,D_p}x_{s_p}}_{\text{Desired Signal}} + \underbrace{h_{S,D_p}x_s}_{\text{Interference Signal}} + \underbrace{n_{D_p}}_{\text{AWGN}}, \quad (2.28)$$

where h_{S_p,D_p} and h_{S,D_p} are the channel gains of $S_p - D_p$ and $S - D_p$ links, respectively, x_s and x_{s_p} are the transmitted information packets of the S and the S_p with $\mathbb{E}[|x_s|^2] = P_s$ and $\mathbb{E}[|x_{s_p}|^2] = P_{s_p}$, respectively, and n_{D_p} is the AWGN at the input of the D_p with constant power spectral density equals to N_o . Using (2.26), (2.27) and (2.28), SINR at R_{i^*} , D and D_p are respectively given as

$$\gamma_{S,R_{i^*}} = \frac{\frac{P_s}{N_o} |h_{S,R_{i^*}}|^2}{\frac{P_{sp}}{N_o} |h_{S_p,R_{i^*}}|^2 + 1}, \quad (2.29)$$

$$\gamma_{R_{i^*},D} = \frac{\frac{P_{R_i}}{N_o} |h_{R_{i^*},D}|^2}{\frac{P_{sp}}{N_o} |h_{S_p,D}|^2 + 1}, \quad (2.30)$$

$$\gamma_{S_p,D_p} = \frac{\frac{P_{sp}}{N_o} |h_{S_p,D_p}|^2}{\frac{P_w}{N_o} |h_{w,D_p}|^2 + 1}, \quad (2.31)$$

where $w \equiv S$ if the S is transmitting or $w \equiv R_{i^*}$ if the R_{i^*} is transmitting.

Using max-link relay selection protocol in the SN, an outage event occurs in the SN if the best selected link is in outage, either when the best selected relay is receiving or transmitting. Based on that fact, outage probability of buffer-aided relaying with max-link relay selection can be generally written by

$$P_{\text{out}} \triangleq \begin{cases} P\left(\frac{1}{2} \log_2(1 + \gamma_{S,R_{i^*}}) < R_0\right) & \text{(for relay reception);} \\ P\left(\frac{1}{2} \log_2(1 + \gamma_{R_{i^*},D}) < R_0\right) & \text{(for relay transmission),} \end{cases} \quad (2.32)$$

or equivalently,

$$P_{\text{out}} \triangleq \begin{cases} P\left(\gamma_{S,R_{i^*}} < (u = 2^{2R_0} - 1)\right) & \text{(for relay reception);} \\ P\left(\gamma_{R_{i^*},D} < (u = 2^{2R_0} - 1)\right) & \text{(for relay transmission).} \end{cases} \quad (2.33)$$

Markov chain modelling is used in the analysis and derivation of the outage

probability of the SN due to the existence of buffers in relays which in turn represents a queuing system with a number of queues equals to the number of relays within the SN. For the system under consideration, at any time slot, a certain state S_j represents the instantaneous buffer states of all buffers in all relays of the network and can be defined as

$$S_j \triangleq (\Psi(R_1) \Psi(R_2) \dots \Psi(R_N)), \quad (2.34)$$

where N denotes the number of relays in the SN. In general, there are $(1 + L)^N$ possible states in the SN that is equipped with N relays each with a buffer B of maximum size L .

For max-link relaying protocol, when the network operates based on a predefined minimum rate R_0 , a state transition occurs only when the selected link is suitable for transmission on a rate that is not less than R_0 . On the other hand if the selected link is not suitable for transmitting on a rate of R_0 or more, an outage occurs on the selected link and no change on the buffers current state happens. Accordingly, the receiving node sends a re-transmission request to the transmitting node. For any arbitrary state S_j , there is a set of states that the network could move to when a successful data transmission takes place. The set of states that is connected to the S_j state is denoted by \mathbf{C}_{S_j} and can be defined as follows

$$\mathbf{C}_{S_j} = \left\{ \bigcup_{1 \leq m \leq (1+L)^N} S_m : \text{where } S_j \text{ and } S_m \text{ are connected} \right\}, \quad (2.35)$$

where two states are said to be connected if it is possible to move from one state to the other with only one time slot. Being at S_j state, the number of available transmissions to be selected to move from S_j state is denoted by D_j and can be found as follows

$$D_j = \sum_{i=1}^N \phi(R_i),$$

where

$$\phi(R_i) = \begin{cases} 2 & \text{if } 0 < \psi(R_i) < L; \\ 1 & \text{otherwise.} \end{cases} \quad (2.36)$$

At state S_j , under the assumption that all states within the set \mathbf{C}_{S_j} are equally likely, the probability to select a certain available transmission from \mathbf{C}_{S_j} set equals to $1/D_j$ regardless of the initial state. Additionally, the probability of moving from state S_j to state $S_i \forall i, j = 1, 2, \dots, (L+1)^N$ [49]

$$A_{i,j} = \begin{cases} \bar{P}_{D_j} & \text{if } i = j \\ P_{D_j} & \text{if } S_i \in \mathbf{C}_{S_j}, \text{ for } i, j \in \{1, 2, \dots, (L+1)^N\} \\ 0 & \text{elsewhere,} \end{cases} \quad (2.37)$$

where P_{D_j} is the probability that a state transition to S_i state coming from S_j state will take place with successful decoding where $S_i \in \mathbf{C}_{S_j}$, \bar{P}_{D_j} is the probability that no state transition occurs due to outage of the best selected link that belongs to \mathbf{C}_{S_j} and the current buffers state remains as S_j state.

If we define $\boldsymbol{\gamma}_j = (\gamma_{S,R_{q_1}}, \gamma_{S,R_{q_2}}, \dots, \gamma_{S,R_{q_M}}, \gamma_{R_{v_1},D}, \gamma_{R_{v_2},D}, \dots, \gamma_{R_{v_K},D})$ as the

SINR vector that contains a set of the possible transitions associated with S_j state, where $q_i, 0 \leq i \leq M$ is the index of the i^{th} selected $S - R$ link that belongs to one of \mathbf{C}_{S_j} possible links and $v_j, 0 \leq j \leq K$ is the index of the i^{th} selected $R - D$ link that belongs to one of \mathbf{C}_{S_j} possible links and M and K are the numbers of possible transmissions connected to S_j on the $S - R$ and $R - D$ links, respectively. In general, at any state S_j , assuming that all states are equally likely to occur, the probability of leaving state S_j can be defined as [49]

$$P_{D_j} = \frac{1}{D_j} [1 - P_r(\max(\gamma_j) \leq u)]. \quad (2.38)$$

To find the CDF of $\max(\gamma_j)$, we first rewrite the point-to-point SINR of the best link as follows

$$\gamma_{v,q} = \frac{\frac{P_v}{N_o} |h_{v,q}|^2}{\frac{P_{sp}}{N_o} |h_{S_p,q}|^2 + 1} = \frac{Y}{X + 1} = \frac{Y}{Z}, \quad (2.39)$$

where $(q, v) \equiv (S, R_{i^*})$ if the best link belongs to $S - R$ links or $(q, v) \equiv (R_{i^*}, D)$ if the best link belongs to $R - D$ links. The CDF of the SINR of the best selected link can be found using the following mathematical expression [48]

$$P_r(\max(\gamma) \leq u) = \int_1^\infty f_Z(z) \int_0^{uz} f_Y(y) dy dz, \quad (2.40)$$

where $f_Z(z)$ is the PDF of the denominator which can be found using a simple

RV transformation and written as

$$f_Z(z) = \lambda_{S_p,w} \exp(-\lambda_{S_p,w}(z-1)), \quad (2.41)$$

where

$$\lambda_{S_p,w} = \begin{cases} \left[\frac{P_{sp}}{N_o} \sigma_{S_p, R_{qw}}^2 \right]^{-1} & 1 \leq w \leq M, \\ \left[\frac{P_{sp}}{N_o} \sigma_{S_p, D}^2 \right]^{-1}, & \text{if } M+1 \leq w \leq D_j. \end{cases} \quad (2.42)$$

The PDF $f_Y(y)$ of the desired signal of the best link conditioned on the set \mathbf{C}_{S_j} can be written as

$$f_Y(y) = \sum_{l=1}^{D_j} \lambda_l \exp(-y\lambda_l) \prod_{m=1, m \neq l}^{D_j} (1 - \exp(-\lambda_m y)), \quad (2.43)$$

where

$$\lambda_x = \begin{cases} \left[\frac{P_{R_{qx}}}{N_o} \sigma_{S, R_{qx}}^2 \right]^{-1}, & \text{if } 1 \leq x \leq M \\ \left[\frac{P_{R_{vx}}}{N_o} \sigma_{R_{vx}, D}^2 \right]^{-1}, & \text{if } M+1 \leq x \leq D_j. \end{cases} \quad (2.44)$$

Using binomial formula, (2.43) can be rewritten as

$$f_Y(y) = \sum_{l=1}^{D_j} \lambda_l \exp(-y\lambda_l) \sum_{n=0}^{D_j-1} \left[(-1)^n \times \sum_{j_1 < \dots < j_n, j_{(\cdot)} \neq l} \exp(-y(\lambda_{j_1} + \dots + \lambda_{j_n})) \right], \quad (2.45)$$

where

$$\lambda_x = \begin{cases} \left[\frac{P_{R_{qx}}}{N_o} \sigma_{S, R_{qx}}^2 \right]^{-1}, & \text{if } 1 \leq x \leq M \\ \left[\frac{P_{R_{vx}}}{N_o} \sigma_{R_{vx}, D}^2 \right]^{-1}, & \text{if } M+1 \leq x \leq D_j, \end{cases} \quad (2.46)$$

where the summation $\sum_{j_1 < \dots < j_n, j_{(\cdot)} \neq l}$ is taken over all $\binom{D_j-1}{n}$ possible subsets of n

from the set $\mathbf{C} = \mathbf{C}_{S_j} - l = \{1, \dots, l-1, l+1, \dots, D_j\}$ and $j_{(\cdot)}$ denotes the index of relay selected from \mathbf{C}_{S_j} . Substituting (2.41) and (2.45) in (2.40), integrating, and simplifying yields

$$P_r(\max(\gamma_j) \leq u) = \sum_{l=1}^{D_j} (-\lambda_l) \sum_{n=0}^{D_j-1} \left[(-1)^n \times \sum_{j_1 < \dots < j_n, j_{(\cdot)} \neq l} \frac{1}{\lambda_{j_1} + \dots + \lambda_{j_n} + \lambda_l} \right. \\ \left. \times \left(1 - \frac{\lambda_{s_p, l} \exp(-(\lambda_{j_1} + \dots + \lambda_{j_n} + \lambda_l) u)}{\lambda_{s_p, l} + (\lambda_{j_1} + \dots + \lambda_{j_n} + \lambda_l) u} \right) \right]. \quad (2.47)$$

Substituting (2.47) in (2.38), the probability of leaving the state S_j to another state is then given by

$$P_{D_j} = \frac{1}{D_j} \left[1 - \left\{ \sum_{l=1}^{D_j} (-\lambda_l) \sum_{n=0}^{D_j-1} \left[(-1)^n \right. \right. \right. \\ \left. \times \sum_{j_1 < \dots < j_n, j_{(\cdot)} \neq l} \times \frac{1}{\lambda_{j_1} + \dots + \lambda_{j_n} + \lambda_l} \left(1 - \right. \right. \quad (2.48) \\ \left. \left. \frac{\lambda_{s_p, l} \exp(-(\lambda_{j_1} + \dots + \lambda_{j_n} + \lambda_l) u)}{\lambda_{s_p, l} + (\lambda_{j_1} + \dots + \lambda_{j_n} + \lambda_l) u} \right) \right] \right\} \right].$$

On the other hand using Markov theory, the probability that the best selected link transmission will suffers from an outage and hence no state change occurs can be given by

$$\bar{P}_{D_j} \triangleq 1 - \sum_{i=1}^{D_j} P_{D_j}, \quad (2.49a)$$

$$= \sum_{l=1}^{D_j} (-\lambda_l) \sum_{n=0}^{D_j-1} \left[(-1)^n \times \sum_{j_1 < \dots < j_n, j_{(\cdot)} \neq l} \frac{1}{\lambda_{j_1} + \dots + \lambda_{j_n} + \lambda_l} \right. \\ \left. \times \left(1 - \frac{\lambda_{s_p, l} \exp(-(\lambda_{j_1} + \dots + \lambda_{j_n} + \lambda_l) u)}{\lambda_{s_p, l} + (\lambda_{j_1} + \dots + \lambda_{j_n} + \lambda_l) u} \right) \right]. \quad (2.49b)$$

After finding all elements of the transition matrix $\mathbf{A} \in \mathbb{C}^{(L+1)^N \times (L+1)^N}$ using (2.37), we are interested in finding the probability of being at a certain state of the network. In [49], it was found that the steady state matrix of Markov model that models a set of buffers is a column stochastic matrix ². The stationary state distribution $\boldsymbol{\pi}$ of a column stochastic Markov chain matrix \mathbf{A} is given by [49]

$$\boldsymbol{\pi} = (\mathbf{A} - \mathbf{I} + \mathbf{B})^{-1} \mathbf{b}, \quad (2.50)$$

where $\boldsymbol{\pi}$ is the stationary distribution, $\mathbf{b} = (1 \ 1 \ \dots \ 1)^T$, $B_{i,j} = 1 \ \forall i, j$, and \mathbf{I} is identity matrix.

It is clear that an outage events only occurs if there is no state transmission, i.e. no change on buffers state. The probability of outage of the SN is then can be expressed as

$$P_{out}^{SN} = \sum_{i=1}^{(L+1)^N} \pi_i \bar{P}_{D_i} = \text{diag}(\mathbf{A}) \boldsymbol{\pi}. \quad (2.51)$$

For the PN, link selection on the SN does not affect the interference signal on the PN. With the assumption of equal variance for all SN channel gains that interfere on the PN, and also the assumption of equal transmission power for all interfering transmission nodes, the outage probability of the PN can be written by

²A column stochastic matrix is a square matrix for which the sum of the elements in each of its columns is 1.

$$P_{out}^{PN} = 1 - \frac{\lambda \exp(-u\lambda_{s_p, D_p})}{\lambda + u\lambda_{s_p, D_p}}, \quad (2.52)$$

where

$$\lambda_{s_p, D_p} = \left[\frac{P_{s_p}}{N_o} \sigma_{S_p, D_p}^2 \right]^{-1},$$

also, λ is the average SNR between any SN transmitting node and the PN receiving node at any arbitrary time slot and is defined by $\lambda = \left[\frac{P}{N_o} \sigma_{x, D_p}^2 \right]^{-1}$, where x denotes any transmitting node of the SN that causes an interference on the PN receiving node.

• Illustrative Example

To show how the transition matrix of the SN is constructed, we assume a network with $N = 2$ relays and $L = 3$ maximum buffer size on each, i.e. there will be $(L + 1)^N = 16$ possible states. The set of all possible states that illustrate the possible buffer contents are shown in Table 2.1 Now, the problem is to first assign the transition matrix by assigning which states are connected by each other. If states S_i and S_j are connected, then it is possible to move from (to) state S_i to (from) state S_j by during one time slot. The state transition matrix for this example is then given by

Again, it is important to mention that outage probability expressions are derived with the assumption that the peak transmission power is always less than the PN interference threshold value I_{th} which indicate that the effect of I_{th} is trivial in this chapter. However, the effect of the PN interference threshold values is investigated in details in the subsequent chapters.

Table 2.1: Possible States

State	$\psi(R_1)$	$\psi(R_2)$
S_1	0	0
S_2	1	0
S_3	2	0
S_4	3	0
S_5	0	1
S_6	1	1
S_7	2	1
S_8	3	1
S_9	0	2
S_{10}	1	2
S_{11}	2	2
S_{12}	3	2
S_{13}	0	3
S_{14}	1	3
S_{15}	2	3
S_{16}	3	3

$$\mathbf{A} = \begin{bmatrix} \bar{P}_{1,1} & P_{1,2} & 0 & 0 & P_{1,5} & 0 & 0 & 0 & 0 & 0 & 0 & 0 & 0 & 0 & 0 & 0 \\ P_{2,1} & \bar{P}_{2,2} & P_{2,3} & 0 & 0 & P_{2,6} & 0 & 0 & 0 & 0 & 0 & 0 & 0 & 0 & 0 & 0 \\ 0 & P_{3,2} & \bar{P}_{3,3} & P_{3,4} & 0 & 0 & P_{3,7} & 0 & 0 & 0 & 0 & 0 & 0 & 0 & 0 & 0 \\ 0 & 0 & P_{4,3} & \bar{P}_{4,4} & 0 & 0 & 0 & P_{4,8} & 0 & 0 & 0 & 0 & 0 & 0 & 0 & 0 \\ P_{5,1} & 0 & 0 & 0 & \bar{P}_{5,5} & P_{5,6} & 0 & 0 & P_{5,9} & 0 & 0 & 0 & 0 & 0 & 0 & 0 \\ 0 & P_{6,2} & 0 & 0 & P_{6,5} & \bar{P}_{6,6} & P_{6,7} & 0 & 0 & P_{6,10} & 0 & 0 & 0 & 0 & 0 & 0 \\ 0 & 0 & P_{7,3} & 0 & 0 & P_{7,6} & \bar{P}_{7,7} & P_{7,8} & 0 & 0 & P_{7,11} & 0 & 0 & 0 & 0 & 0 \\ 0 & 0 & 0 & P_{8,4} & 0 & 0 & P_{8,7} & \bar{P}_{8,8} & 0 & 0 & 0 & P_{8,12} & 0 & 0 & 0 & 0 \\ 0 & 0 & 0 & 0 & P_{9,5} & 0 & 0 & 0 & \bar{P}_{9,9} & P_{9,10} & 0 & 0 & P_{9,13} & 0 & 0 & 0 \\ 0 & 0 & 0 & 0 & 0 & P_{10,6} & 0 & 0 & P_{10,9} & \bar{P}_{10,10} & P_{10,11} & 0 & 0 & P_{10,14} & 0 & 0 \\ 0 & 0 & 0 & 0 & 0 & 0 & P_{11,7} & 0 & 0 & P_{11,10} & \bar{P}_{11,11} & P_{11,12} & 0 & 0 & P_{11,15} & 0 \\ 0 & 0 & 0 & 0 & 0 & 0 & 0 & P_{12,8} & 0 & 0 & P_{12,11} & \bar{P}_{12,12} & 0 & 0 & 0 & P_{12,16} \\ 0 & 0 & 0 & 0 & 0 & 0 & 0 & 0 & P_{13,9} & 0 & 0 & 0 & \bar{P}_{13,13} & P_{13,14} & 0 & 0 \\ 0 & 0 & 0 & 0 & 0 & 0 & 0 & 0 & 0 & P_{14,10} & 0 & 0 & P_{14,13} & \bar{P}_{14,14} & P_{14,15} & 0 \\ 0 & 0 & 0 & 0 & 0 & 0 & 0 & 0 & 0 & 0 & P_{15,11} & 0 & 0 & P_{15,14} & \bar{P}_{15,15} & P_{15,16} \\ 0 & 0 & 0 & 0 & 0 & 0 & 0 & 0 & 0 & 0 & 0 & P_{16,12} & 0 & 0 & P_{16,15} & \bar{P}_{16,16} \end{bmatrix}$$

2.4 Simulation Results

In this section we present simulation results of the outage behavior of the PN and the SN with conventional and buffer-aided relaying schemes. A performance

comparison between conventional and buffer-aided relaying is also presented.

2.4.1 Conventional Unbuffered Relaying

In this part, all simulation results generated with 1000,000 iterations of Monte-Carlo simulation. Simulation results are presented to validate the derived expressions. For simplicity of the simulation, all channel gains are assumed to have equal variances, i.e., $\mathbb{E}[|h_{i,j}|^2] = \sigma^2 \forall(i, j)$, which means $\lambda_{i,j} = \lambda \forall(i, j)$.

Figure 2.4 shows the probability of outage of the SN of both simulation results and analytical expressions for different number of active relays N .

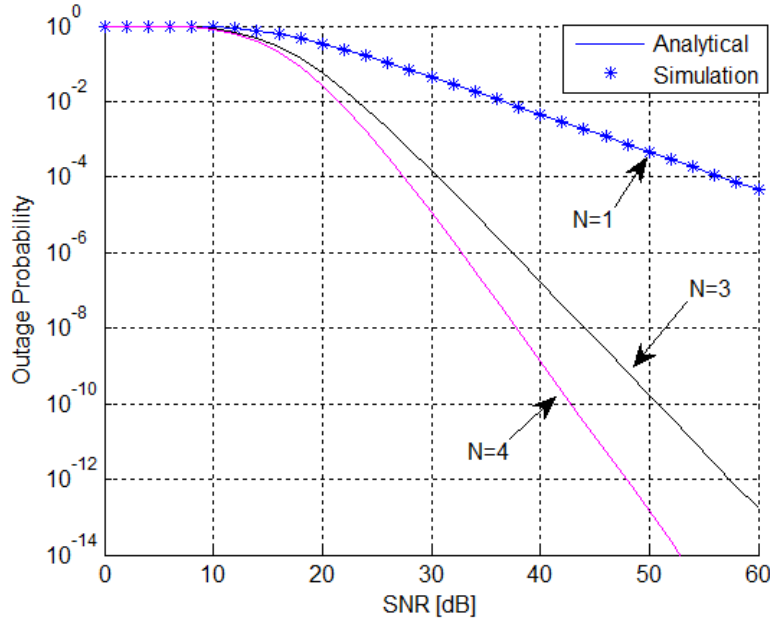


Figure 2.4: Outage probability of the SN with equal-power interferers and different number of relays N with $\gamma_{th} = 5$ dB.

It can be depicted from this figure that when the number of relays in the SN increases, the diversity gain of the SN is significantly enhanced. For example, a gain of around 10 dB is achieved at SNR equals to 30 dB when increasing $N = 1$ to

$N = 3$. However, the effect of increasing the number of relays within the network decays as N goes large.

The effect of the PN interference power on the SN probability of outage is shown in Figure 2.5. It can be depicted from this figure that increasing the PN

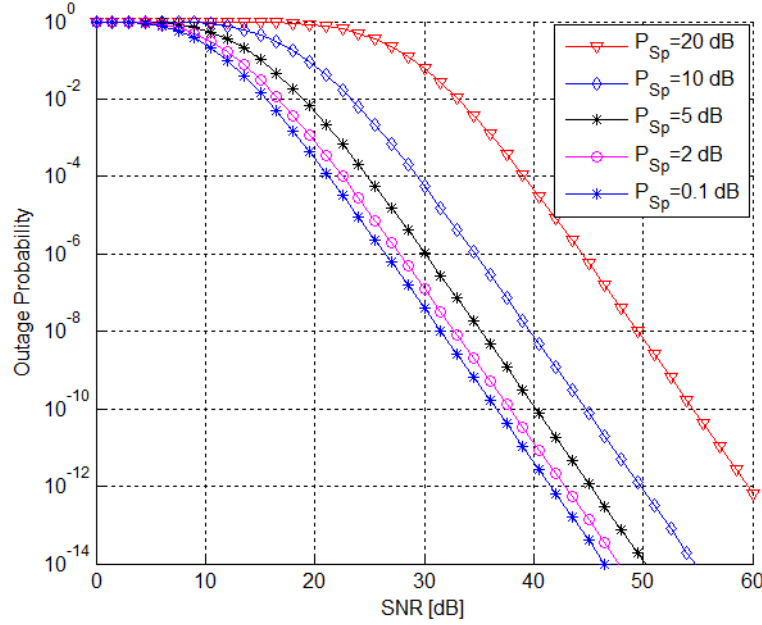


Figure 2.5: Outage probability of the SN with different PN interference power with $\gamma_{th} = 5$ dB.

interference power degrades the outage performance of the SN significantly. In the other hand, decreasing the PN interference power enhances the SN outage performance significantly until it reaches a certain point that further decrement on the PN interference power does not enhance the SN outage performance. This is due to the fact that the at low PN interference, the SINR of the SN depends mainly on the AWGN and channel quality.

The PN outage performance with difference interference power is shown in Figure 2.6. It can be seen from this figure the number of active relays N on the

SN does not affect outage probability of the PN, as expected.

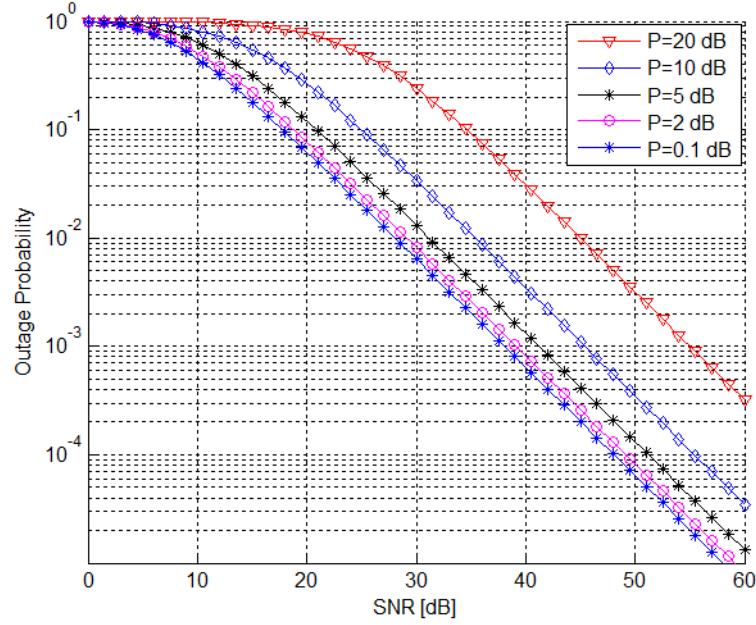


Figure 2.6: Outage probability of the PN with different interference powers $\gamma_{th} = 5$ dB.

Figure 2.7 shows a performance comparison of outage behavior of both PN and SN. It can be seen from this figure that outage probability of the PN is a bit better than that of the SN for the case of $N = 1$. This is due to the fact that the PN outage is taken over one single e2e hope while in the SN, the outage event occurs in either the first or second hope. However, increasing the number of relays in the SN enhances the outage performance of the SN significantly and does not affect the performance of the PN. This is due to the fact that diversity gain acquired by relays only enhance the SN outage probability not the PN.

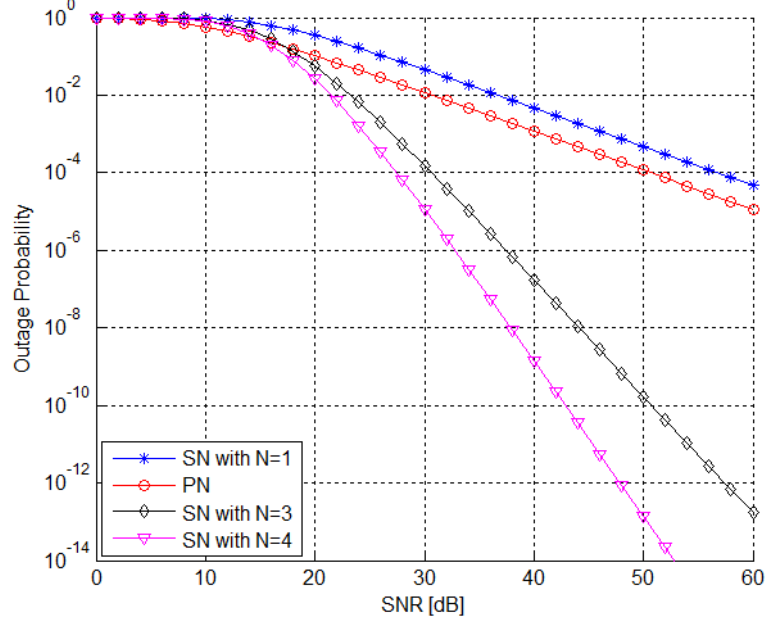


Figure 2.7: Outage probability of the PN with equal-power interferers $\gamma_{th} = 5$ dB.

2.4.2 Buffer-Aided Relaying

This section presents analytical results for outage behavior of the PN and SN with buffer-aided relaying scheme. Simulation results are generated with 1000,000 iterations of Monte-Carlo simulation presented to validate the derived expressions. For simplicity of the simulation, all channel gains are assumed to have equal variances i.e. $\mathbb{E}[|h_{i,j}|^2] = \sigma^2 \forall(i, j)$, which means $\lambda_{i,j} = \lambda \forall(i, j)$.

Figure 2.8 shows the simulation and analytical results of outage probability of the SN that uses buffer-aided relaying scheme for different number of relays with $P_{S_p} = 8$ dB, $\gamma_{th} = 5$ dB.

The diversity gain achieved in this figure is due to the increase of number of relays on the network.

The effect of maximum buffer size L on outage behavior of the SN is investi-

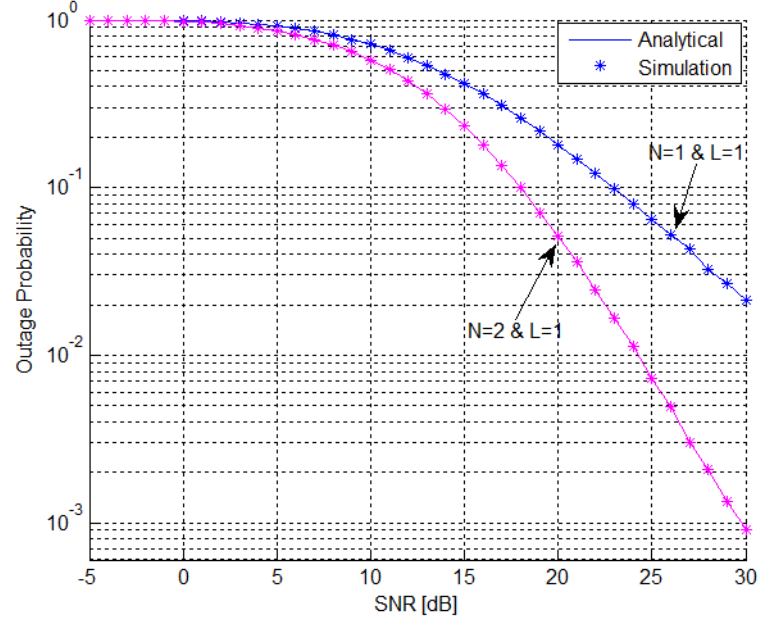


Figure 2.8: Simulation and analytical results of outage probability of the SN that uses buffer-aided relaying scheme under different number of relays with $P_{S_p} = 8$ dB, $\gamma_{th} = 5$ dB.

gated in Figure 2.9. It can be noticed from this figure that for $N = 1$, increasing

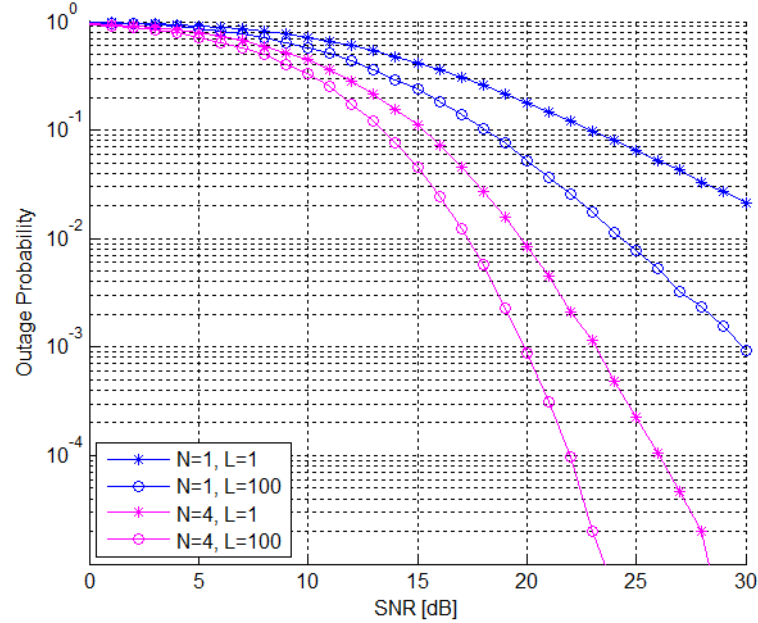


Figure 2.9: Outage probability of the SN with different number of relays and different number of maximum buffer size L with $P_{S_p} = 8$ dB, $\gamma_{th} = 5$ dB.

the maximum buffer size from $L = 1$ to $L = 100$ enhances the outage behavior of the SN significantly (a gain of 7 dB to achieve the same performance as that of $\bar{\gamma} = 30$ dB in the case of $L = 1$). For higher number of relays, the enhancement on outage behavior of the SN is still high but not as much as that achieved with $N = 1$. This is due to the fact that the system is already enhanced by increasing the number of relays on the network and the effect of increasing buffer size will be decreased as the number of relays increases.

Figure 2.10 compares the outage behavior of the SN and PN with equal interference values used in generating the results.

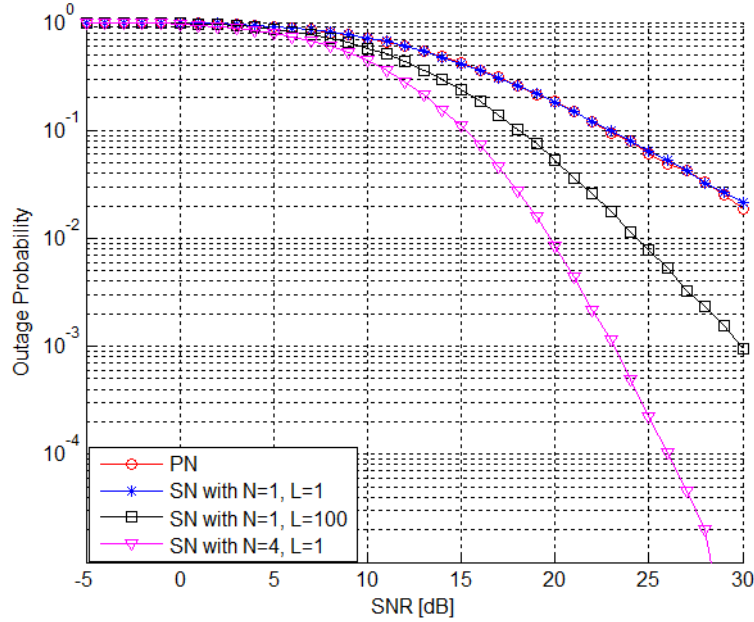


Figure 2.10: Outage probability of the SN and PN $P_{interference} = 8$ dB and $\gamma_{th} = 5$ dB.

It can be seen from this figure that the outage behavior of the PN with that of SN with one relay and $L = 1$ is almost identical. However, for higher buffer size and/or higher number of relays, the SN outage performance is being superior

to that of the PN.

2.4.3 Conventional versus Buffer-Aided Relaying

In this section, the performance enhancement achieved when moving from conventional relaying schemes to buffer-aided relay networks is investigated.

Figure 2.11 shows the probability of outage of the SN for both conventional unbuffered and buffer-aided relaying schemes with different values of maximum buffer size L .

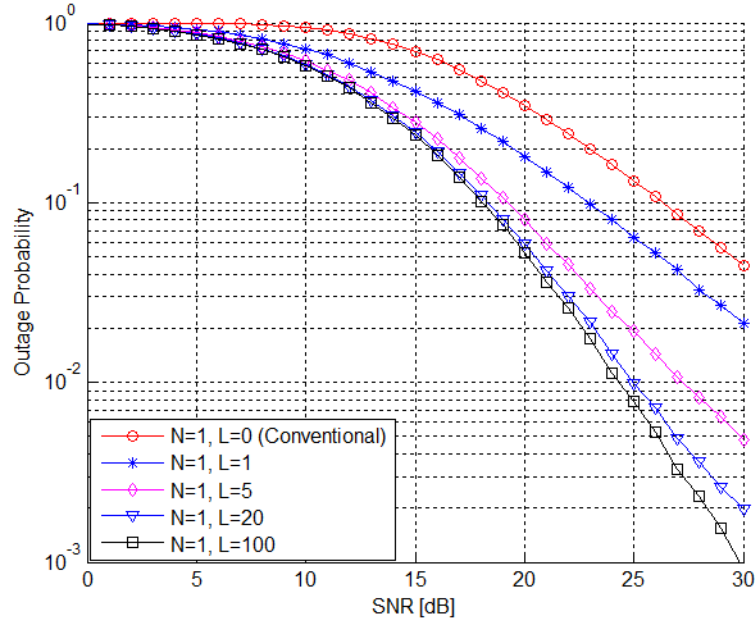


Figure 2.11: outage probability of the SN for both conventional unbuffered and buffer-aided relaying schemes with different values of maximum buffer size L $P_{S_p} = 8$ dB, $\gamma_{th} = 5$ dB, and $N = 1$.

It can be noticed from this figure that the SN outage behavior significantly enhanced when equipping the relay node with buffer of maximum size $L = 1$. This enhancement can be classified as a coding gain outage enhancement. Coding gain shifts the whole outage curve to the left by amount of around 3.5 dB. In the other

hand, any additional increment on maximum buffer size L is found to achieve a significant amount of diversity gain, especially at high SNR values. Diversity gain enhances the outage behavior of the SN as the peak transmission power increases. For example, a gain of around 10 dB is achieved to get the same performance as the conventional relaying scheme that operate on 30 dB, this gain is achieved when equipping the relay by a buffer of maximum size $L = 100$. However, it can be also noticed from the previous figure that diversity gain is not increasing linearly with the increasing of maximum buffer size, instead, it is large at low values of buffers and as the maximum buffer size increases, it becomes difficult to achieve a significant diversity gain.

Figure 2.12 shows the outage performance of the SN for both conventional and buffer-aided relaying scheme with a significantly high number of relays on the network $N = 4$. It can be noticed from this figure that the amount of enhancement added to the SN outage performance is less than that when the number of relays was one. This is due to the fact that adding more relays enhances the network diversity gain and any further enhancement using buffer-aided relaying will be smaller than the case with only single relay.

In the previous analyzes, the delay effect of buffering is not investigated or studied. However, information packet delay represents an important factor, especially in real-time applications at which high delay would significantly affect the quality of received data such as online gaming and video conferencing. Delay effect and analyses were investigated in the following two chapters with the

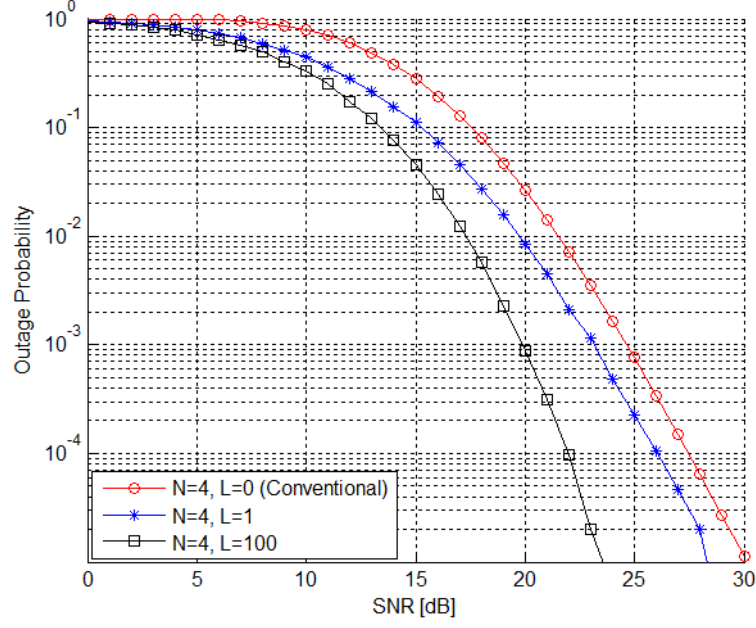


Figure 2.12: outage probability of the SN for both conventional unbuffered and buffer-aided relaying schemes with different values of maximum buffer size L $P_{S_p} = 8$ dB, $\gamma_{th} = 5$ dB, and $N = 4$.

proposition of an efficient delay-limited relaying protocols.

As can be noticed in the previous results, buffer-aided relaying represents an efficient and a smart enhancement for cooperative relaying schemes. Physical layer buffering can be used in SN to compensate for the interference threshold constraints of the PN. The advantages of buffer-aided relaying compared to conventional unbuffered relaying networks has motivated us toward the design and analysis of more complicated buffer-aided networks such as bidirectional schemes and MIMO-equipped buffer-aided cognitive networks.

2.5 Conclusions

In this chapter, the outage behavior of cognitive unbuffered and buffer-aided DF relay network was investigated. Closed-form expressions for outage probability of both the PN and SN were derived for conventional unbuffered cognitive radio network. The SN uses opportunistic relay selection strategy to select the best relay among a set of available relays. For the case of buffer-aided relaying, closed-form expressions for outage probability of the SN and PN were derived and analyzed. Also, the effect of maximum buffer size on outage behavior was also investigated. Additionally, the outage performance of conventional unbuffered relaying scheme was compared to that of buffer-aided relaying network. It was found that buffer-aided relaying added significant amount of coding gain to the SN system performance compared to the conventional unbuffered relaying. Furthermore, results showed that diversity gain is enhanced significantly as the maximum buffer size increases and it reaches a certain level at which further increment of buffer size does not add any significant gain.

CHAPTER 3

DESIGN AND ANALYSIS OF SINGLE-ANTENNA COGNITIVE DF RELAYING SCHEMES

3.1 Introduction

This chapter considers unidirectional/bidirectional relaying and transmission power allocation schemes in cognitive single-input single-output (SISO) buffer-aided DF relay networks. First, optimal transmission power allocation scheme that maximizes the PN and SN sum rate in unidirectional relaying networks that uses max-link relaying protocol is proposed and evaluated. Second, a low complexity bidirectional relaying protocol that maximizes the normalized sum of the sec-

ondary and primary rate networks and bounds the average delay per packet of the secondary network is proposed. Additionally, optimal/sub-optimal expressions for transmission power of both primary and secondary networks operating under all possible transmission modes are derived. The derived expressions allocate a maximum power budget per transmission mode among primary and secondary networks such that the SN interference on the PN does not exceed a certain threshold value. Furthermore, the average delay per information packet that is caused by buffering is investigated for the case of unidirectional relaying protocol and simulated for the proposed bidirectional relaying protocol. The impacts of different network parameters such as the buffer size and the interference threshold on the network performance are studied. Findings show that applying buffering significantly enhances the secondary network performance while slightly degrades the primary network performance.

The remainder of this chapter is organized as follows: Section 3.2 studies the design and analysis of unidirectional cognitive SISO buffer-aided DF relay networks. The design and analysis of bidirectional cognitive SISO buffer-aided DF relay networks are presented in Section 3.3. Average information packet delay of the SN is investigated in Section 3.4. Section 3.5 presents some analytical and simulation results of the considered systems. Finally, Section 3.6 concludes the chapter and provides the key results.

3.2 Unidirectional Transmission Relaying

In this section, unidirectional cognitive SISO buffer-aided DF relaying system is investigated. First, the system and channel models are introduced. Second, the max-link protocol is explained with some details. Then, optimal transmission power allocation scheme that allocates a maximum power budget among the PN and the SN sources is proposed and investigated.

3.2.1 System and Channel Models

This section considers a CR network that consists of a PN with one PU source (S_p), one PU destination (D_p), and a SN with one SU source (S), one SU destination (D), and N cognitive DF relays $[R_i]_{i=1}^N$, as shown in Figure 3.1. In this figure, the solid and dotted lines represent the desired and interfering signals at any possible transmission mode, respectively.

Each relay R_i is assumed to be equipped with a buffer B_i of maximum size L , where L is the maximum number of packets that can be stored in B_i before an overflow occurs. We denote the instantaneous number of stored information packets at the buffer of the i^{th} relay by $\Psi(R_i)$, where $0 \leq \Psi(R_i) \leq L$.

Without loss of generality, the direct $S - D$ link is not considered in this model as it is assumed to be suffering from sever fading and shadowing effects. In addition, PUs and SUs are assumed to access the spectrum simultaneously. In order to maintain a certain QoS level at the PU, the SN interference on the PN should not exceed I_{th} [33]. We define P_T as the maximum available power

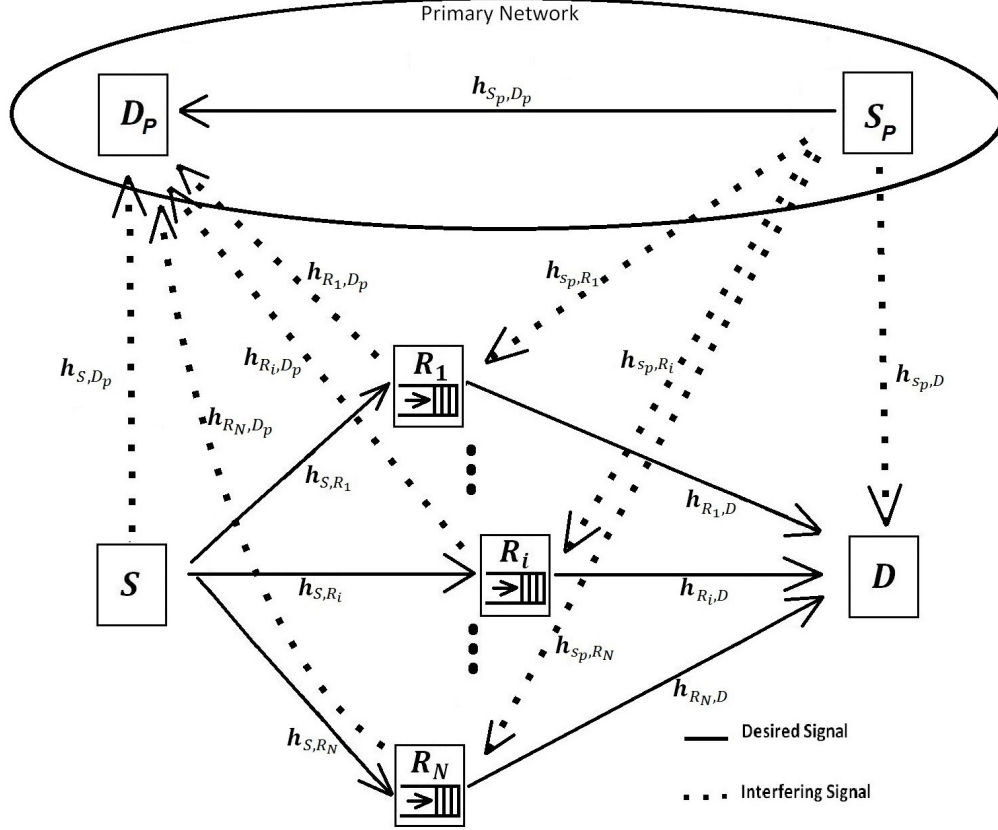


Figure 3.1: Cognitive radio network with buffer-aided DF relays (solid lines: desired signals, dotted lines: interfering signals).

budget assigned for the whole network at any arbitrary time slot and it is defined as $P_T = P_{S_p} + P_x$ or $P_T = P_{S_p} + P_{R_i}$ depending on whether the $S - R_i$ or $R_i - D$ link is selected for transmission, respectively.

All channel coefficients are assumed to be i.i.d. slowly varying Rayleigh fading random variables such that they remain unchanged during one time slot. We denote $h_{x,y}$ as the channel gain factor between terminals x and y . Each receiving terminal is assumed to experience an AWGN at its input with constant power spectral density N_o . Transmitted signals from S , R_i , and S_p are denoted by X_S , X_{R_i} , and X_{S_p} respectively. To avoid the need for heavy and fast back-haul links, a central processing unit that performs the relay selection and power allocation

operations is assumed to exist in the network with a full CSI knowledge.

3.2.2 Transmission Power Allocation

In this section, optimal transmission power allocation scheme for the system model in figure 3.1 is proposed. A maximum power budget P_T is optimally allocated between the PN and the SN transmitters per time slot such that their sum rate is optimized.

Using the above system model, the relaying is achieved using the max-link relay selection protocol described in Section 2.3.1. However, the index of the best relay that is related to the best link is found using the modified max-link protocol as follows

$$i^* = \arg \max_{R_i \in \mathcal{C}} \left\{ \bigcup_{R_i \in \mathcal{C}: \Psi(R_i) \neq L} \left\{ \frac{|h_{S_i R_i}|^2 P_T}{|h_{S_p, R_i}|^2 P_T + 2N_o} \right\}, \right. \\ \left. \bigcup_{R_i \in \mathcal{C}: \Psi(R_i) \neq 0} \left\{ \frac{|h_{R_i, D}|^2 P_T}{|h_{S_p, D}|^2 P_T + 2N_o} \right\} \right\}. \quad (3.1)$$

This modified relay selection scheme is identical to max-link relay selection with a difference that the interference caused by the PN at the SN is considered while, the link with the highest SINR is selected. It is important to mention that in order to reduce the complexity and processing delay of system operation, the relay selection is performed using equal power distribution strategy while the optimal transmission power allocation schemes are performed after selecting the best relay.

If at any arbitrary time slot t_1 , the $S - R_i$ link is selected for transmission, with i being the index of the best relay selected using the max-link relaying protocol,

the signal received by the i^{th} relay is given by

$$y_{R_i}^{(t_1)} = \underbrace{h_{S,R_i}^{(t_1)} X_S^{(t_1)}}_{\text{Desired Signal}} + \underbrace{h_{S_p,R_i}^{(t_1)} X_{S_p}^{(t_1)}}_{\text{Interfering Signal}} + \underbrace{n_{R_i}^{(t_1)}}_{\text{AWGN}}, \quad (3.2)$$

where $X_S^{(t_1)}$ and $X_{S_p}^{(t_1)}$ are the transmitted message signals from S and S_p at time instate t_1 , respectively, $n_{R_i}^{(t_1)}$ is the AWGN at the input of the i^{th} selected relay. In the same time instant t_1 , the PN source S_p is assumed to be transmitting a message signal to the PN destination D_p and hence, the signal received by D_p at t_1 is given by

$$y_{D_p}^{(t_1)} = \underbrace{h_{S_p,D_p}^{(t_1)} X_{S_p}^{(t_1)}}_{\text{Desired Signal}} + \underbrace{h_{S,D_p}^{(t_1)} X_S^{(t_1)}}_{\text{Interfering Signal}} + \underbrace{n_{D_p}^{(t_1)}}_{\text{AWGN}}. \quad (3.3)$$

If, after an arbitrary number of time slots $\tau = t_2 - t_1$, the $R_i - D$ link is selected for transmission with i is the index of the best relay selected using the max-link relaying protocol, the received signal at the D at time instant t_2 can be written as

$$y_D^{(t_2)} = \underbrace{h_{R_i,D}^{(t_2)} X_{R_i}^{(t_2)}}_{\text{Desired Signal}} + \underbrace{h_{S_p,R_i}^{(t_2)} X_{S_p}^{(t_2)}}_{\text{Interfering Signal}} + \underbrace{n_D^{(t_2)}}_{\text{AWGN}}, \quad (3.4)$$

where $X_{R_i}^{(t_2)}$ and $X_{S_p}^{(t_2)}$ are the transmitted message signals from R_i and S_p at time instance t_2 , respectively, $n_{R_i}^{(t_2)}$ is the AWGN at the input of the i^{th} selected relay. At the same time instant t_2 , the PN source S_p is assumed to be transmitting a message signal to the PN destination D_p and hence, the signal received by D_p at t_2 is given by

$$y_{D_p}^{(t_2)} = \underbrace{h_{S_p, D_p}^{(t_2)} X_{S_p}^{(t_2)}}_{\text{Desired Signal}} + \underbrace{h_{R_i, D_p}^{(t_2)} X_{R_i}^{(t_2)}}_{\text{Interfering Signal}} + \underbrace{n_{D_p}^{(t_2)}}_{\text{AWGN}}. \quad (3.5)$$

For the aim of math notation simplicity, the time scripts will be removed in future analysis. However, it is important to emphasize that the number of time slots required to achieve one complete e2e information packet transmission is not restricted to two time slots which means that a packet could be stored in the buffer for a certain number of time slots, that is $\psi(R_i) \leq \tau \leq \infty$. The normalized rate at $S - R_i$, $R_i - D$, and $S_p - D_p$ links are respectively given by

$$R_{S, R_i} = \log_2 \left(1 + \frac{|h_{S, R_i}|^2 P_S}{|h_{S_p, R_i}|^2 P_{S_p} + N_o} \right), \quad (3.6)$$

$$R_{R_i, D} = \log_2 \left(1 + \frac{|h_{R_i, D}|^2 P_{R_i}}{|h_{S_p, R_i}|^2 P_{S_p} + N_o} \right), \quad (3.7)$$

$$R_{S_p, D_p}^{(t_1)} = \log_2 \left(1 + \frac{|h_{S_p, D_p}|^2 P_{S_p}}{|h_{S, D_p}|^2 P_S + N_o} \right), \quad (3.8)$$

$$R_{S_p, D_p}^{(t_2)} = \log_2 \left(1 + \frac{|h_{S_p, D_p}|^2 P_{S_p}}{|h_{R_i, D_p}|^2 P_{R_i} + N_o} \right). \quad (3.9)$$

The problem in our hand is to allocate a maximum power budget between the PN and SN such that the normalized sum rate is maximized. The transmission power allocation problem when the $S - R_i$ link is selected can be written as

$$\begin{aligned} & \underset{P_{S_p}, P_S}{\text{maximize}} && R_{S_p, D_p}^{(t_1)} + R_{S, R_i} \\ & \text{subject to} && 0 \leq P_{S_p} + P_S \leq P_T, \\ & && |h_{S, D_p}|^2 P_S \leq I_{th}. \end{aligned} \quad (3.10)$$

On the other hand, the transmission power allocation problem when the $R_i - D$ link is selected can be written as

$$\begin{aligned}
& \underset{P_{S_p}, P_{R_i}}{\text{maximize}} && R_{S_p, D_p}^{(t_2)} + R_{R_i, D} \\
& \text{subject to} && 0 \leq P_{S_p} + P_S \leq P_T, \\
& && |h_{S, D_p}|^2 P_{R_i} \leq I_{th}.
\end{aligned} \tag{3.11}$$

To solve the optimization problem in (3.10), the Lagrangian multiplier method is used [12]. First, the PN transmission power is written as a function of the SN transmission power as $P_{s_p} = P_T - P_s$. Then, the optimization problem in (3.10) is rewritten as

$$\begin{aligned}
& \underset{P_S}{\text{maximize}} && R_{S_p, D_p}^{(t_1)} + R_{S, R_i} \\
& \text{subject to} && 0 \leq P_S \leq P_T, \\
& && |h_{S, D_p}|^2 P_S \leq I_{th},
\end{aligned} \tag{3.12}$$

where

$$R_{S_p, D_p}^{(t_1)} = \log_2 \left(1 + \frac{|h_{S_p, D_p}|^2 (P_T - P_S)}{|h_{S, D_p}|^2 P_S + N_o} \right), \tag{3.13}$$

$$R_{S, R_i} = \log_2 \left(1 + \frac{|h_{S, R_i}|^2 P_S}{|h_{S_p, R_i}|^2 (P_T - P_S) + N_o} \right). \tag{3.14}$$

The Lagrangian function related to problem (3.12) is given by

$$\mathcal{L}(P_S, \lambda_1, \lambda_2) = R_{S_p, D_p}^{(t_1)} + R_{S, R_i} - \lambda_1 (P_S - P_T) - \lambda_2 (|h_{S, D_p}|^2 P_S - I_{th}), \tag{3.15}$$

where λ_1 and λ_2 denote the Lagrangian multipliers related to the first and second constraints of (3.12), respectively. By differentiating (3.15) with respect to P_S and equating the result to zero, we end up with a quartic equation that is given by

$$(P_S)^4 + a(P_S)^3 + b(P_S)^2 + c(P_S) + d, \quad (3.16a)$$

where

$$a = \left[\frac{h_2 N_o + N_2 |h_{S,D_p}|^2}{h_1 h_2 |h_{S,D_p}|^2} + \frac{N_1 |h_{S,K}|^2}{h_1 |h_{S_p,K}|^2} \right], \quad (3.16b)$$

$$b = \left[\frac{N_o N_2}{h_2 |h_{S,D_p}|^2} - \frac{N_1 |h_{S,K}|^2 (h_2 N_o + N_2 |h_{S,D_p}|^2)}{\lambda h_1 h_2 |h_{S_p,K}|^2 |h_{S,D_p}|^2} - \frac{N_1 |h_{S,K}|^2}{\lambda h_2 |h_{S,D_p}|^2} - \frac{N_3}{\lambda h_1 |h_{S_p,K}|^2} \right], \quad (3.16c)$$

$$c = \left[\frac{(h_2 N_o + N_2 |h_{S,D_p}|^2) (|h_{S,K}|^2 N_1 - N_3 - \lambda N_1^2) - \lambda N_o N_1 N_2 |h_{S,K}|^2}{\lambda h_1 h_2 |h_{S_p,K}|^2 |h_{S,D_p}|^2} \right], \quad (3.16d)$$

$$d = \left[\frac{N_o N_2 (N_1 |h_{S,K}|^2 - \lambda N_1^2 - N_3)}{\lambda h_1 h_2 |h_{S_p,K}|^2 |h_{S,D_p}|^2} \right], \quad (3.16e)$$

where

$$\begin{aligned} h_1 &= |h_{S,K}|^2 - |h_{S_p,K}|^2 & \& \quad N_1 = |h_{S_p,K}|^2 P_T + N_o, \\ h_2 &= |h_{S,D_p}|^2 - |h_{S_p,D_p}|^2 & \& \quad N_2 = |h_{S_p,D_p}|^2 P_T + N_o, \\ N_3 &= |h_{S_p,D_p}|^2 (|h_{S,D_p}|^2 P_T + N_o) & \& \quad \lambda = \ln 2 (\lambda_1 |h_{S,D_p}|^2 + \lambda_2). \end{aligned} \quad (3.16f)$$

We propose to use the quartic formula to find the roots of (3.16a) as follows

$$P_J^* = \left[-\frac{b}{4a} \pm S \pm \frac{1}{2} \sqrt{-4S^2 - 2p + \frac{q}{s}} \right]^+, \quad (3.17a)$$

where

$$p = \frac{8ac - 3b^2}{8a^2} \quad \& \quad q = \frac{b^3 - 4abc + 8a^2d}{8a^3}, \quad (3.17b)$$

$$S = \frac{1}{2} \sqrt{-\frac{2}{3}p + \frac{1}{3}a \left(Q + \frac{\delta_o}{Q} \right)}, \quad (3.17c)$$

$$Q = \sqrt[3]{\frac{\delta_1 + \sqrt{\delta_1^2 - 4\delta_o^3}}{2}}, \quad (3.17d)$$

$$\delta_o = c^2 - 3bd + 12ae, \quad (3.17e)$$

$$\delta_1 = 3c^3 - 9bcd + 27b^2e + 27ad^2 - 72ace, \quad (3.17f)$$

where $[\zeta]^+ = \max(\zeta, 0)$, and a, b, c, d are the coefficients of the quartic equation in (3.16a). The value of PN optimal transmission power for those modes is then given by

$$P_{S_p}^* = P_T - P_S^*. \quad (3.18)$$

The values of the Lagrangian multipliers λ_1 and λ_2 are chosen such that they minimize the Lagrangian function $\mathcal{L}(\lambda_1, \lambda_2)$ given in (3.15). One efficient method to find λ_1 and λ_2 is called sub-gradient update method and it is given by [50]

$$\begin{aligned} \lambda_1^{(m+1)} &= \left[\lambda_1^{(m)} + \mu^{(m)} (P_S^* - P_T) \right]^+, \\ \lambda_2^{(m+1)} &= \left[\lambda_2^{(m)} + \mu^{(m)} (|h_{S,D_p}|^2 P_S - I_{th}) \right]^+, \end{aligned} \quad (3.19)$$

where m denotes the iteration index and $\mu^{(m)}$ is a sequence of scalar step sizes. It was found that due to the convexity of the target function, the sub-gradient method converges to the optimal values as long as $\mu^{(m)}$ is chosen to be sufficiently small [50].

3.3 Bidirectional Transmission Relaying

In this section, data transmission in bidirectional buffer-aided DF relay network is investigated. First, the system and channel models of the considered system are in-

troduced. Then, after formulating the problem of relay selection and transmission power allocation, a low complexity bidirectional transmission relaying protocol for the SN is proposed. Finally, theoretical analysis of the power allocation between the PN and the SN for each possible transmission mode is derived and analysed.

3.3.1 System and Channel Models

This section considers a CR network that consists of a PN with one PU source (S_p) and one PU destination (D_p), and a SN with a pair of SU transceiver nodes U_1 and U_2 , and N cognitive bidirectional half-duplex DF relays $[R_i]_{i=1}^N$, as shown in Figure 3.2. In this figure, the solid and dotted lines represent the desired and interfering signals in each possible transmission mode, respectively. Each relay is provided with two buffers denoted by $B_1(R_i)$ and $B_2(R_i)$ to store received information packets from U_1 and U_2 respectively. $B_m(R_i)$ has maximum size of L_m , where L_m is the maximum number of information packets received from terminal $U_m, m = 1, 2$ that can be stored before an overflow occurs. We denote the instantaneous number of stored information packets at the m^{th} buffer of the i^{th} relay by $\Psi_m(R_i)$, where $0 \leq \Psi_m(R_i) \leq L_m$.

Without loss of generality, the direct $U_1 - U_2$ link is not considered in this model as it is assumed to be suffering from sever fading and shadowing effects. In addition, PUs and SUs are assumed to access the spectrum simultaneously. In order to maintain a certain QoS level at the PU, the average received interference power due to SUs should not exceed a certain interference threshold denoted by

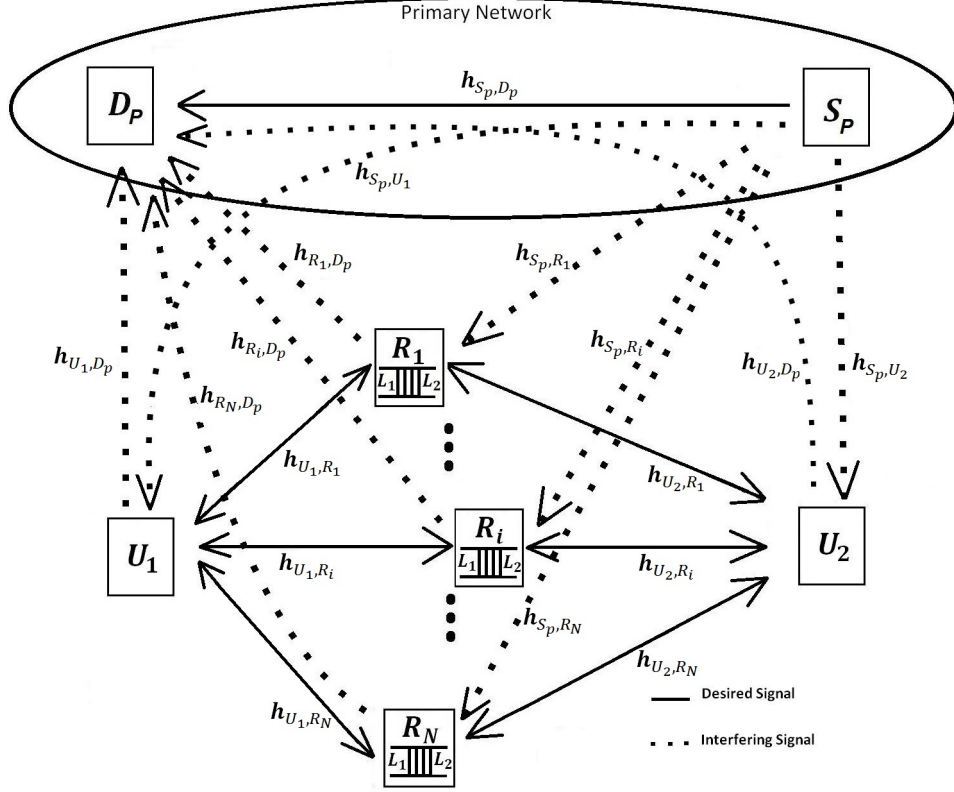


Figure 3.2: System model for cognitive radio network with buffer-aided DF half duplex bidirectional relays (solid lines: desired signal, dotted lines: interfering signal).

I_{th} [33]. We define P_T as the maximum available power budget assigned for the whole network at any arbitrary time slot and it is defined as $P_T = P_{S_p} + P_{U_m}$, where ($m = 1$ or 2) or $P_T = P_{S_p} + P_{R_i}$ if $U_m - R_i$ or $R_i - U_m$ link is selected, respectively.

All channel coefficients are assumed to be i.i.d. slowly varying Rayleigh fading RVs such that they remain unchanged during one time slot. We denote $h_{x,y}$ as the channel coefficient between terminals x and y . Channel gains of bidirectional links are assumed to be symmetric which means, at a certain time instant t , the channel coefficient in $U_m - R_i$ link is identical to that in the $R_i - U_m$ inverse

link¹. Each receiving terminal is assumed to experience an AWGN at its input with a constant variance N_o . Transmitted signals from U_1 , U_2 , R_i , and S_p are denoted by X_{U_1} , X_{U_2} , X_{R_i} , and X_{S_p} respectively. To avoid the need for heavy and fast back-haul links, a central processing unit that performs relay selection and power allocation operations is assumed to exist in the network with a full CSI acknowledgement.

3.3.2 Problem Formulation

In buffer-aided half-duplex bidirectional relaying scheme, there exists mainly five possible transmission modes occur in the SN at any arbitrary time slot denoted by $\mathcal{M}_i, i = 1, \dots, 5$ as shown in Figure 3.3. PN is assumed to be transmitting

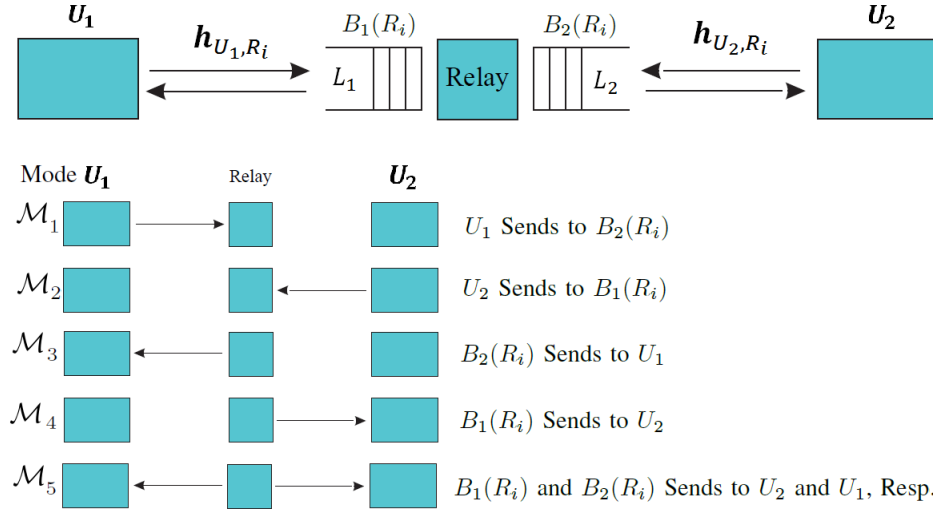


Figure 3.3: Possible bidirectional transmission modes of the secondary network.

information packets at every time slot during network operation. The received

¹Most of the previous works in the literature used the symmetric channel gain assumption to simplify the analysis without any effect on the final results and conclusions of the analysis [37].

signals at the i^{th} relay in modes \mathcal{M}_1 and \mathcal{M}_2 are, respectively given by

$$y_{R_i}^{(\mathcal{M}_1)} = \underbrace{h_{U_1,R_i}X_{U_1}}_{\text{Desired Signal}} + \underbrace{h_{S_p,R_i}X_{S_p}}_{\text{Interfering Signal}} + \underbrace{n_{R_i}}_{\text{AWGN}}, \quad (3.20)$$

$$y_{R_i}^{(\mathcal{M}_2)} = \underbrace{h_{U_2,R_i}X_{U_2}}_{\text{Desired Signal}} + \underbrace{h_{S_p,R_i}X_{S_p}}_{\text{Interfering Signal}} + \underbrace{n_{R_i}}_{\text{AWGN}}, \quad (3.21)$$

where X_{U_1} and X_{U_2} are the transmitted message signals from U_1 and U_2 with powers P_{U_1} and P_{U_2} , respectively, n_{R_i} is the AWGN at the input of R_i with power N_o . Information packet received from U_1 or U_2 is stored at buffer $B_1(R_i)$ or $B_2(R_i)$, respectively. At a certain time slot, when the selected relay is chosen to transmit to one or both user terminals U_1 and U_2 , the received signals at U_1 and U_2 are respectively given by

$$y_{U_1}^{(\mathcal{M}_3,\mathcal{M}_5)} = \underbrace{h_{U_1,R_i}X_{R_i}}_{\text{Desired Signal}} + \underbrace{h_{S_p,U_1}X_{S_p}}_{\text{Interfering Signal}} + \underbrace{n_{U_1}}_{\text{AWGN}}, \quad (3.22)$$

$$y_{U_2}^{(\mathcal{M}_4,\mathcal{M}_5)} = \underbrace{h_{U_2,R_i}X_{R_i}}_{\text{Desired Signal}} + \underbrace{h_{S_p,U_2}X_{S_p}}_{\text{Interfering Signal}} + \underbrace{n_{U_2}}_{\text{AWGN}}. \quad (3.23)$$

Mode \mathcal{M}_5 is called broadcasting mode since R_i combines two signals from $B_1(R_i)$ and $B_2(R_i)$ and broadcasts the resultant to U_1 and U_2 with transmission power P_{R_i} . Each terminal receiver is assumed to have some self-interference cancellation strategy. The received signal at D_p at any arbitrary time slot is given by

$$y_{D_p} = \underbrace{h_{S_p,D_p}X_{S_p}}_{\text{Desired Signal}} + \underbrace{h_{W,D_p}X_W}_{\text{Interfering Signal}} + \underbrace{n_{D_p}}_{\text{AWGN}}, \quad (3.24)$$

where W depends on the transmission mode of SN. The normalized rate at modes \mathcal{M}_1 to \mathcal{M}_5 are respectively given by

$$R_{U_1, R_i}^{(\mathcal{M}_1)} = \log_2 \left(1 + \frac{|h_{U_1, R_i}|^2 P_{U_1}}{|h_{S_p, R_i}|^2 P_{S_p} + N_o} \right), \quad (3.25)$$

$$R_{U_2, R_i}^{(\mathcal{M}_2)} = \log_2 \left(1 + \frac{|h_{U_2, R_i}|^2 P_{U_2}}{|h_{S_p, R_i}|^2 P_{S_p} + N_o} \right), \quad (3.26)$$

$$R_{R_i, U_1}^{(\mathcal{M}_3, \mathcal{M}_5)} = \log_2 \left(1 + \frac{|h_{U_1, R_i}|^2 P_{R_i}}{|h_{S_p, U_1}|^2 P_{S_p} + N_o} \right), \quad (3.27)$$

$$R_{R_i, U_2}^{(\mathcal{M}_4, \mathcal{M}_5)} = \log_2 \left(1 + \frac{|h_{U_2, R_i}|^2 P_{R_i}}{|h_{S_p, U_2}|^2 P_{S_p} + N_o} \right), \quad (3.28)$$

while the PN rate at any arbitrary time slot is given by

$$R_{S_p, D_p} = \log_2 \left(1 + \frac{|h_{S_p, D_p}|^2 P_{S_p}}{|h_{W, D_p}|^2 P_W + N_o} \right). \quad (3.29)$$

The problem in our hand is first to select the best relay and the corresponding transmission mode for the SN and then allocate a maximum power budget between PN and SN such that the normalized sum rate is maximized. In this work, the aim of the bidirectional transmission mode protocol is to maximize the normalized sum rate and bound the average packet delay of the SN by a predefined number of time slots μ . The transmission power optimization problem at modes \mathcal{M}_1 to

\mathcal{M}_4 is given by

$$\begin{aligned}
& \underset{P_{S_p}, P_J^{(\mathcal{M}_i)}}{\text{maximize}} && R_{S_p, D_p} + R_{J, K}^{(\mathcal{M}_i)} \\
& \text{subject to} && 0 \leq P_{S_p} + P_J^{(\mathcal{M}_i)} \leq P_T, \\
& && |h_{J, D_p}|^2 P_J^{(\mathcal{M}_i)} \leq I_{th}.
\end{aligned} \tag{3.30}$$

For mode \mathcal{M}_1 , $(J, K) \equiv (U_1, R_i)$, for mode \mathcal{M}_2 , $(J, K) \equiv (U_2, R_i)$, for mode \mathcal{M}_3 , $(J, K) \equiv (R_i, U_1)$, and for mode \mathcal{M}_4 , $(J, K) \equiv (R_i, U_2)$. For mode \mathcal{M}_5 , the optimization problem is given by

$$\begin{aligned}
& \underset{P_{S_p}, P_{R_i}^{(\mathcal{M}_5)}}{\text{maximize}} && R_{S_p, D_p} + R_{R_i, U_1}^{(\mathcal{M}_5)} + R_{R_i, U_2}^{(\mathcal{M}_5)} \\
& \text{subject to} && 0 \leq P_{S_p} + P_{R_i}^{(\mathcal{M}_5)} \leq P_T, \\
& && |h_{R_i, D_p}|^2 P_{R_i}^{(\mathcal{M}_5)} \leq I_{th}.
\end{aligned} \tag{3.31}$$

In the following two sections, we propose a low complexity bidirectional relaying protocol and some optimal/sub-optimal transmission power allocation schemes.

3.3.3 A New Bidirectional Relaying Protocol for Buffer-Aided DF Relay Network

In this section, a low complexity bidirectional relaying protocol that controls the two-way data flow between terminals U_1 and U_2 in the SN is introduced. The proposed protocol is not restricted by a predefined scheduling for data exchange, instead, it selects the best transmission mode from a set of five possible modes. Mode selection is achieved according to the instantaneous channel coefficients,

buffers states, and average information packet delay. Figure 4.5 shows a descriptive flowchart of the proposed bidirectional relaying protocol. From the flowchart,

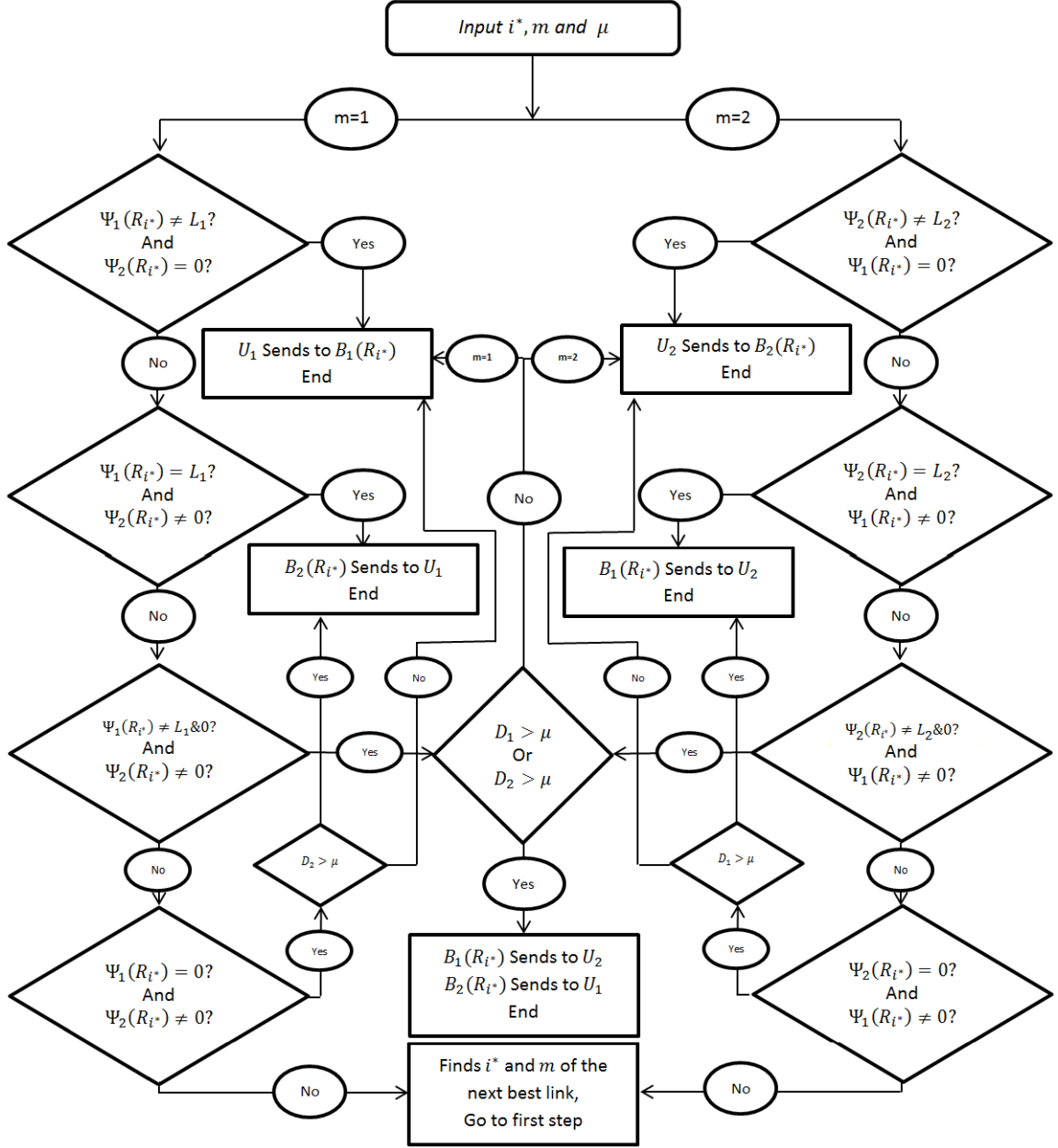


Figure 3.4: Flowchart for the proposed bidirectional relaying protocol.

D_1 and D_2 represent the number of time slots since the oldest information packet has been buffered at $B_1(R_i)$ and $B_2(R_i)$ of the selected relay, respectively.

The best relay R_{i^*} is proposed to be found using the following relay selection

scheme

$$R_i^* = \arg \max_{R_i} \{ \min \{ \gamma_{U_1, R_i}, \gamma_{R_i, U_1} \}, \min \{ \gamma_{U_2, R_i}, \gamma_{R_i, U_2} \} \},$$

where

$$\begin{aligned} \gamma_{U_1, R_i} &= \frac{|h_{U_1, R_i}|^2 P_{U_1}}{|h_{S_p, R_i}|^2 P_{S_p} + N_o}, \\ \gamma_{R_i, U_1} &= \frac{|h_{U_1, R_i}|^2 P_{R_i}}{|h_{S_p, U_1}|^2 P_{S_p} + N_o}, \\ \gamma_{U_2, R_i} &= \frac{|h_{U_2, R_i}|^2 P_{U_2}}{|h_{S_p, R_i}|^2 P_{S_p} + N_o}, \\ \gamma_{R_i, U_2} &= \frac{|h_{U_2, R_i}|^2 P_{R_i}}{|h_{S_p, U_2}|^2 P_{S_p} + N_o}. \end{aligned} \tag{3.32}$$

This modified relay selection scheme considers the interference caused by the PN at the SN at any possible transmission mode. It is important to mention that in order to reduce the complexity and processing delay of system operation, the relay selection is performed using equal power distribution strategy while the optimal transmission power allocation schemes are performed after selecting the best relay.

The delay of this is bounded by the fact that the transmission priority is higher for those packets that have been stored in buffers for a predefined number of time slots denoted by μ . This protocol does not require the derivation of complicated optimal mode selection problems. Instead, a set of conditions are examined and a transmission mode is selected accordingly.

3.3.4 Transmission Power Allocation Scheme

In this section, optimal and sub-optimal transmission power allocation schemes are proposed for each possible transmission mode.

Convex optimization theory is used in the derivation of optimal transmission power at modes \mathcal{M}_1 through \mathcal{M}_4 [51]. By substituting $P_{S_p} = P_T - P_J^{(\mathcal{M}_i)}$, changing the peak power condition in (4.31) to $P_J^{(\mathcal{M}_i)} \leq P_T$, and using the Lagrangian multiplier method, the Lagrangian function of the optimization problem given by (4.31) is defined by

$$\mathcal{L}\left(P_J^{(\mathcal{M}_i)}, \lambda_1, \lambda_2\right) = R_{S_p, D_p} + R_{J, K}^{(\mathcal{M}_i)} - \lambda_1 \left(P_J^{(\mathcal{M}_i)} - P_T\right) - \lambda_2 \left(|h_{J, D_p}|^2 P_J^{(\mathcal{M}_i)} - I_{th}\right), \quad (3.33)$$

where λ_1 and λ_2 are the Lagrangian multipliers related to the peak source transmission power and interference constraints, respectively, and (J, K) is as defined in (4.31). When deriving $\mathcal{L}\left(P_J^{(\mathcal{M}_i)}, \lambda_1, \lambda_2\right)$ with respect to $P_J^{(\mathcal{M}_i)}$ and equating the result to zero we end up with a quartic equation that can be written as

$$\left(P_J^{(\mathcal{M}_i)}\right)^4 + a\left(P_J^{(\mathcal{M}_i)}\right)^3 + b\left(P_J^{(\mathcal{M}_i)}\right)^2 + c\left(P_J^{(\mathcal{M}_i)}\right) + d, \quad (3.34a)$$

where

$$a = \left[\frac{h_2 N_o + N_2 |h_{J, D_p}|^2}{h_1 h_2 |h_{J, D_p}|^2} + \frac{N_1 |h_{J, K}|^2}{h_1 |h_{S_p, K}|^2} \right], \quad (3.34b)$$

$$b = \left[\frac{N_o N_2}{h_2 |h_{J, D_p}|^2} - \frac{N_1 |h_{J, K}|^2 (h_2 N_o + N_2 |h_{J, D_p}|^2)}{\lambda h_1 h_2 |h_{S_p, K}|^2 |h_{J, D_p}|^2} - \frac{N_1 |h_{J, K}|^2}{\lambda h_2 |h_{J, D_p}|^2} - \frac{N_3}{\lambda h_1 |h_{S_p, K}|^2} \right], \quad (3.34c)$$

$$c = \left[\frac{(h_2 N_o + N_2 |h_{J, D_p}|^2) (|h_{J, K}|^2 N_1 - N_3 - \lambda N_1^2) - \lambda N_o N_1 N_2 |h_{J, K}|^2}{\lambda h_1 h_2 |h_{S_p, K}|^2 |h_{J, D_p}|^2} \right], \quad (3.34d)$$

$$d = \left[\frac{N_o N_2 (N_1 |h_{J,K}|^2 - \lambda N_1^2 - N_3)}{\lambda h_1 h_2 |h_{S_p,K}|^2 |h_{J,D_p}|^2} \right], \quad (3.34e)$$

where

$$\begin{aligned} h_1 &= |h_{J,K}|^2 - |h_{S_p,K}|^2 & \& \quad N_1 &= |h_{S_p,K}|^2 P_T + N_o, \\ h_2 &= |h_{J,D_p}|^2 - |h_{S_p,D_p}|^2 & \& \quad N_2 &= |h_{S_p,D_p}|^2 P_T + N_o, \\ N_3 &= |h_{S_p,D_p}|^2 (|h_{J,D_p}|^2 P_T + N_o) & \& \quad \lambda &= \ln 2 (\lambda_1 |h_{J,D_p}|^2 + \lambda_2). \end{aligned} \quad (3.34f)$$

We propose to use the quartic formula to find the roots of (3.34a) as follows

$$(P_J^*)^{(\mathcal{M}_i)} = \left[-\frac{b}{4a} \pm S \pm \frac{1}{2} \sqrt{-4S^2 - 2p + \frac{q}{s}} \right]^+, \quad (3.35a)$$

where

$$p = \frac{8ac - 3b^2}{8a^2} \quad \& \quad q = \frac{b^3 - 4abc + 8a^2d}{8a^3}, \quad (3.35b)$$

$$S = \frac{1}{2} \sqrt{-\frac{2}{3}p + \frac{1}{3}a \left(Q + \frac{\delta_o}{Q} \right)}, \quad (3.35c)$$

$$Q = \sqrt[3]{\frac{\delta_1 + \sqrt{\delta_1^2 - 4\delta_o^3}}{2}}, \quad (3.35d)$$

$$\delta_o = c^2 - 3bd + 12ae, \quad (3.35e)$$

$$\delta_1 = 3c^3 - 9bcd + 27b^2e + 27ad^2 - 72ace, \quad (3.35f)$$

where $[\zeta]^+ = \max(\zeta, 0)$. The value of PN optimal transmission power for those modes is then given by

$$P_{S_p}^* = P_T - (P_J^*)^{(\mathcal{M}_i)}. \quad (3.36)$$

The value of Lagrangian multipliers λ_1 and λ_2 are chosen such that they maximize the Lagrangian function $\mathcal{L}(\lambda_1, \lambda_2)$ given by (4.16). One efficient method to

find λ_1 and λ_2 is called sub-gradient update method and it is given by [?]

$$\begin{aligned}\lambda_1^{(m+1)} &= \left[\lambda_1^{(m)} + \mu^{(m)} \left((P_J^*)^{(\mathcal{M}_i)} - P_T \right) \right]^+, \\ \lambda_2^{(m+1)} &= \left[\lambda_2^{(m)} + \mu^{(m)} \left(|h_{J,D_p}|^2 (P_J^*)^{(\mathcal{M}_i)} - I_{th} \right) \right]^+, \end{aligned} \quad (3.37)$$

where m is the iteration index and $\mu^{(m)}$ is a sequence of scalar step sizes. It was found that due to the convexity of the target function, the sub-gradient method converges to the optimal values as long as $\mu^{(m)}$ is chosen to be sufficiently small [?].

For mode \mathcal{M}_5 , at which R_i broadcasts a combined signal to U_1 and U_2 , using convex optimization problem ends up with a 6th order equation which requires the use of some numerical algorithms to find its roots. However, in this section, we propose to use a genetic algorithm to solve the optimization problem in (4.32). The proposed algorithm is shown at Algorithm 4.1.

In this algorithm, $h_{x,y}$ represents all possible channel coefficients of PN and SN during a certain time slot. Due to the convexity of the target optimized function, the proposed algorithm is said to converge to a global maxima point which is equivalent to the optimal solution, especially for high n_p .

3.3.5 Complexity Analysis

Solving the problems in (4.32) via exhaustive search (ES) numerical programming algorithm requires $\sum_{i=0}^q \binom{2N}{i} (q-1)^i = O(q^{2N})$ operations to find the optimal solution [?], while the proposed GA requires at most $(n_p \times \text{Iterations})$ operations,

Algorithm 3.1 Genetic Algorithm that finds P_{S_p} and $(P_{R_i}^{\mathcal{M}_5})$ that maximize $R_{sum} = R_{S_p, D_p}^{\mathcal{M}_5} + R_{R_i, U_1}^{(\mathcal{M}_5)} + R_{R_i, U_2}^{(\mathcal{M}_5)}$

```

1: Input:  $h_{x,y}, P_T, N_o, n_p, n_{parents}, Iterations$ 
2: Generate  $n_p$  initial population of  $\mathbf{P}^j = \left[ P_{S_p}^j (P_{R_i}^{\mathcal{M}_5})^j \right]$ , with  $0 \leq P_{S_p}^j + (P_{R_i}^{\mathcal{M}_5})^j \leq P_T, \forall j = 1, \dots, n_p$ 
3: Count=1
4:  $R_{max} = 0$ 
5: while (Count  $\leq$  Iterations, or stopping condition hold), do
6:   for  $m = 1 : n_p$  do
7:     if Constrains in (4.32) are satisfied then
8:        $R_m = R_{S_p, D_p}(P_{S_p}^j, (P_{R_i}^{\mathcal{M}_5})^j) + R_{R_i, U_1}^{(\mathcal{M}_5)}(P_{S_p}^j, (P_{R_i}^{\mathcal{M}_5})^j) + R_{R_i, U_2}^{(\mathcal{M}_5)}(P_{S_p}^j, (P_{R_i}^{\mathcal{M}_5})^j)$ 
9:     else
10:       $R_m = 0$ 
11:    end if
12:  end for
13:   $R_{max} = \max_m R_m$ 
14:  Take the best  $n_{parents}$  vectors of  $\mathbf{P}^j$  and use crossover and mutation go generate  $(n_p - n_{parents})$  next population vectors.
15: end while

```

where q is the quantization levels of the ES algorithm. Table 4.1 shows the central processing unit time duration in seconds of the ES and GA algorithms for 100 channel realizations.

Table 3.1: Central processing unit times (seconds) for 100 channel realization

Optimal	GA
$\{N, q\} = \{4, 64\}$	
$2 \times 10^7, \infty$	1120, 0.45
$\{N, q\} = \{4, 128\}$	
$3 \times 10^{14}, \infty$	1120, 0.45
$\{N, q\} = \{4, 256\}$	
$8 \times 10^{28}, \infty$	1120, 0.45

3.4 Effect of Delay in Buffer-Aided DF Relaying

In this section, the effect of physical layer buffering on the average packet delay is studied for both unidirectional and bidirectional relaying schemes. Additionally, the effect of buffer size on the average packet delay is investigated as well.

In the DF max-link scheme with multiple relays, data is not transmitted from source (relay) only if the corresponding $S-R$ ($R-D$) link is selected. Accordingly, at the terminal destination, packets received in a random order and recombined by reading their index number. Additionally, the delay introduced to each packet is different from the other packets due to the random nature of different links. The problem of packet delay is considered as the main problem of buffer-aided relaying scheme [36].

Packet delay takes place either at user terminal or at relay node. As an example, consider Figure 3.5 In this figure, a source S has three packets S_1 ,

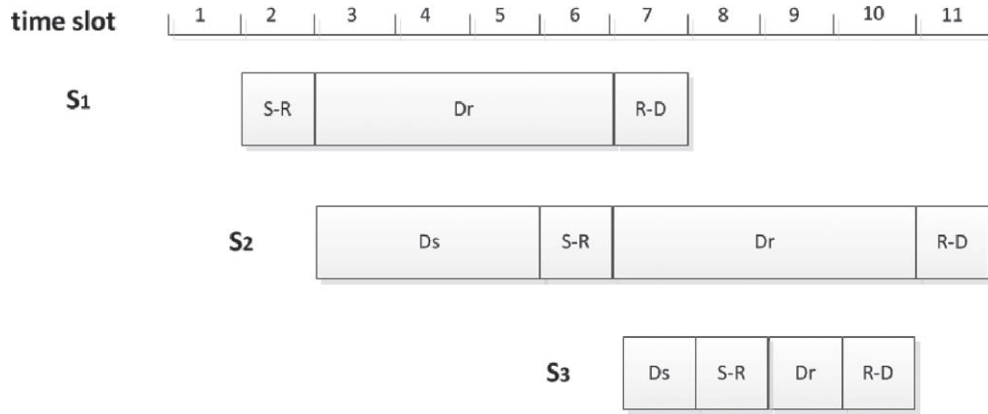


Figure 3.5: Illustrative example of different packet delay in the DF max-link scheme.

S_2 , and S_3 to be transmitted to the destination D through N DF relay nodes. Each packet has its own transmission time that is illustrated by horizontal bars.

The delay in time slots of the source and the relay are indicated respectively by D_s and D_r . As an example, at time slot 2, the packet S_1 is transmitted from the source to a certain relay node. After that, the relays are selected to transmits other packets to the destination. After waiting for three time slots (slots $3 \rightarrow 5$), the packet S_2 is chosen to be transmitted to a certain relay. After S_2 arrives at the relay at slot 6, it waits for another four time slots (slots $7 \rightarrow 10$) before it is eventually transmitted to the destination at slot 11. Thus, the delays for S_2 at the source and relay nodes are 3 and 4, respectively. Packet S_3 is chosen for transmission at time slot 8 after waiting only for one time slot at the source and at the relay it waits only for one time slot and then transmitted to the destination at time slot 10. We can also notice from this example that the packets received at the destination out of order in the form $[S_1 S_3 S_2]$. Despite the fact that different packets suffers from different delays, it's important to mention that the system throughput is not sacrificed since there is always a packet transmitted at every time slot. Average packet delay is usually defined as the average number of time slots required for a packet to be transmitted from the source into the destination. If we neglect the propagation delay, the packet delay will be as the number of time slots a packet is held at a certain buffer of a certain node, either a source or a relay. For this queuing system, we can use the Littles formula to define the average packet delay at a certain node as [52]

$$E[T] = \frac{E[\psi(R)]}{A} \text{ (time slot)}, \quad (3.38)$$

where $E[\psi(R)]$ is the average buffer length defined by $E[\psi(R)] = \lim_{t \rightarrow \infty} \sum_{t=1}^{\infty} \frac{\psi(R_t)}{t}$, where t is the number of time slots, and A is the arrival rate at the destination or the so called throughput. The average packet delay at both the source and relay nodes is derived in the following sections.

3.4.1 Average Packet Delay at the Source

For a system with a single source, N DF relays, and a single destination, the average throughput of the transmitting source is defined as [34]

$$R = \frac{1}{2}(\text{packet/time slot}). \quad (3.39)$$

This result is due to the fact that with single source, the average throughput at the source node is the same for the overall system. The queuing length at the source will depend on how fast the data leaves the source node. This in term is directly related to the probability of selecting the $S-R$ link. To avoid losing data packets permanently, the probability of selecting the $S-R$ link must be equal to the probability of selecting the $R-D$ link, which means

$$P_{S-R} = P_{R-D} = \frac{1}{2}. \quad (3.40)$$

By merging (3.39) and (3.40), we conclude that the average packet delay for the source is given by

$$D_s = \frac{\frac{1}{2}}{\frac{1}{2}} = 1 \text{ time slot}. \quad (3.41)$$

3.4.2 Average Packet Delay at the Relay

As the probabilities of selecting any of the relays are the same, the average packet delays at any of the relays are also the same. Hence, the average throughput at any relay is given by

$$R_i = \frac{1}{2N}. \quad (3.42)$$

The number 2 appeared in (3.42) due to the fact that the i^{th} selected relay is approximately transmitting for half of its operating time and receiving for the other half. This is exactly true when the operating time of the relay goes to infinity.

For N relay nodes each with maximum buffer size of L , the total number of possible buffer states is given by

$$M = (L + 1)^N. \quad (3.43)$$

The average buffer or queue length is defined as [34]

$$E[\psi(R)] = \sum_{l=1}^M \pi_l \psi_r^{(s_l)}, \quad (3.44)$$

where π_l is the steady state probability of being at S_l state, and $\psi_r^{(s_l)}$ is the average number of packets per buffer at S_l state. A closed-form expression for the steady state probability of unidirectional buffer-aided DF relaying system was derived in

2.3.3. The average packet delay at the relay node is then defined by

$$D_r = 2N \sum_{l=1}^M \pi_l \psi_r^{(s_l)} \text{ time slot.} \quad (3.45)$$

The over all packet delay of the complete end-to-end packet transmission is given by

$$D = D_s + D_r = 1 + 2N \sum_{l=1}^M \pi_l \psi_r^{(s_l)} \text{ time slot.} \quad (3.46)$$

3.5 Simulation Results

In this section of the thesis work, some simulation and analytical results of the discussed topics are presented and investigated. Simulations were performed based on a set of assumptions that simplify the simulation process and guarantee a fair comparisons between the different schemes. The first assumption is that all relays are provided with buffers of equal maximum size, that is $L_i = L, \forall i = 1, 2, \dots, N$ for the case of unidirectional, and $L_1 = L_2$ for all relays in the case of bidirectional relaying. Another assumption is that each receiving node experiences an AWGN with a constant variance N_o at each time slot. All simulation results were obtained using 1,000,000 Monte-Carlo runs.

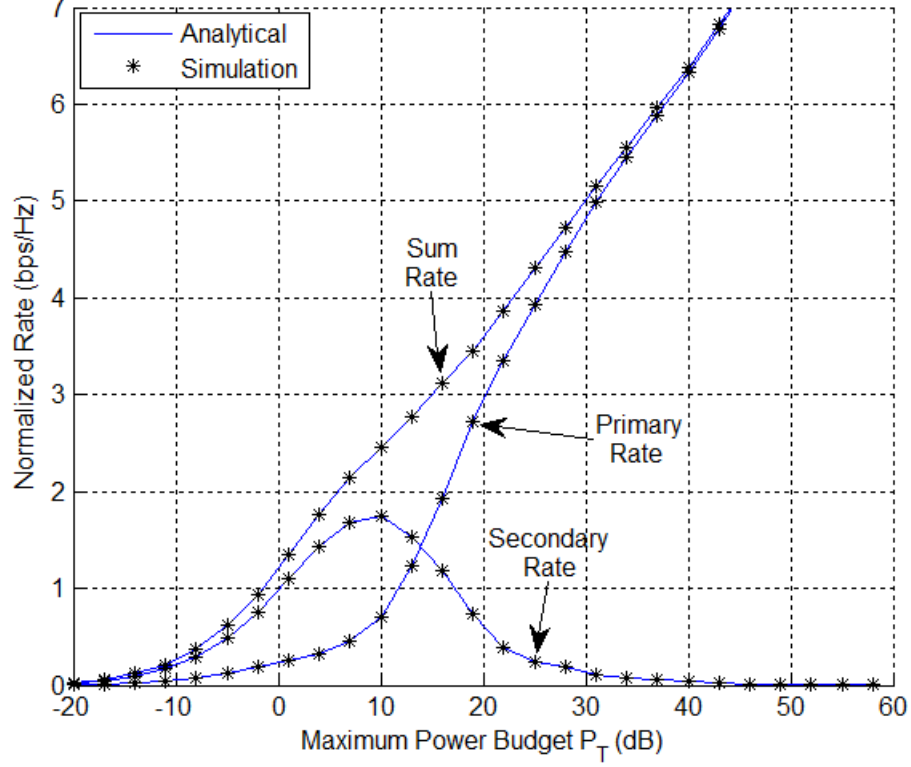


Figure 3.6: Simulation and analytical results of the achievable normalized PN, SN and sum rates with $N = 4$, $L = 50$, and $I_{th} = 10$ dB.

3.5.1 Unidirectional Transmission

This section presents analytical and simulation results of the unidirectional relaying schemes. Figure 3.6 shows the simulation results along with the analytically derived expression results of the achievable normalized PN, SN and sum rates. It can be seen from this figure that for peak transmission power P_T values that is less than the assigned interference threshold value $I_{th} = 10$ dB, the SN normalized rate is larger to that of the PN. This is due to the fact that the SU transmission power is not bounded by I_{th} , beside the fact that the SN has achieved higher spacial diversity gain due to the use of cooperative relay nodes. For values of P_T that are higher than I_{th} , the SU rate begins to decay until it reaches 0 bps/Hz.

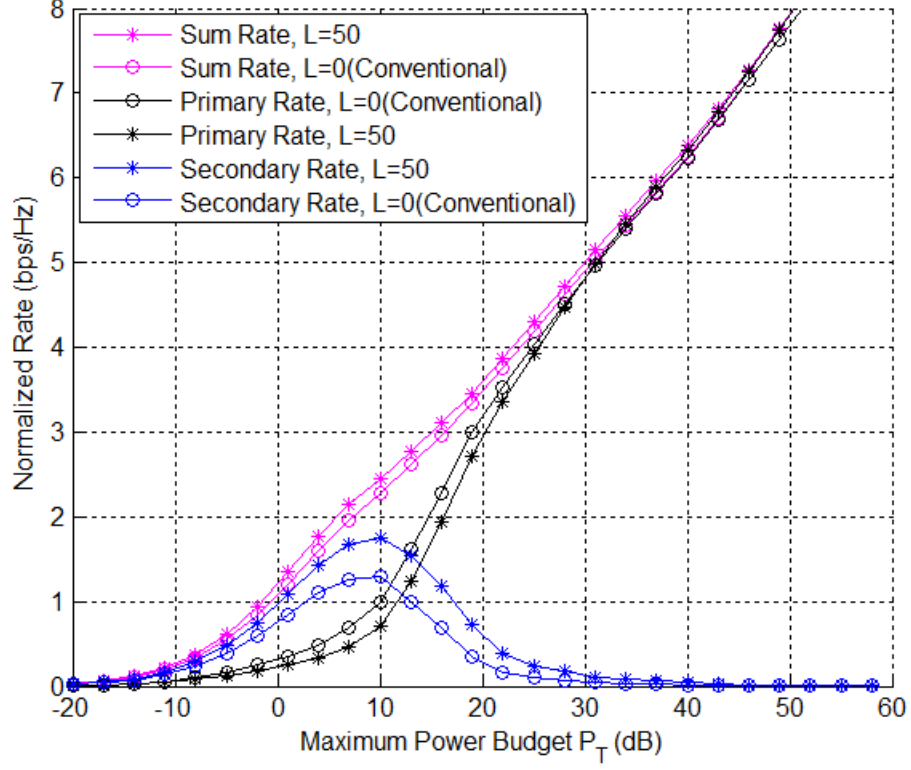


Figure 3.7: Achievable normalized rate of the PN, SN and their sum rate for both conventional and buffer-aided ($L = 20$) relaying schemes with $N = 4$ and $I_{th} = 10$ dB.

This is due to the fact that, most of the power budget is pumped to the PN due to the interference restriction on the SN transmission power, consequently, the interference caused by the PN on SN increases and hence, decreasing the SN rate.

To study the effect of physical layer buffering relaying networks compared to conventional relaying, Figure 3.7 shows the achievable normalized rate of the PN, SN and their sum for both conventional and buffer-aided relaying schemes. It can be seen from this figure that equipping the SN relays with buffers of maximum size of $L = 50$ enhances the SN rate at most by an amount of 0.5 bps/Hz at $P_T = 10$ dB. On the other hand, buffering in the SN relays degrades the performance of the PN slightly. This is due to the fact that buffering guarantees better channel

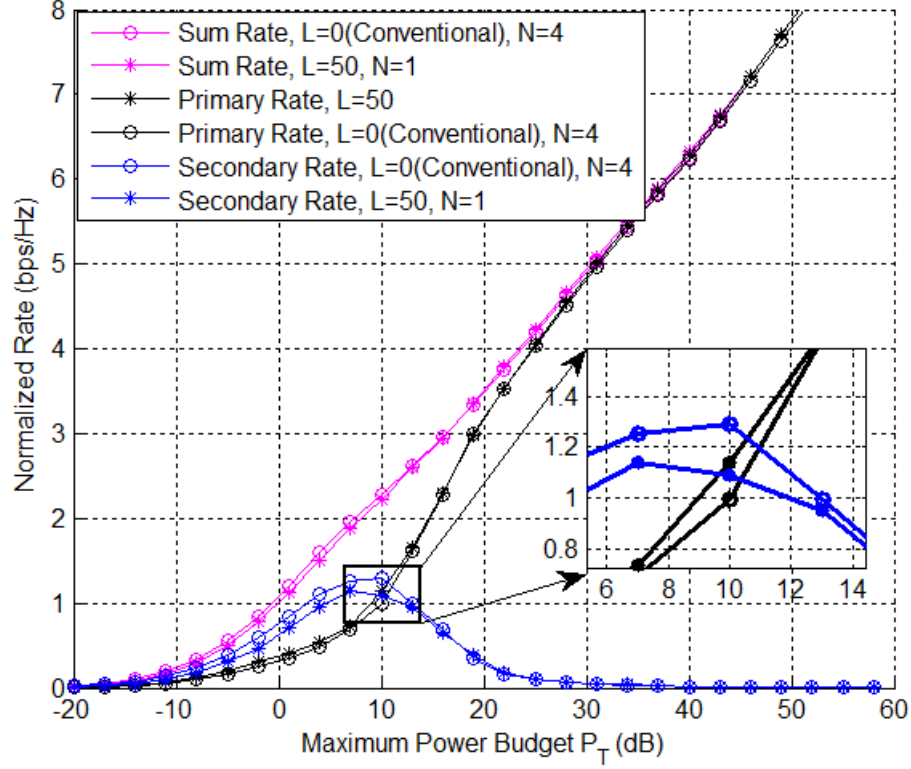


Figure 3.8: Achievable normalized rate of the PN, SN and their sum rate with $I_{th} = 10$ dB for conventional and buffer-aided relaying using different number of relays and buffer sizes.

gains for SN links and since the power allocation follows the water-filling strategy, more power is pumped in these links which enhances the SN performance at the expense of degrading the PN performance. However, the overall effect of buffering that occurs in the sum rate shows that a better rate is achieved using buffer-aided relaying at the SN compared to the conventional relaying. Additionally, it can be seen that physical layer buffering could represent an excellent alternative for multiple relays scenario. Figure (3.8) shows a comparison of the conventional relaying system with four relays available for transmission with that of buffer-aided relaying network with only one available relay.

Also, it can be seen from this figure that a single relay that is equipped

with buffers could achieve a performance level that is close to four relays without buffers. However, buffering introduces a serious delay and to overcome this problem they should contain some delay control methodology.

3.5.2 Bidirectional Transmission

In this section, we provide numerical simulation results of the proposed bidirectional relaying protocol and validate the derived expressions of transmission power allocation schemes. We also study the effect of different network parameters in the overall system performance.

To evaluate the proposed bidirectional relaying protocol, it is practical to compare the normalized rates per user of the proposed bidirectional relaying protocol with that of the unidirectional normalized rates. The unidirectional relaying is achieved using max-link relay selection scheme as in the previous section with a similar simulation parameters. Such a comparison metric is valid due to the fact that the unidirectional max-link relaying scheme represents a lower bound for normalized rate for any other bidirectional relaying scheme. This is due to the fact that, in unidirectional buffer-aided relaying it takes an average of two time slots to achieve a complete e2e packet transmission. In the other hand, for any bidirectional buffer-aided relaying protocol, it takes an average of one and half time slot to achieve a complete e2e packet transmission.

Figure 3.9 shows the achievable normalized PN, SN, and sum rates per user versus maximum power budget for both unidirectional and bidirectional relaying

schemes. It can be seen from this figure that the proposed bidirectional relaying

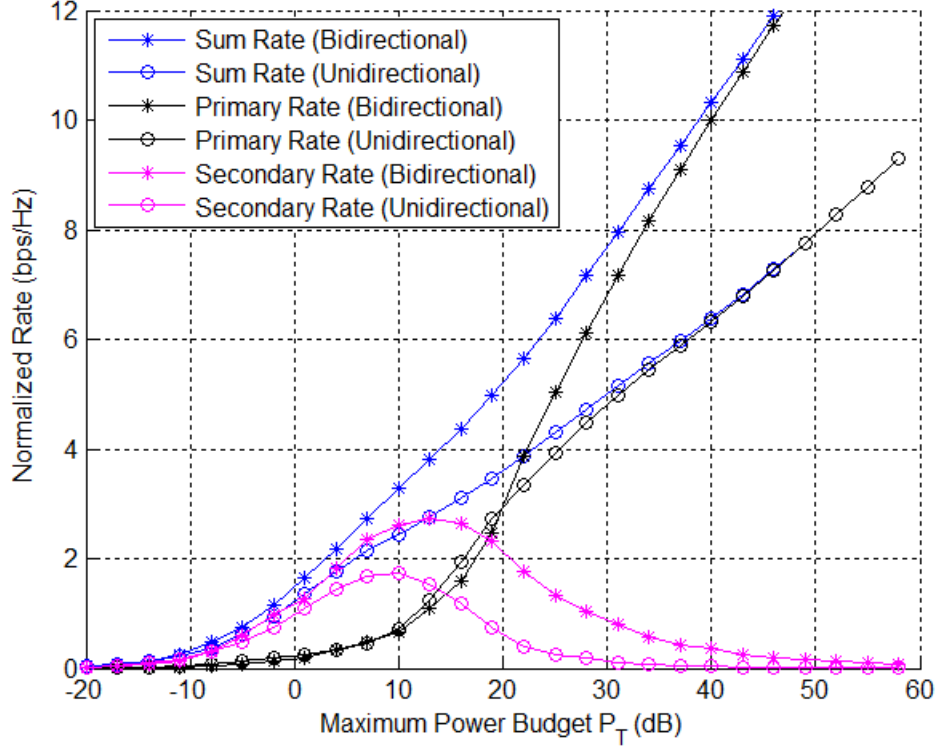


Figure 3.9: Achievable normalized PN, SN, and sum rates per user versus maximum power budget for both unidirectional and bidirectional relaying schemes with $I_{th} = 10$ dB, $L = L_1 = L_2 = 50$, $\mu = 200$, and $N = 4$.

protocol achieves normalized rates that are significantly higher than that of the unidirectional case. Additionally, it is clear that the delay is bounded in the proposed bidirectional relaying protocol while for unidirectional max-link protocol, the delay ranges between one and infinity. The superiority of bidirectional relaying rates compared to those of unidirectional relaying is due to the fact that the unidirectional relaying takes an average of two time slot to achieve one complete e2e transmission, while for bidirectional relaying, only 1.5 time slot is required to achieve a complete e2e transmission.

To evaluate the performance of the proposed GA scheme, Figure 3.10 shows the

achievable normalized PN, SN, and sum rates per user versus maximum power budget P_T of the optimal and the proposed scenarios. We mean by optimal

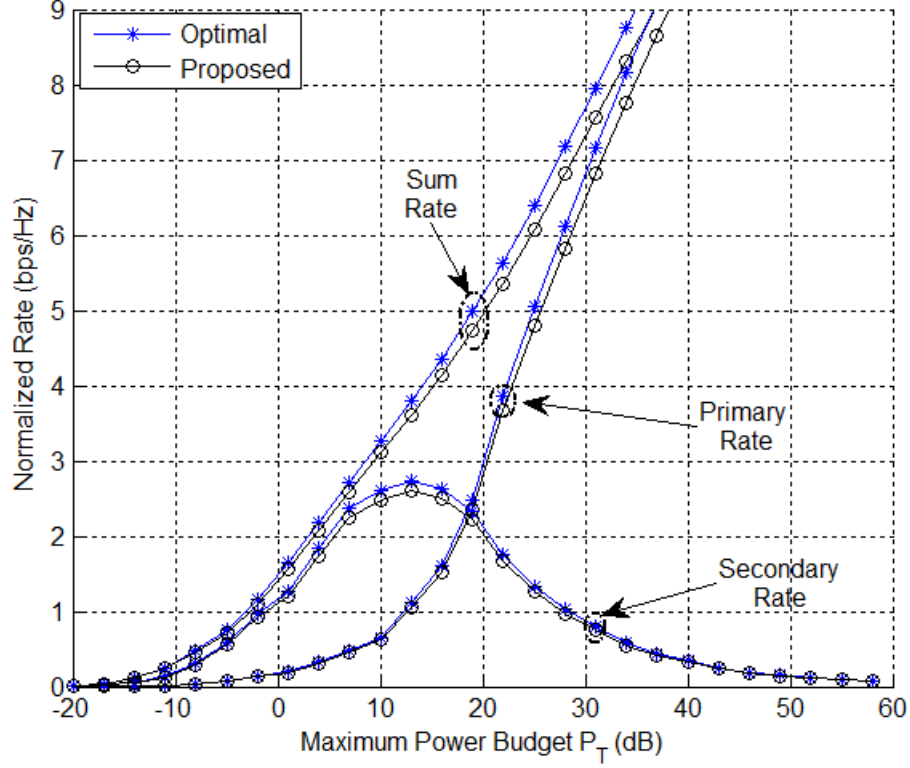


Figure 3.10: Achievable normalized PN, SN, and sum rates per user versus maximum power budget P_T for both optimal and proposed schemes with $I_{th} = 10$ dB, $L = 50$, $\mu = 200$, and $N = 4$.

solution that for the broadcast mode \mathcal{M}_5 , the sum rate is optimized using an exhaustive search rather than a GA. It can be seen that at $P_T = 7$ dB, there is only a 0.25 bps/Hz degradation in the performance of the proposed scheme compared to the optimal one. Additionally, it is obvious that the SN rate starts to decay to zero after passing I_{th} value in order to maintain the PN interference threshold constraint.

Figure 3.11 shows the achievable normalized rate for the PN, SN and their sum rates versus different maximum buffer sizes. It can be seen from this figure

that a rate increment of around 0.7 bps/Hz is achieved in the SN rate at $P_T = 10$.

Additionally, it can be seen from that the physical layer buffering on the SN

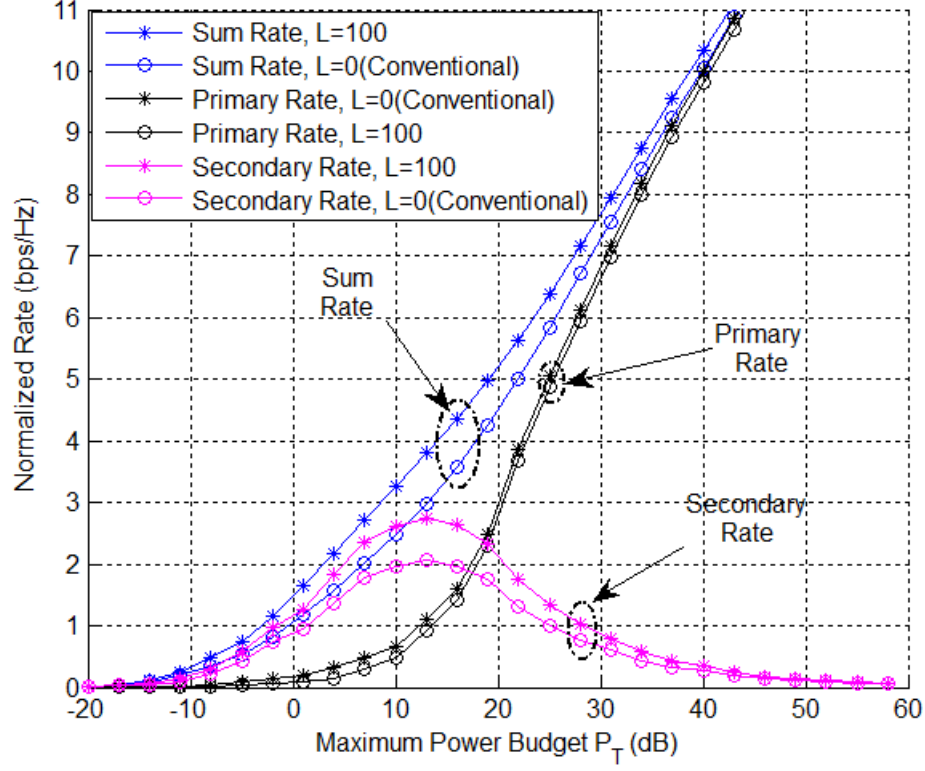


Figure 3.11: Achievable PN, SN, and sum rates per user versus maximum power budget P_T for conventional and buffer-aided relaying with $I_{th} = 10$ dB, $\mu = 200$, and $N = 4$.

relay nodes decreases the normalized rate of the PN. This is due to the fact that the buffering guarantees a better channel gains for SN links and since the power allocation follows a water-filling strategy, more power is pumped in these links which enhances the SN performance on the expense of PN performance.

Finally, Figure 3.12 shows the achievable PN, SN, and sum rates per user versus maximum allowable delay μ , where μ is the maximum number of time slots the oldest buffered information packet can be stored. It can be seen from this figure that a better rate is achieved as μ increases with a rate floor appears after

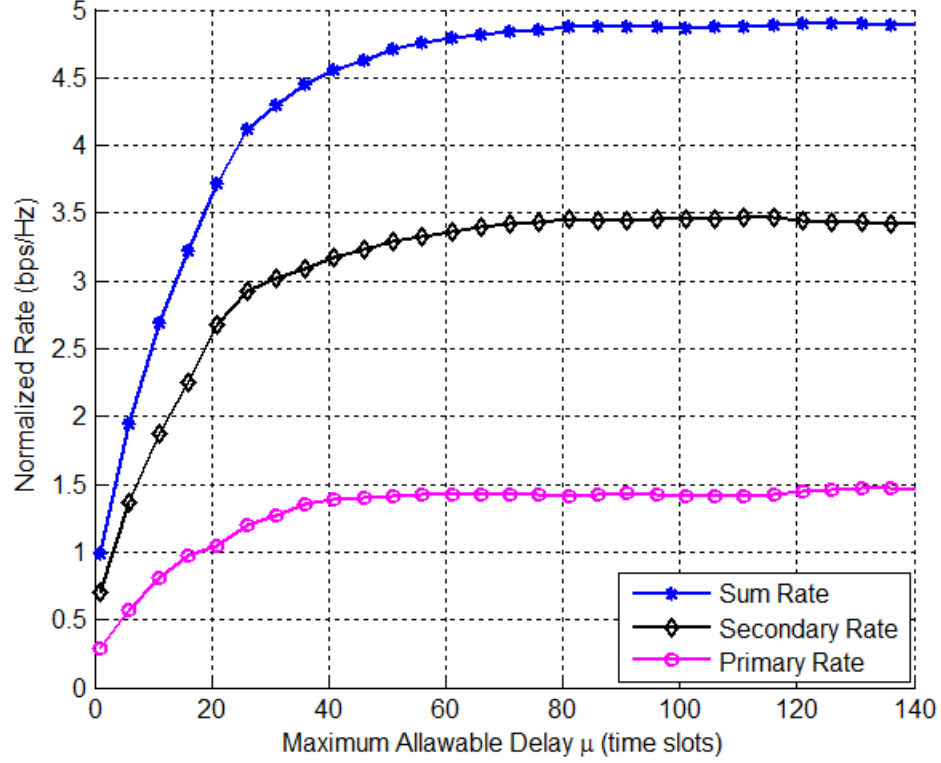


Figure 3.12: Achievable PN, SN, and sum rates per user versus maximum allowable delay μ with $P_T = 10$ dB, $I_{th} = 10$ dB, $L = 50$, and $N = 4$.

$\mu = 40$ (time slots). The rate floor occurs since for high values of μ , the probability that a packet will be stored for longer time slots that μ goes to zero and hence further increase in μ will not affect the rate any more. However, increasing μ means that some information packets will be delayed for a considerably long time which is not efficient for real-time communication systems.

3.5.3 Delay Effect in Buffer-Aided Relaying

This section presents the simulation results of average package delay for both unidirectional and bidirectional relaying schemes as a function of different network parameters.

Figure 3.13, shows the delay measured by number of time slots required to achieve a complete packet transmission between two users as a function of buffer size for both unidirectional and bidirectional relaying. It can be seen that our proposed bidirectional relaying protocol outperforms the unidirectional max-link relaying protocol for the two cases $N = 1$ and $N = 4$. This is due to the fact that in the max-link relaying protocol, the only factor that controls the mode selection process is the channel quality, while in our proposed protocol, the state of buffers and average waiting time at the buffer have been considered in the mode selection process. That means that packet delay is restricted and in case reaches a specific value, the best channel condition may be sacrificed and select the link related to a considerably high load buffer rather than the link with maximum gain.

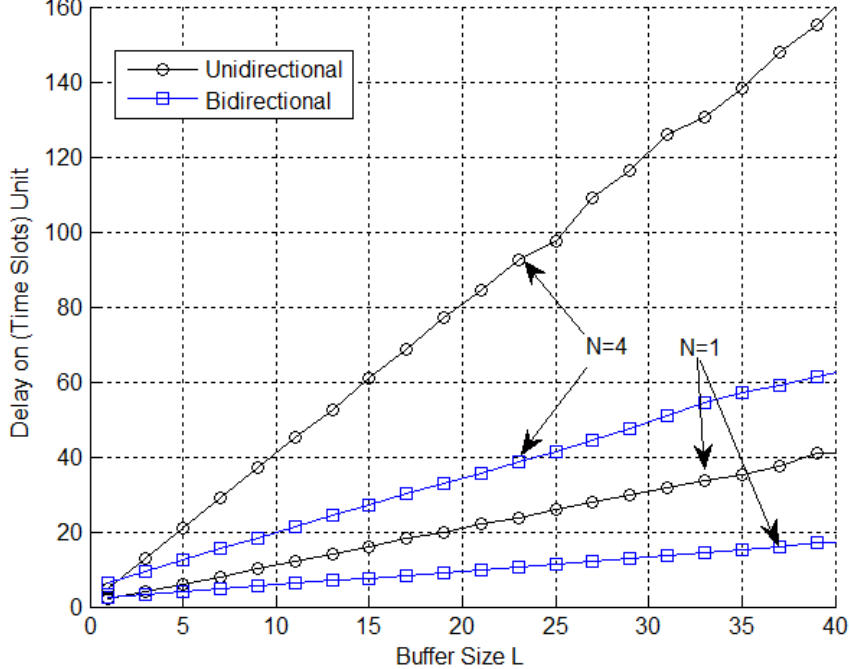


Figure 3.13: Packet average delay versus buffer size for bidirectional relaying with $L_1 = L_2 = L$, and unidirectional relaying with two different number of relays, $N = 1$ and $N = 4$.

Finally, Figure 3.14 shows the average packet delay as a function of number of available relays within the network. For a buffer size of one, we can see that the max-link protocol slightly outperforms our bidirectional relaying protocol, however, for $L = 10$, a considerably high delay of the max-link protocol compared to our proposed bidirectional relaying protocol.

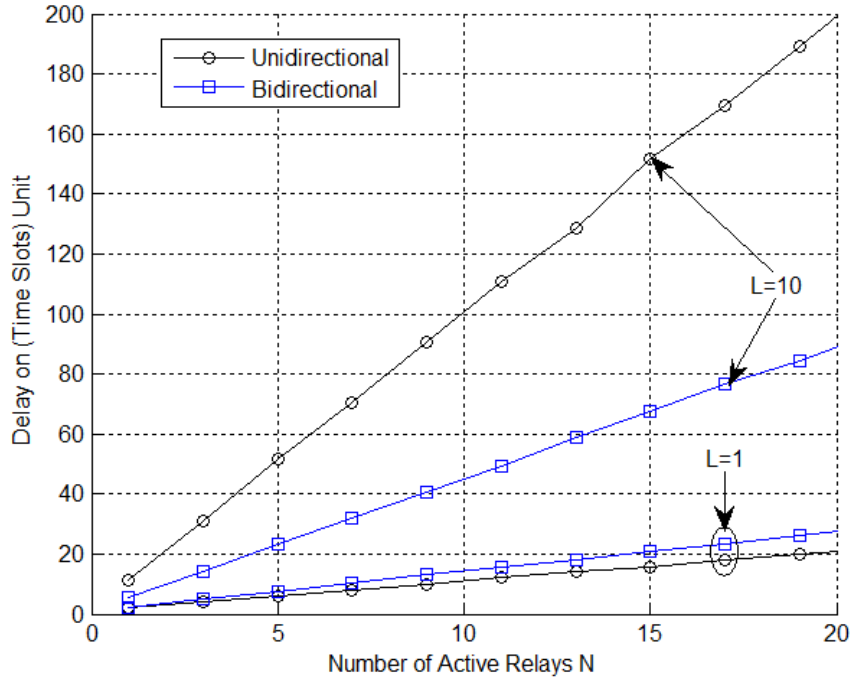


Figure 3.14: Packet average delay versus the number of relays for both bidirectional relaying with $(L_1 = L_2 = L)$, and unidirectional relaying with two different buffer sizes, $L = 1, L = 10$.

3.6 Conclusions

In this chapter, an optimal transmission power scheme for unidirectional buffer-aided DF relay network was proposed and evaluated. Additionally, a low complexity protocol which efficiently achieves bidirectional relaying and utilizes the

freedom acquired by physical layer buffering was proposed. The presented protocol controls the information packet delay of SN buffered data. Optimal transmission power expressions which allocate a maximum power budget P_T among PN and SN and maximize the normalized sum rate were provided. It was found that applying buffering at SN relays enhances the SN performance significantly, while degrading the PN performance slightly. Additionally, for a higher delay bound, the sum rate was shown to be enhanced with the cost of increasing the information packet delay in the SN.

CHAPTER 4

DESIGN AND ANALYSIS OF MULTIPLE-ANTENNA SCHEMES

4.1 Introduction

In this chapter, we consider DF buffer-aided relay selection and transmission power allocation for underlay CR network that is equipped with MIMO antenna scheme. We propose a low complexity MIMO-based relay selection scheme that maximizes the single-hop normalized rate of the SN. Also, we propose a sub-optimal allocation scheme of antenna transmission power that maximizes the overall normalized sum rate of primary and secondary cognitive networks. We first derive optimal expressions for antenna transmission power of both primary and SNs. The derived expressions are then used in an iterative algorithm to produce a near-optimum

solution. The analysis is applied to the cases of unidirectional and bidirectional relaying as well. Simulation results are provided to evaluate the performance of the proposed MIMO-based relay selection and antenna power allocation schemes and compare their performance with that of optimal schemes. Impacts of several system parameters including buffer maximum size, interference threshold, and number of antennas on network performance are also investigated. Results reveal that the proposed sub-optimal relay selection and transmission power allocation schemes introduce a satisfactory performance with much lower complexity compared to optimal relay selection and power allocation schemes. Findings also show that using buffer-aided relays significantly enhances the secondary network while slightly decreases the PN performance.

The remaining of this chapter is divided as follows: Section 4.2 studies the design and analysis of unidirectional cognitive MIMO buffer-aided DF relay networks. The design and analysis of bidirectional cognitive MIMO buffer-aided DF relay networks are studied in Section 4.3. Section 4.4 presents and investigates simulation results. Finally, Section 4.5 concludes the chapter and discusses the analytical and simulation results.

4.2 Unidirectional Relaying

In this section, DF buffer-aided relay selection and transmission power allocation for unidirectional underlay CR network that is equipped with MIMO antenna scheme is proposed and analysed.

4.2.1 System Model

In this section, we consider a CR network that consists of a PN with one PU source (S_p) and one PU destination (D_p), and a SN with one SU source (S), one SU destination (D), and N cognitive DF relays $[R_i]_{i=1}^N$. Each relay is assumed to be equipped with a buffer of maximum size L , where L is the number of data packets that can be stored in the buffer before an overflow occurs. The nodes S_p , D_p , S , D and the i^{th} selected relay are assumed to be equipped with M_{S_p} , M_{D_p} , M_S , M_D , and M_{R_i} antennas, respectively. A MIMO scheme is used to achieve multiplexing gain using SVD method. We denote the instantaneous number of stored decoded information packets in the i^{th} relay buffer by $\Psi(R_i)$, where $0 \leq \Psi(R_i) \leq L$. Figure 4.1 shows the considered system model in this work. In this figure, solid lines represent the desired signals at any possible transmission, while dotted lines represent the interfering signals at any possible transmission. Without loss of generality, the direct $S - D$ link is not considered in this model as it is assumed to be suffering from sever fading and shadowing effects. In addition, PUs and SUs are assumed to access the spectrum simultaneously. In order to maintain a certain QoS level to the PU, the average received interference power due to SUs should not exceed a certain interference threshold denoted by I_{th} [46]. At a certain time slot t_1 , if the $S - R$ link is selected, the source transmits its signals $\mathbf{X}_S = [X_s^1, X_s^2, \dots, X_s^{M_s}]^T$ with a power vector given by $\mathbf{P}_S = [p_s^1, p_s^2, \dots, p_s^{M_s}]^T$ where $[.]^T = Transpose[.]$. On the other hand, if the $R - D$ link is selected, the i^{th} best relay transmits its stored information packet that is given by $\mathbf{X}_{R_i} = [X_{R_i}^1, X_{R_i}^2, \dots, X_{R_i}^{M_{R_i}}]^T$ with a power

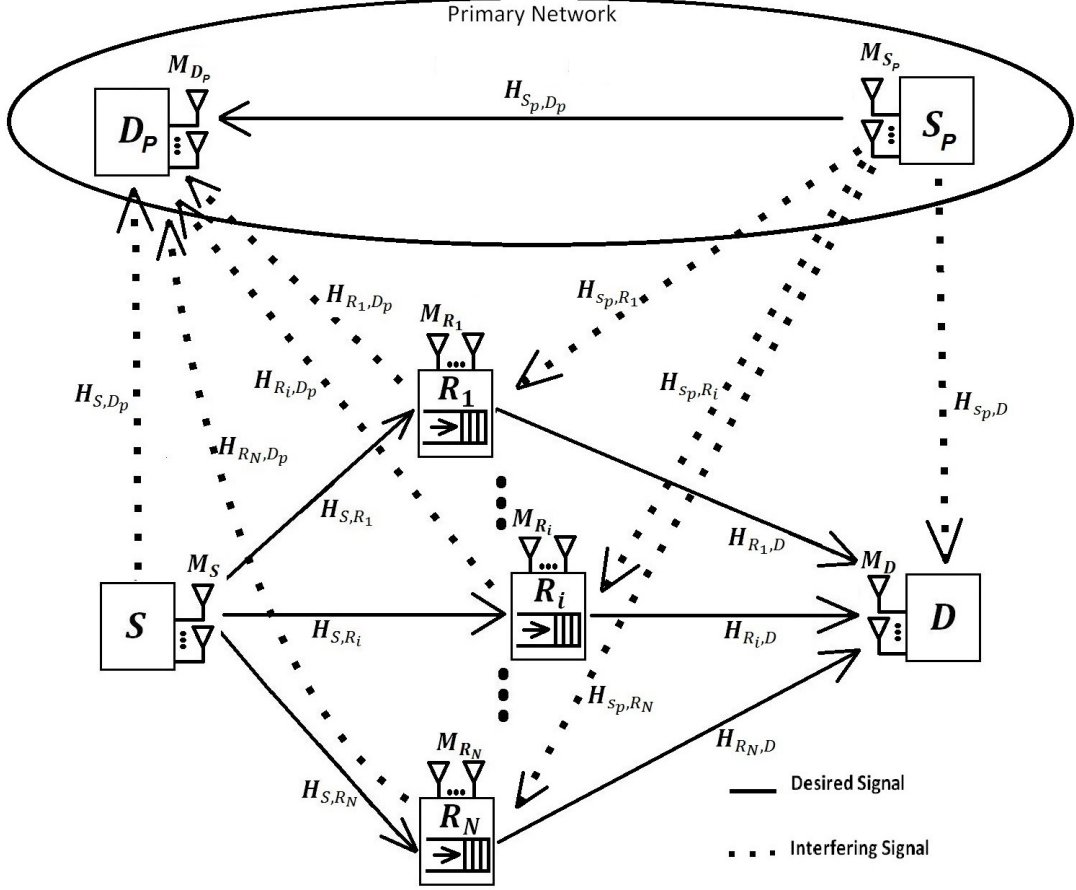


Figure 4.1: Cognitive radio network with MIMO buffer-aided DF relays (solid lines: desired signals at any possible transmission, dotted lines: interfering signals at any possible transmission).

vector given by $\mathbf{P}_{R_i} = [p_{R_i}^1, p_{R_i}^2, \dots, p_{R_i}^{M_{R_i}}]^T$. PN is assumed to be transmitting at every time slot t during network operation. The transmitted information packet in the $S_p - D_p$ link is given by $\mathbf{X}_{S_p} = [X_{s_p}^1, X_{s_p}^2, \dots, X_{s_p}^{M_{s_p}}]^T$ with a power vector given by $\mathbf{P}_{S_p} = [p_{s_p}^1, p_{s_p}^2, \dots, p_{s_p}^{M_{s_p}}]^T$. We define P_T , as the maximum available power budget assigned for the whole network at any arbitrary time slot and it is given by $P_T = p_s^1 + \dots + p_s^{M_s} + p_{s_p}^1 + \dots + p_{s_p}^{M_{s_p}}$ or $P_T = p_{R_i}^1 + \dots + p_{R_i}^{M_{R_i}} + p_{s_p}^1 + \dots + p_{s_p}^{M_{s_p}}$ if the $S - R_i$ or $R_i - D$ link is selected for transmission, respectively. Also, we define $\mathbf{H}_{S, R_i} \in \mathbb{C}^{M_{R_i} \times M_S}$, $\mathbf{H}_{S, D_p} \in \mathbb{C}^{M_{D_p} \times M_S}$, $\mathbf{H}_{R_i, D} \in \mathbb{C}^{M_D \times M_{R_i}}$, $\mathbf{H}_{R_i, D_p} \in \mathbb{C}^{M_{D_p} \times M_{R_i}}$,

$\mathbf{H}_{S_p, D_p} \in \mathbb{C}^{M_{D_p} \times M_{S_p}}$, $\mathbf{H}_{S_p, R_i} \in \mathbb{C}^{M_{R_i} \times M_{S_p}}$, and $\mathbf{H}_{S_p, D} \in \mathbb{C}^{M_D \times M_{S_p}}$ as the complex channel gain matrices between S and R_i , S and D_p , R_i and D , R_i and D_p , S_p and D_p , S_p and R_i , and S_p and D , respectively. We assume that all channel coefficients are independent and identically distributed (i.i.d.) slowly varying Rayleigh fading random variables such that they remain unchanged during one time slot. To avoid the need for heavy and fast back-haul links, a central processing unit that performs relay selection and power allocation operations is assumed to exist in the network with a full knowledge CSI.

4.2.2 Problem Formulation

If an information packet is transmitted from the source to the i^{th} selected relay at time instant t_1 , the received signal vector at the i^{th} selected relay is given by

$$\mathbf{Y}_{R_i} = \underbrace{\mathbf{H}_{S, R_i} \mathbf{X}_S}_{\text{Desired Signal}} + \underbrace{\mathbf{H}_{S_p, R_i} \mathbf{X}_{S_p}}_{\text{Interfering Signal}} + \underbrace{\mathbf{n}_{R_i}}_{\text{AWGN}}, \quad (4.1)$$

where \mathbf{n}_{R_i} is the AWGN vector at the input of the relay receiving antennas given by $\mathbf{n}_{R_i} = [n_{R_i}^1, n_{R_i}^2, \dots, n_{R_i}^{M_{R_i}}]$.

When the $R_i - D$ link is selected at t_2 after an arbitrary number of time slots $\tau = t_2 - t_1$ that lies in the period $\Psi(R_i) \leq \tau < \infty$, the i^{th} relay takes the oldest stored information packet, modulates it, and transmits it to destination. The

received signal vector at the D at time slot t_2 is given by

$$\mathbf{Y}_D = \underbrace{\mathbf{H}_{R_i,D}\mathbf{X}_{R_i}}_{\text{Desired Signal}} + \underbrace{\mathbf{H}_{S_p,D}\mathbf{X}_{S_p}}_{\text{Interfering Signal}} + \underbrace{\mathbf{n}_D}_{\text{AWGN}}. \quad (4.2)$$

At any arbitrary time slot t , the received signal at D_p from S_p is given by

$$\mathbf{Y}_{D_p} = \underbrace{\mathbf{H}_{S_p,D_p}\mathbf{X}_{S_p}}_{\text{Desired Signal}} + \underbrace{\mathbf{H}_{y,D}\mathbf{X}_y}_{\text{Interfering Signal}} + \underbrace{\mathbf{n}_{D_p}}_{\text{AWGN}}, \quad (4.3)$$

where $y = S$ or $y = R_i$ depending on whether $S - R_i$ or $R_i - D$ is selected for transmission, respectively.

To fully utilize the existence of MIMO scheme within the network, we use SVD method which advantage of the fact that a MIMO channel \mathbf{H} can be decomposed to a number of $\mathcal{R}_{\mathbf{H}}$ parallel independent channels, where $\mathcal{R}_{\mathbf{H}}$ is the rank of the channel \mathbf{H} . By multiplexing independent data to these independent channels, we get an $\mathcal{R}_{\mathbf{H}}$ -fold increase in data rate compared to that with a single antenna system [3].

In general MIMO channel normalized rate at the $S - R_i$ link can be written as [3]

$$R_{S,R_i} = \log_2 \det [\mathbf{I}_{M_{R_i}} + \mathbf{H}_{S,R_i}\mathbf{R}_{SS}\mathbf{H}_{S,R_i}^T\mathbf{C}_{z_1z_1}^{-1}], \quad (4.4)$$

where $\mathbf{P}_S = \text{diag}(\mathbf{R}_{SS})$, $\mathbf{I} \in \mathbb{C}^{M_{R_i} \times M_{R_i}}$ is the identity matrix, and $\mathbf{C}_{z_1z_1} \in \mathbb{C}^{M_{R_i} \times M_{S_p}}$ where $\mathbf{C}_{z_1z_1}$ is the covariance matrix of the interfering signal.

In general, the covariance matrix $\mathbf{C}_{z_1 z_1}$ is given by

$$\mathbf{C}_{z_1 z_1} = \mathbb{E} \left[(\mathbf{H}_{S_p, R_i} \mathbf{X}_{S_p} + \mathbf{n}_{R_i}) (\mathbf{H}_{S_p, R_i} \mathbf{X}_{S_p} + \mathbf{n}_{R_i})^H \right], \quad (4.5)$$

where $(\cdot)^H$ is the Hermitian transpose operation. Since \mathbf{H}_{S_p, R_i} and \mathbf{n}_{R_i} are assumed to be uncorrelated, the covariance matrix is simplified to be

$$\mathbf{C}_{z_1 z_1} = \mathbb{E} \left[(\mathbf{H}_{S_p, R_i} \mathbf{X}_{S_p}) (\mathbf{H}_{S_p, R_i} \mathbf{X}_{S_p})^T \right] + \mathbb{E} [\mathbf{n}_{R_i} \mathbf{n}_{R_i}^T]. \quad (4.6)$$

Under the i.i.d. assumption of all MIMO channel matrices, AWGN noises and the assumption that all MIMO channel gains are constants during one time slot duration, the covariance matrix is simplified to be equals to

$$\begin{bmatrix} \sum_{j=1}^{M_{S_p}} |h_{S_p, R_i}^{1,j}|^2 p_{s_p}^j + N_o & 0 & \dots & 0 \\ 0 & \sum_{j=1}^{M_{S_p}} |h_{S_p, R_i}^{2,j}|^2 p_{s_p}^j + N_o & \dots & 0 \\ \dots & \dots & \dots & \dots \\ 0 & 0 & \dots & \sum_{j=1}^{M_{S_p}} |h_{S_p, R_i}^{M_{R_i}, j}|^2 p_{s_p}^j + N_o \end{bmatrix} \quad (4.7)$$

From matrix theory, the SVD of the $S - R_i$ channel matrix \mathbf{H}_{S, R_i} can be obtained as follows

$$\mathbf{H}_{S, R_i} = \mathbf{U} \mathbf{\Sigma} \mathbf{V}^T, \quad (4.8)$$

where $\mathbf{U} \in \mathbb{C}^{M_{R_i} \times M_{R_i}}$, $\mathbf{\Sigma} \in \mathbb{C}^{M_{R_i} \times M_S}$, and $\mathbf{V}^T \in \mathbb{C}^{M_S \times M_S}$ are unitary matrices such that for a unitary matrix \mathbf{U} , we have $\mathbf{U} \mathbf{U}^T = \mathbf{I}$. The matrices \mathbf{V} and \mathbf{U} are used for precoding and decoding at the source transmitting and relay receiving

antennas, respectively. Σ is a diagonal matrix of singular values $[\sigma_i]_{i=1}^{j=M_1}$, where $M_1 = \min(M_S, M_{R_i})$ and $\sigma_j^2 = \lambda_j$, where λ_j is the j^{th} eigen value of \mathbf{H}_{S,R_i} . If the best relay is selected to receive data from source, SVD takes place on both transmitting and receiving antennas of the source and the i^{th} selected relay. Substituting the precoding and decoding matrices in (4.24) and simplifying yields

$$R_{S,R_i} = \sum_{u=1}^{M_1} \log_2 \left(1 + \frac{\sigma_u^2 p_s^u}{\sum_{j=1}^{M_{S_p}} |h_{S_p,R_i}^{u,j}|^2 p_{s_p}^j + N_o} \right). \quad (4.9)$$

In a similar procedure, the normalized rate at the $R_i - D$ and $S_p - D_p$ links can be respectively written as

$$\begin{aligned} R_{R_i,D} &= \sum_{v=1}^{M_2} \log_2 \left(1 + \frac{\sigma_v^2 p_{R_i}^v}{\sum_{j=1}^{M_{S_p}} |h_{S_p,D}^{v,j}|^2 p_{s_p}^j + N_o} \right), \\ R_{S_p,D_p} &= \sum_{l=1}^{M_3} \log_2 \left(1 + \frac{\sigma_l^2 p_{s_p}^l}{\sum_{j=1}^{M_y} |h_{y,D_p}^{l,j}|^2 p_y^j + N_o} \right), \end{aligned} \quad (4.10)$$

where $M_2 = \min(M_{R_i}, M_D)$, $M_3 = \min(M_{S_p}, M_{D_p})$, and $y = S$ or $y = R_i$ if $S - R_i$ or $R_i - D$ link is selected for transmission, respectively.

The problem in our hands is first to select the i^{th} best relay for reception or transmission and then efficiently allocate a maximum power budget P_T among all primary and secondary transmitting antennas at a certain time slot to maximize the normalized sum rate of the network. The optimization problem involved when

the $S - R_i$ link is selected can be formulated as follows

$$\begin{aligned}
& \underset{\mathbf{P}_S, \mathbf{P}_{S_p}}{\text{maximize}} && R_{S,R_i} + R_{S_p,D_p} \\
& \text{subject to} && 0 \leq \sum_{u=1}^{M_S} p_s^u + \sum_{v=1}^{M_{s_p}} p_{s_p}^v \leq P_T, \\
& && \sum_{v=1}^{M_{D_p}} \sum_{u=1}^{M_S} |h_{S,D_p}^{v,u}|^2 p_s^u \leq I_{th}.
\end{aligned} \tag{4.11}$$

On the other hand, the optimization problem involved when the $R_i - D$ link is selected can be formulated as follows

$$\begin{aligned}
& \underset{\mathbf{P}_{R_i}, \mathbf{P}_{S_p}}{\text{maximize}} && R_{R_i-D} + R_{S_p,D_p}, \\
& \text{subject to} && 0 \leq \sum_{u=1}^{M_{R_i}} p_{R_i}^u + \sum_{v=1}^{M_{s_p}} p_{s_p}^v \leq P_T, \\
& && \sum_{v=1}^{M_{D_p}} \sum_{u=1}^{M_{R_i}} |h_{R_i,D_p}^{v,u}|^2 p_{R_i}^u \leq I_{th}.
\end{aligned} \tag{4.12}$$

In the following two subsections, a low complexity relay selection and sub-optimal antenna transmission power allocation schemes are proposed.

4.2.3 New MIMO-based Relay Selection Scheme

In buffer-aided relaying, the i^{th} relay that receives an information packet from the source when the $S - R_i$ link is selected is not necessarily the same j^{th} relay that transmits an information packet to the destination when the $R_j - D$ link is selected after an arbitrary number of time slots. This fact means that, in buffer-aided relaying, the best receiving and transmitting relays are selected separately.

In MIMO cooperative buffer-aided relay networks, the optimal relay from multiplexing gain point of view is the one that results in a maximum normalized rate. Finding the maximum normalized rate requires first optimizing antenna transmission power for all active relays and then selecting the link which gives maximum rate. This relay selection procedure is tedious and time consuming [31]

$$i_{Opt} = \max_i (R_{S,R_i}, R_{R_i,D}). \quad (4.13)$$

Max-link relay selection also takes into consideration the content of relay buffers i.e. full buffers are not selected for receiving and empty buffers are not selected for transmission. In this work, we propose to select the best relay utilizing the concept of SVD with the assumption of equal power allocation. The proposed relay selection scheme is performed based on the following criterion

$$i^* = \max (f_{S,R_i}, f_{R_i,D}), \quad (4.14a)$$

where

$$f_{S,R_i} = \max_i \prod_{v=1}^{M_{y1}} \left(1 + \frac{\lambda_{v,1}^i P_T}{P_T \sum_{j=1}^{M_{Sp}} |h_{Sp,R_i}^{v,j}|^2 + N_o M_{T_2}} \right), \quad (4.14b)$$

$$f_{R_i,D} = \max_i \prod_{v=1}^{M_{y2}} \left(1 + \frac{\lambda_{v,2}^i P_T}{P_T \sum_{j=1}^{M_{Sp}} |h_{Sp,D}^{v,j}|^2 + N_o M_{T_2}} \right), \quad (4.14c)$$

where $M_{y1} = \min(M_S, M_{R_i})$, $M_{y2} = \min(M_{R_i}, M_D)$, $M_{T_1} = M_S + M_{Sp}$, $M_{T_2} = M_{R_i} + M_{Sp}$, $\lambda_{v,1}^i$ is the v^{th} eigen value generated from the channel matrix \mathbf{H}_{S,R_i} , and $\lambda_{v,2}^i$ is the v^{th} eigen value generated from the channel matrix $\mathbf{H}_{R_i,D}$. The proposed relay selection scheme takes all possible MIMO channel gains into consideration

and selects the one that maximizes the $S - R$ or $R - D$ normalized rate. Also, it considers the interference caused by the PN.

4.2.4 Antenna Transmission Power Allocation Scheme

Deriving of an optimal solution for problems in (4.28, 4.29) is a very complicated procedure due to the high non-linearity of the target functions. This has motivated us to propose a sub-optimal solution of antenna transmission power allocation problem. In the proposed scheme, we first derive the optimal transmission power allocation expressions of each primary and SN independently and then combine the derived expressions in an iterative algorithm that maximizes the overall sum rate. In each optimization problem, the interference power values are assumed to be known and constants.

The optimization problem related to the $S - R_i$ link can be formulated as follows

$$\begin{aligned}
& \underset{\mathbf{P}_S}{\text{maximize}} && R_{S,R_i} \\
& \text{subject to} && 0 \leq \sum_{u=1}^{M_S} p_s^u + \sum_{v=1}^{M_{S_p}} p_{s_p}^v \leq P_T, \\
& && \sum_{v=1}^{M_{D_p}} \sum_{u=1}^{M_S} |h_{S,D_p}^{v,u}|^2 p_s^u \leq I_{th}.
\end{aligned} \tag{4.15}$$

To solve this optimization problem, the Lagrangian multiplier method is used

[12]. The Lagrangian function and its optimal solution can be written as follows

$$\begin{aligned} \mathcal{L}_1(\mathbf{P}_s, \lambda_1, \lambda_2) = & \sum_{u=1}^{M_1} \log_2 \left(1 + \frac{\sigma_u^2 p_s^u}{\sum_{j=1}^{M_{S_p}} |h_{S_p, R_i}^{u,j}|^2 p_{s_p}^j + N_o} \right) \\ & - \lambda_1 \left(\sum_{u=1}^{M_S} p_s^u + \sum_{v=1}^{M_{S_p}} p_{s_p}^v - P_T \right) - \lambda_2 \left(\sum_{v=1}^{M_{D_p}} \sum_{u=1}^{M_S} |h_{S, D_p}^{v,u}|^2 p_s^u - I_{th} \right), \end{aligned} \quad (4.16)$$

where λ_1 and λ_2 are the Lagrangian multipliers related to peak source transmission power, and interference constraints, respectively,

$$p_s^u = \frac{1}{\log_e 2 \left[\lambda_1 + \lambda_2 \sum_{v=1}^{M_{D_p}} |h_{S, D_p}^{v,u}|^2 \right]} - \frac{\sum_{j=1}^{M_{S_p}} |h_{S_p, R_i}^{u,j}|^2 p_{s_p}^j + N_o}{\sigma_u^2}, \quad (4.17)$$

where $1 \leq u \leq M_S$. The value of Lagrangian multipliers λ_1 and λ_2 are chosen such that they minimize $\mathcal{L}_1(\lambda_1, \lambda_2)$ in (4.16). However, their optimal values lie between one and zero.

One efficient method to find λ_1 and λ_2 is called sub-gradient update method [?] and it is given by

$$\begin{aligned} \lambda_1^{(m+1)} &= \left[\lambda_1^{(m)} + \mu^{(m)} \left(\sum_{u=1}^{M_S} (p_s^m)^u + \sum_{v=1}^{M_{S_p}} p_{s_p}^v - P_T \right) \right]^+, \\ \lambda_2^{(m+1)} &= \left[\lambda_2^{(m)} + \mu^{(m)} \left(\sum_{v=1}^{M_{D_p}} \sum_{u=1}^{M_S} |h_{S, D_p}^{v,u}|^2 (p_s^m)^u - I_{th} \right) \right]^+, \end{aligned} \quad (4.18)$$

where m is the iteration index, $\mu^{(m)}$ is a sequence of scalar step sizes, and $[\zeta]^+ = \max(\zeta, 0)$. It was found that due to the convexity of the target function, the sub-gradient method is found to converge to the optimal values as long as $\mu^{(m)}$ is

chosen to be sufficiently small.

In a similar procedure, the optimal antenna transmission power expressions for i^{th} selected relay and primary user can be derived and is given respectively as

$$p_{R_i}^u = \frac{1}{\log_e 2 \left[\lambda_3 + \lambda_4 \sum_{v=1}^{M_{D_p}} |h_{R_i, D_p}^{v,u}|^2 \right]} - \frac{\sum_{j=1}^{M_{S_p}} |h_{S_p, D}^{u,j}|^2 p_{s_p}^j + N_o}{\sigma_u^2}, \quad (4.19)$$

where $1 \leq u \leq M_{R_i}$, λ_3 , and λ_4 are the Lagrangian multipliers of first and second constraints related to the problem of optimizing $R_{R_i, D}$,

$$p_{s_p}^u = \frac{1}{\lambda_5 \log_e 2} - \frac{\sum_{j=1}^{M_y} |h_{y, D_p}^{u,j}|^2 p_y^j + N_o}{\sigma_u^2}, \quad (4.20)$$

where $(M_S \text{ or } M_{R_i}) + 1 \leq u \leq (M_S \text{ or } M_{R_i}) + M_{S_p}$, depending on whether $R_{S_p, D_p} + R_{S, R_i}$ or $R_{S_p, D_p} + R_{R_i, D}$ is maximized, respectively, and λ_5 is the Lagrangian multiplier related the maximum power constraint of the problem of maximizing R_{S_p, D_p} .

In the proposed scheme, we first define a global power vector $\mathbf{P} = [\mathbf{P}_S^T : \mathbf{P}_{S_p}^T]^T$ then use an iterative algorithm to repeatedly allocate power values to each optimal expression using the results of the previous iterations. Figure 4.2 shows a simplified flowchart of the proposed scheme that is used to maximize $R_{S, R_i} + R_{S_p, D_p}$ when the $S - R_i$ link is selected.

The same algorithm can be used to maximize $R_{R_i, D} + R_{S_p, D_p}$ whenever the $R_i - D$ link is selected.

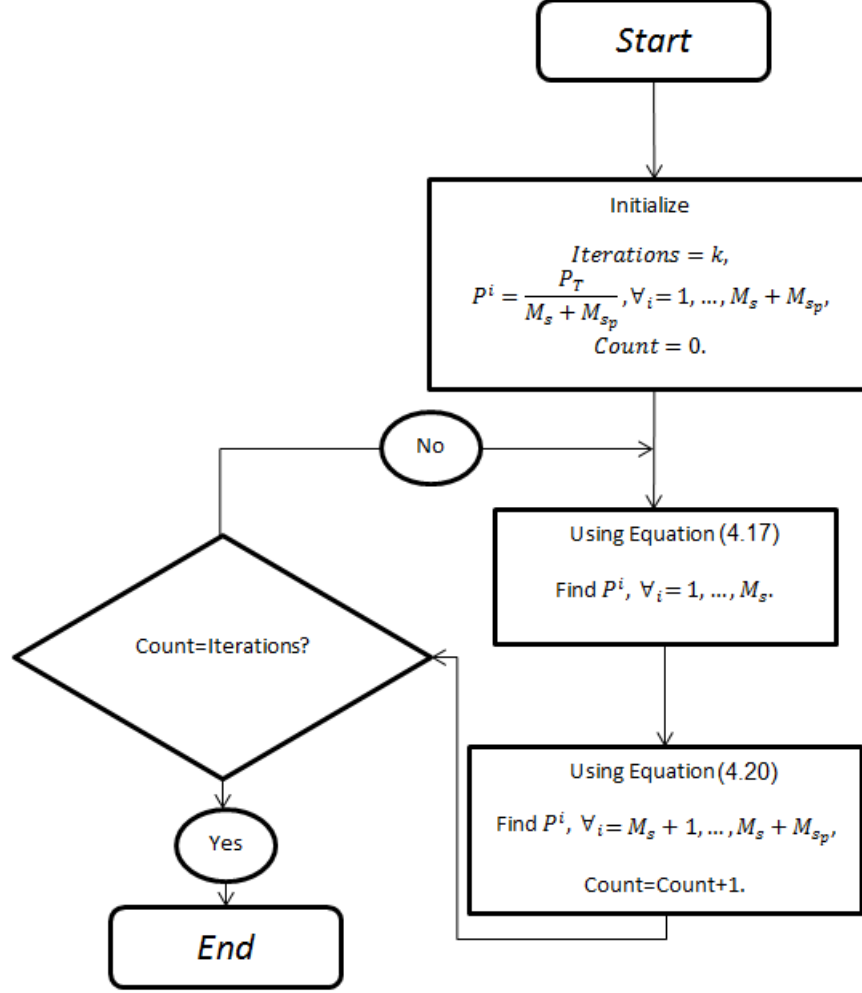


Figure 4.2: Proposed antenna transmission power allocation scheme applied for maximizing $R_{S,R_i} + R_{S_p,D_p}$ when the $S - R_i$ link is selected.

4.2.5 Complexity Analysis

Solving problems (4.28, 4.29) via exhaustive search (ES) numerical programming algorithm requires $\sum_{i=0}^q \binom{NM}{i} (q-1)^i = O(q^{NM})$ operations to find the optimal solution [?], while our proposed sub-optimal solution requires $2Mk = O(Mk)$ operations, where q is the quantization levels of ES algorithm and M is the sum PN and SN transmitting antennas at a certain time slot. For example, with $\{M, N, q, k\} = \{4, 4, 64, 5\}$, the complexity order is $\{8 \times 10^{28}, 120.18, 2\}$ for ES,

Table 4.1: Central processing unit times (seconds), for 100 channel realization.

Optimal	Proposed	Separate
	$\{M, N, q, k\} = \{1, 4, 64, 1\}$	
$2 \times 10^7, \infty$	15	11.7
	$\{M, N, q, k\} = \{2, 4, 64, 3\}$	
$3 \times 10^{14}, \infty$	60.43	11.7
	$\{M, N, q, k\} = \{4, 4, 64, 5\}$	
$8 \times 10^{28}, \infty$	120.18	11.7

proposed, and separate schemes, respectively. Table 1 shows the central processing unit time duration of different schemes for 100 channel realization.

4.3 Bidirectional Relaying

In this section, a similar procedure of bidirectional cognitive SISO buffer-aided relaying network is presented for the case of MIMO scheme.

4.3.1 System Model

In this section, we consider a CR network that consists of a PN with one PU source (S_p) and one PU destination (D_p), and a SN with one SU source (S), one SU destination (D), and N cognitive DF relays $[R_i]_{i=1}^N$. The nodes S_p , D_p , U_1 , U_2 and the i^{th} selected relay are assumed to be equipped with M_{S_p} , M_{D_p} , M_{U_1} , M_{U_2} , and M_{R_i} antennas, respectively. A MIMO scheme is used to achieve multiplexing gain using SVD method.

Each relay is provided with two buffers to store received information packets from U_1 and U_2 and denoted by $B_1(R_i)$ and $B_2(R_i)$, respectively. $B_m(R_i)$ has maximum size of L_m , where L_m is the maximum number of information packets

received from terminal $U_m, m = 1, 2$ that can be stored before an overflow occurs. We denote the instantaneous number of stored information packets at the m^{th} buffer of the i^{th} relay by $\Psi_m(R_i)$, where $0 \leq \Psi_m(R_i) \leq L_m$. Figure 4.3 shows the system model used in this section. As illustrated in this Figure, the solid and dotted lines represent desired and interfering signals in each possible transmission mode, respectively.

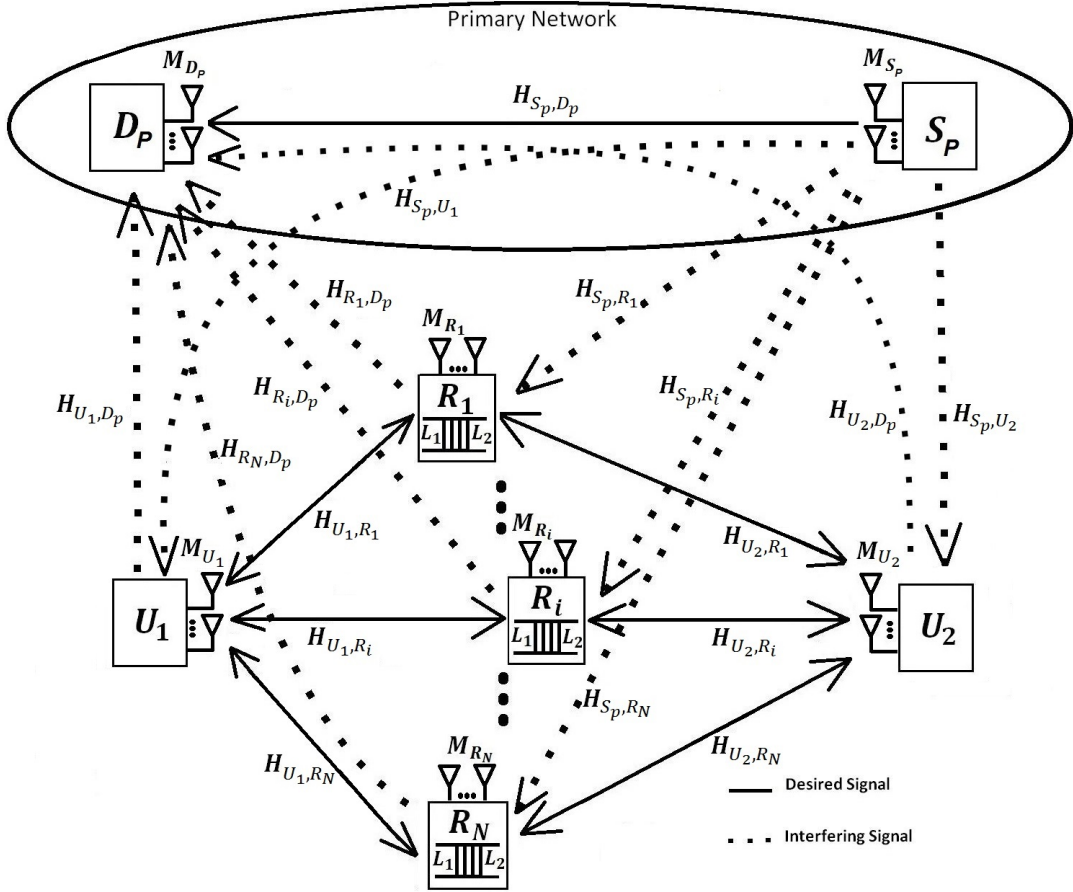


Figure 4.3: Cognitive radio network with MIMO buffer-aided DF relays (solid lines: desired signals, dotted lines: interfering signals).

Without loss of generality, the direct $U_1 - U_2$ link is not considered in this model as it is assumed to be suffering from sever fading and shadowing effects. In addition, PUs and SUs are assumed to access the spectrum simultaneously. In

order to maintain a certain QoS level to the PU, the average received interference power due to SUs should not exceed a certain interference threshold denoted by I_{th} [33].

All channel coefficients are assumed to be i.i.d. slowly Rayleigh fading random variables such that they remain unchanged during one time slot. We denote $\mathbf{H}_{x,y}$ as the channel matrix between terminals x and y . Channel gains of bidirectional links are assumed to be symmetric which means, at a certain time instant t , channel coefficient in $U_m - R_i$ link is identical to that in $R_i - U_m$ inverse link¹. Each receiving terminal is assumed to experience an AWGN at its input with constant variance N_o .

At a certain time slot t_1 , if the U_m terminal is selected for transmission, $m = 1, 2$, the terminal transmits its signals $\mathbf{X}_{U_m} = [X_{U_m}^1, X_{U_m}^2, \dots, X_{U_m}^{M_{U_m}}]^T$ with a power vector given by $\mathbf{P}_{U_m} = [p_{U_m}^1, p_{U_m}^2, \dots, p_{U_m}^{M_{U_m}}]^T$. On the other hand, if the relay that is related to the selected link is chosen for transmission, it transmits one its oldest stored information packet that is given by $\mathbf{X}_{R_i} = [X_{R_i}^1, X_{R_i}^2, \dots, X_{R_i}^{M_{R_i}}]^T$ with a power vector given by $\mathbf{P}_{R_i} = [p_{R_i}^1, p_{R_i}^2, \dots, p_{R_i}^{M_{R_i}}]^T$. PN is assumed to be transmitting at every time slot t during network operation. The transmitted information packet in the $S_p - D_p$ link is given by $\mathbf{X}_{S_p} = [X_{s_p}^1, X_{s_p}^2, \dots, X_{s_p}^{M_{s_p}}]^T$ with a power vector given by $\mathbf{P}_{S_p} = [p_{s_p}^1, p_{s_p}^2, \dots, p_{s_p}^{M_{s_p}}]^T$. We define P_T , as the maximum available power budget assigned for the whole network at any arbitrary time slot and it is given by $P_T = p_{U_1}^1 + \dots + p_{U_1}^{M_{U_1}} + p_{s_p}^1 + \dots + p_{s_p}^{M_{s_p}}$ or $P_T =$

¹Most of the previous works in the literature used the symmetric channel gain assumption to simplify the analysis without any effect in the final results and conclusions of the analysis [37].

$p_{R_i}^1 + \dots + p_{R_i}^{M_{R_i}} + p_{s_p}^1 + \dots + p_{s_p}^{M_{s_p}}$ or $P_T = p_{U_2}^1 + \dots + p_{U_2}^{M_{U_2}} + p_{s_p}^1 + \dots + p_{s_p}^{M_{s_p}}$ if the U_1 , R_i , or U_2 is selected for transmission in the SN, respectively.

To avoid the need for heavy and fast back-haul links, a central processing unit that performs relay selection and power allocation operations is assumed to exist in the network with a full CSI acknowledgement.

4.3.2 Problem Formulation

In buffer-aided half-duplex bidirectional relaying scheme, there are mainly five possible transmission modes occur in the SN at any arbitrary time slot denoted by $\mathcal{M}_i, i = 1, \dots, 5$ as shown in Figure 4.4. The PN is assumed to be transmitting

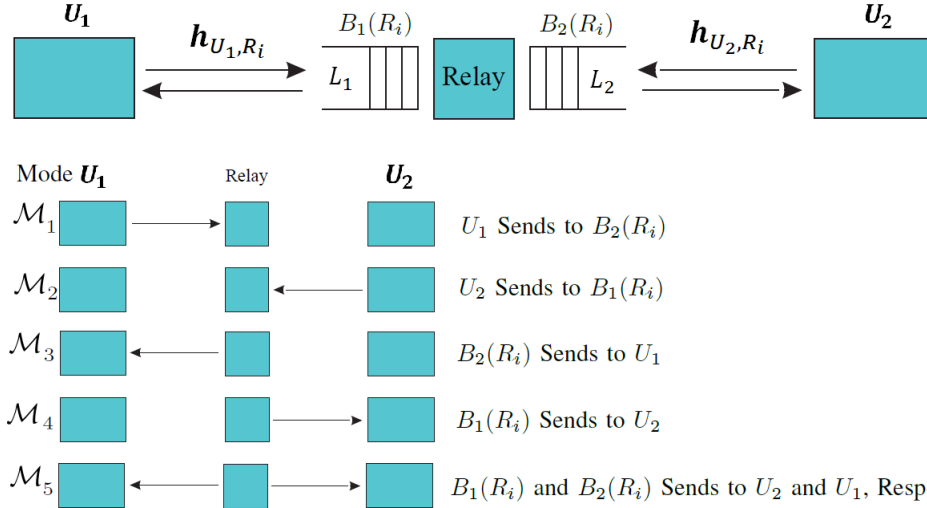


Figure 4.4: Possible bidirectional transmission modes of the secondary network.

information packets at every time slot during network operation. The received signal vector at the i^{th} relay for modes \mathcal{M}_1 and \mathcal{M}_2 are respectively given by

$$\mathbf{y}_{R_i}^{(\mathcal{M}_1)} = \underbrace{\mathbf{H}_{U_1, R_i} \mathbf{X}_{U_1}}_{\text{Desired Signal}} + \underbrace{\mathbf{H}_{S_p, R_i} \mathbf{X}_{S_p}}_{\text{Interfering Signal}} + \underbrace{\mathbf{n}_{R_i}}_{\text{AWGN}}, \quad (4.21)$$

$$\mathbf{y}_{R_i}^{(\mathcal{M}_2)} = \underbrace{\mathbf{H}_{U_2, R_i} \mathbf{X}_{U_2}}_{\text{Desired Signal}} + \underbrace{\mathbf{H}_{S_p, R_i} \mathbf{X}_{S_p}}_{\text{Interfering Signal}} + \underbrace{\mathbf{n}_{R_i}}_{\text{AWGN}}, \quad (4.22)$$

where \mathbf{X}_{U_1} and \mathbf{X}_{U_2} are the message signal vectors which transmitted from U_1 and U_2 with power vectors \mathbf{P}_{U_1} and \mathbf{P}_{U_2} , respectively, \mathbf{n}_{R_i} is the AWGN vector at the input of R_i relay with power N_o at each antenna input. Information packet received from U_1 or U_2 is stored at buffer $B_1(R_i)$ or $B_2(R_i)$, respectively. At a certain time slot, when the selected relay is chosen to transmit to one or both user terminals U_1 and U_2 , the received signal vectors at U_1 and U_2 are respectively given by

$$\mathbf{y}_{U_1}^{(\mathcal{M}_3, \mathcal{M}_5)} = \underbrace{\mathbf{H}_{U_1, R_i} \mathbf{X}_{R_i}}_{\text{Desired Signal}} + \underbrace{\mathbf{H}_{S_p, U_1} \mathbf{X}_{S_p}}_{\text{Interfering Signal}} + \underbrace{\mathbf{n}_{U_1}}_{\text{AWGN}}, \quad (4.23)$$

$$\mathbf{y}_{U_2}^{(\mathcal{M}_4, \mathcal{M}_5)} = \underbrace{\mathbf{H}_{U_2, R_i} \mathbf{X}_{R_i}}_{\text{Desired Signal}} + \underbrace{\mathbf{H}_{S_p, U_2} \mathbf{X}_{S_p}}_{\text{Interfering Signal}} + \underbrace{\mathbf{n}_{U_2}}_{\text{AWGN}}. \quad (4.24)$$

Mode \mathcal{M}_5 is called the broadcasting mode since R_i combines two signal vectors from $B_1(R_i)$ and $B_2(R_i)$ and broadcast the resultant to U_1 and U_2 with transmission power vector \mathbf{P}_{R_i} . Each terminal receiver is assumed to have some self-interference cancellation strategy. The received signal at D_p at any arbitrary time slot is given by

$$\mathbf{y}_{D_p} = \underbrace{\mathbf{H}_{S_p, D_p} \mathbf{X}_{S_p}}_{\text{Desired Signal}} + \underbrace{\mathbf{H}_{W, D_p} \mathbf{X}_W}_{\text{Interfering Signal}} + \underbrace{\mathbf{n}_{D_p}}_{\text{AWGN}}, \quad (4.25)$$

where W depends on the transmission mode of the SN.

By going through the same analyses procedure as that of Section 4.2.2, the

normalized rate at modes \mathcal{M}_1 to \mathcal{M}_5 are given respectively by

$$R_{U_1, R_i}^{(\mathcal{M}_1)} = \sum_{u=1}^{M_1} \log_2 \left(1 + \frac{\sigma_u^2 p_{U_1}^u}{\sum_{j=1}^{M_{S_p}} |h_{S_p, R_i}^{u,j}|^2 p_{s_p}^j + N_o} \right), \quad (4.26)$$

$$R_{U_2, R_i}^{(\mathcal{M}_2)} = \sum_{u=1}^{M_1} \log_2 \left(1 + \frac{\sigma_u^2 p_{U_2}^u}{\sum_{j=1}^{M_{S_p}} |h_{S_p, R_i}^{u,j}|^2 p_{s_p}^j + N_o} \right), \quad (4.27)$$

$$R_{R_i, U_1}^{(\mathcal{M}_3, \mathcal{M}_5)} = \sum_{v=1}^{M_2} \log_2 \left(1 + \frac{\sigma_v^2 p_{R_i}^v}{\sum_{j=1}^{M_{S_p}} |h_{S_p, U_1}^{v,j}|^2 p_{s_p}^j + N_o} \right), \quad (4.28)$$

$$R_{R_i, U_2}^{(\mathcal{M}_3, \mathcal{M}_5)} = \sum_{v=1}^{M_2} \log_2 \left(1 + \frac{\sigma_v^2 p_{R_i}^v}{\sum_{j=1}^{M_{S_p}} |h_{S_p, U_2}^{v,j}|^2 p_{s_p}^j + N_o} \right), \quad (4.29)$$

while the PN rate at any arbitrary time slot is given by

$$R_{S_p, D_p} = \sum_{l=1}^{M_3} \log_2 \left(1 + \frac{\sigma_l^2 p_{s_p}^l}{\sum_{j=1}^{M_y} |h_{y, D_p}^{l,j}|^2 p_y^j + N_o} \right). \quad (4.30)$$

The problem in our hand is first to select the best relay and the corresponding transmission mode for the SN and then allocate a maximum power budget between both the PN and the SN such that the normalized sum rate is maximized. Bidirectional transmission mode selection protocol should maximize the normalized sum rate and bounds the average packet delay of the SN by a predefined number of time slots μ . For MIMO system, the transmission power optimization

problems at modes \mathcal{M}_1 to \mathcal{M}_4 is given by

$$\begin{aligned}
& \underset{\mathbf{P}_{S_p}, \mathbf{P}_J^{(\mathcal{M}_i)}}{\text{maximize}} && R_{S_p, D_p} + R_{J, K}^{(\mathcal{M}_i)} \\
& \text{subject to} && 0 \leq \sum_{v=1}^{M_{S_p}} P_{S_p}^v + \sum_{u=1}^{M_J} P_J^u \leq P_T \\
& && \sum_{v=1}^{M_{S_p}} \sum_{u=1}^{M_J} |h_{J, D_p}^{v, u}|^2 P_J^u \leq I_{th}.
\end{aligned} \tag{4.31}$$

For mode \mathcal{M}_1 , $(J, K) \equiv (U_1, R_i)$, for mode \mathcal{M}_2 , $(J, K) \equiv (U_2, R_i)$, for mode \mathcal{M}_3 , $(J, K) \equiv (R_i, U_1)$, and for mode \mathcal{M}_4 , $(J, K) \equiv (R_i, U_2)$. For mode \mathcal{M}_5 , the optimization problem is given by

$$\begin{aligned}
& \underset{bmP_{S_p}, \mathbf{P}_{R_i}^{(\mathcal{M}_5)}}{\text{maximize}} && R_{S_p, D_p} + R_{R_i, U_1}^{(\mathcal{M}_5)} + R_{R_i, U_2}^{(\mathcal{M}_5)} \\
& \text{subject to} && 0 \leq \sum_{v=1}^{M_{S_p}} P_{S_p}^v + \sum_{u=1}^{M_{R_i}} P_{R_i}^u \leq P_T, \\
& && \sum_{v=1}^{M_{S_p}} \sum_{u=1}^{M_{R_i}} |h_{R_i, D_p}^{v, u}|^2 P_{R_i}^u \leq I_{th}.
\end{aligned} \tag{4.32}$$

In the following two sections, we introduce the used bidirectional relaying protocol and then investigate some optimal/sub-optimal antenna transmission power allocation schemes of the PN and the SN.

4.3.3 Bidirectional Relaying Protocol

In this section, a low complexity bidirectional relaying protocol that controls the two-way data flow between terminals U_1 and U_2 in the SN is introduced. The proposed protocol is not restricted to a predefined scheduling for data exchange,

instead, it selects the best transmission mode from a set of five possible modes. Mode selection is achieved according to the instantaneous channel coefficients, buffers states, and average information packet delay. Figure 4.5 shows a descriptive flowchart of the proposed bidirectional relaying protocol. From the flowchart,

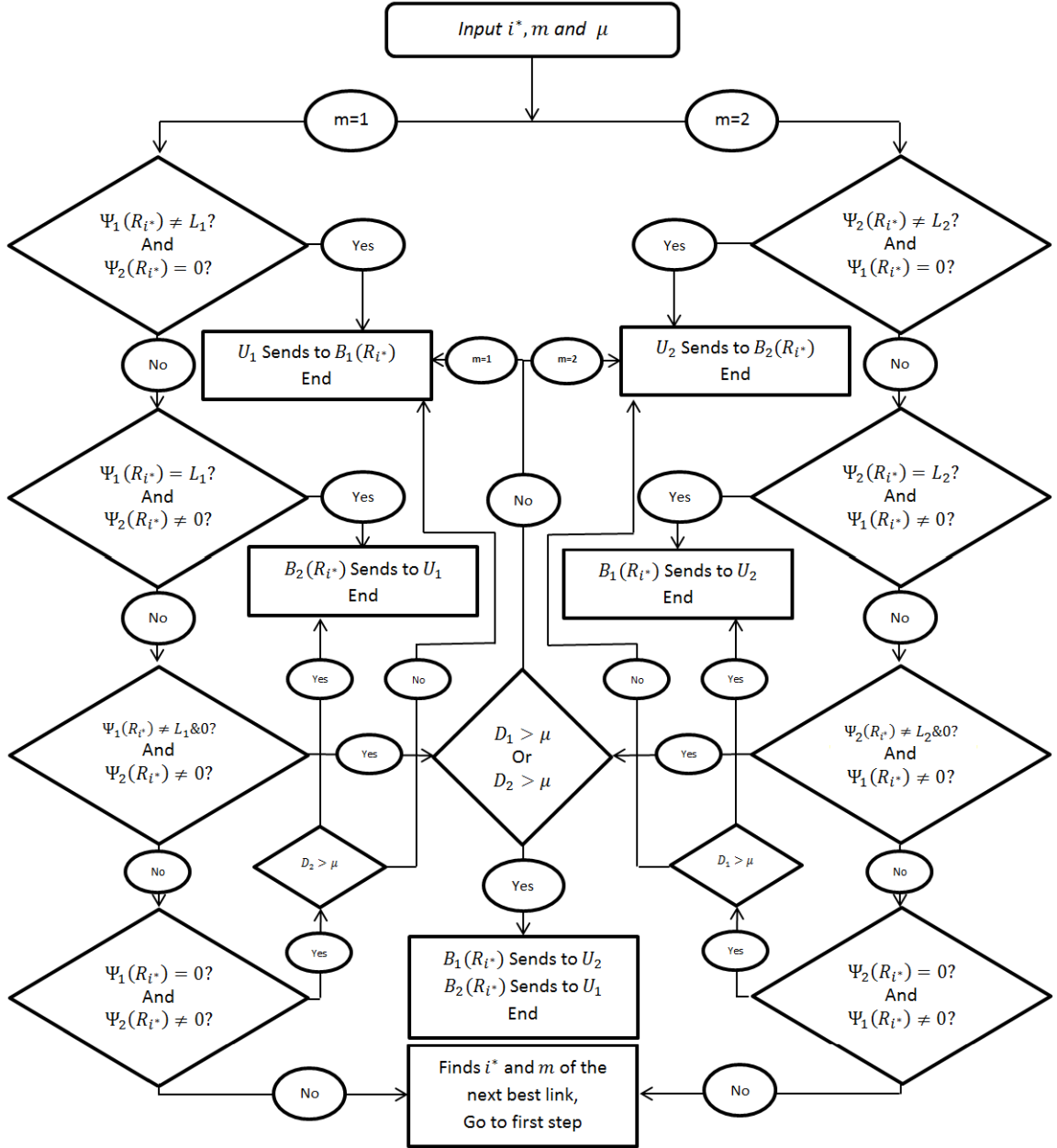


Figure 4.5: A flowchart for the proposed bidirectional relaying protocol.

D_1 and D_2 represent the number of time slots since the oldest information packet

have been buffered at $B_1(R_i)$ and $B_2(R_i)$ of the selected relay, respectively.

The index of the best relay i^* is proposed to be found using the following relay selection scheme

$$i^* = \arg \max_{R_i} \{ \min \{ f_{U_1, R_i}, f_{R_i, U_1} \}, \min \{ f_{U_2, R_i}, f_{R_i, U_2} \} \},$$

where

$$\begin{aligned} \gamma_{U_1, R_i} &= \max_i \prod_{v=1}^{M_{y1}} \left(1 + \frac{\lambda_{v,1}^i P_T}{P_T \sum_{j=1}^{M_{Sp}} |h_{S_p, R_i}^{v,j}|^2 + N_o M_{T_1}} \right), \\ \gamma_{R_i, U_1} &= \max_i \prod_{v=1}^{M_{y1}} \left(1 + \frac{\lambda_{v,1}^i P_T}{P_T \sum_{j=1}^{M_{Sp}} |h_{S_p, U_1}^{v,j}|^2 + N_o M_{T_1}} \right), \\ \gamma_{U_2, R_i} &= \max_i \prod_{v=1}^{M_{y2}} \left(1 + \frac{\lambda_{v,2}^i P_T}{P_T \sum_{j=1}^{M_{Sp}} |h_{S_p, R_i}^{v,j}|^2 + N_o M_{T_2}} \right), \\ \gamma_{R_i, U_2} &= \max_i \prod_{v=1}^{M_{y2}} \left(1 + \frac{\lambda_{v,2}^i P_T}{P_T \sum_{j=1}^{M_{Sp}} |h_{S_p, U_2}^{v,j}|^2 + N_o M_{T_2}} \right), \end{aligned} \quad (4.33)$$

where $M_{y1} = \min(M_{U_1}, M_{R_i})$, $M_{y2} = \min(M_{R_i}, M_{U_2})$, $M_{T_1} = M_S + M_{S_p}$, $M_{T_2} = M_S + M_{S_p}$, $\lambda_{v,1}^i$ is the v^{th} eigen value generated from the channel matrix \mathbf{H}_{U_1, R_i} , and $\lambda_{v,2}^i$ is the v^{th} eigen value generated from the channel matrix \mathbf{H}_{U_2, R_i} .

This modified relay selection scheme considers the interference caused by the PN in the SN at any possible transmission mode. It is important to mention that to reduce the complexity and processing delay of system operation, relay selection is achieved before any transmission power allocation scheme with the assumption that maximum power budget P_T is equally divided between the PN and the SN at any arbitrary time slot.

The significance behind this protocol is that the delay is bounded by the fact

that the transmission priority is higher for those packets that have been stored for a predefined number of time slots denoted by μ . This protocol does not require the derivation of complicated optimal mode selection problems. Instead, a set of conditions are examined and a transmission mode is selected accordingly.

4.3.4 Transmission power allocation

In this section, optimal and sub-optimal transmission power allocation schemes are proposed for each possible transmission mode.

A similar antenna transmission power allocation schemes are used for modes \mathcal{M}_1 to \mathcal{M}_4 as that used for unidirectional cognitive MIMO buffer-aided DF relaying network presented in Section 4.2.4

Optimal antenna transmission power expressions of the SN at modes \mathcal{M}_1 to mode \mathcal{M}_4 that were derived separately without considering the PN are respectively given by

$$(p_{U_1}^u)^{\mathcal{M}_1} = \frac{1}{\log_e 2 \left[\lambda_1 + \lambda_2 \sum_{v=1}^{M_{D_p}} |h_{U_1, D_p}^{v,u}|^2 \right]} - \frac{\sum_{j=1}^{M_{S_p}} |h_{S_p, R_i}^{u,j}|^2 p_{s_p}^j + N_o}{\sigma_u^2}, \quad (4.34)$$

$$(p_{U_2}^u)^{\mathcal{M}_2} = \frac{1}{\log_e 2 \left[\lambda_3 + \lambda_4 \sum_{v=1}^{M_{D_p}} |h_{U_2, D_p}^{v,u}|^2 \right]} - \frac{\sum_{j=1}^{M_{S_p}} |h_{S_p, R_i}^{u,j}|^2 p_{s_p}^j + N_o}{\sigma_u^2}, \quad (4.35)$$

$$(p_{R_i}^u)^{\mathcal{M}_3} = \frac{1}{\log_e 2 \left[\lambda_5 + \lambda_6 \sum_{v=1}^{M_{D_p}} |h_{R_i, D_p}^{v,u}|^2 \right]} - \frac{\sum_{j=1}^{M_{S_p}} |h_{S_p, U_1}^{u,j}|^2 p_{s_p}^j + N_o}{\sigma_u^2}, \quad (4.36)$$

$$(p_{R_i}^u)^{\mathcal{M}_4} = \frac{1}{\log_e 2 \left[\lambda_7 + \lambda_8 \sum_{v=1}^{M_{D_p}} |h_{R_i, D_p}^{v,u}|^2 \right]} - \frac{\sum_{j=1}^{M_{S_p}} |h_{S_p, U_2}^{u,j}|^2 p_{s_p}^j + N_o}{\sigma_u^2}, \quad (4.37)$$

where λ_1 to λ_8 are Lagrangian multipliers related to the optimization problems of modes \mathcal{M}_1 to \mathcal{M}_4 . The Lagrangian multipliers can be found using sub-gradient update method as in the case of unidirectional relaying. For example, when mode \mathcal{M}_1 is selected, λ_1 and λ_2 are found using the following two iterative schemes

$$\begin{aligned} \lambda_1^{(m+1)} &= \left[\lambda_1^{(m)} + \mu^{(m)} \left(\sum_{u=1}^{M_{U_1}} (p_{U_1}^m)^u + \sum_{v=1}^{M_{S_p}} p_{s_p}^v - P_T \right) \right]^+, \\ \lambda_2^{(m+1)} &= \left[\lambda_2^{(m)} + \mu^{(m)} \left(\sum_{v=1}^{M_{D_p}} \sum_{u=1}^{M_{U_1}} |h_{S, D_p}^{v,u}|^2 (p_{U_1}^m)^u - I_{th} \right) \right]^+, \end{aligned} \quad (4.38)$$

where m is the iteration index, $\mu^{(m)}$ is a sequence of scalar step sizes, and $[\zeta]^+ = \max(\zeta, 0)$. It was found that due to the convexity of the target function, the sub-gradient method is found to converge to the optimal values as long as $\mu^{(m)}$ is chosen to be sufficiently small.

The optimal antenna transmission power allocation scheme for the PN that is

derived separately irrespective of the SN is given by

$$p_{s_p}^u = \frac{1}{\lambda_9 \log_e 2} - \frac{\sum_{j=1}^{M_{S_p}} |h_{y,D_p}^{u,j}|^2 p_{s_p}^j + N_o}{\sigma_u^2}, \quad (4.39)$$

where y depends on the transmission mode of the SN.

Similar to unidirectional case, if mode \mathcal{M}_1 is selected, a global power vector $\mathbf{P} = [\mathbf{P}_{U_1}^T : \mathbf{P}_{s_p}^T]^T$ is defined then an iterative algorithm that repeatedly allocate power values to each optimal expression using the results of the previous iterations is used. Figure 4.6 shows a simplified flowchart of the proposed scheme that is used to maximize $R_{U_1,R_i} + R_{S_p,D_p}$ when the \mathcal{M}_1 mode is selected. The same algorithm can be used for modes \mathcal{M}_2 , \mathcal{M}_3 , and \mathcal{M}_4 .

For mode \mathcal{M}_5 , at which R_i broadcasts a combined signal vector to U_1 and U_2 , using the previous sub-optimal algorithm will be a complicated and the process will present more delay. However, in this section, we propose to use a genetic algorithm to solve the optimization problem that maximizes $R_{S_p,D_p} + R_{R_i,U_1} + R_{R_i,U_2}$. The proposed algorithm is shown at Algorithm 4.1.

In this algorithm, $h_{x,y}$ represents all possible channel coefficients of the PN and the SN during a certain time slot. Due to the convexity of the target optimized function, the proposed algorithm is said to converge to a global maxima point which is considerably close to the optimal solution, especially for high n_p .

Algorithm 4.1 Genetic Algorithm that finds P_{S_p} and $(P_{R_i}^{\mathcal{M}_5})$ that maximize $R_{sum} = R_{S_p, D_p}^{\mathcal{M}_5} + R_{R_i, U_1}^{(\mathcal{M}_5)} + R_{R_i, U_2}^{(\mathcal{M}_5)}$

```

1: Input:  $H_{x,y}, P_T, N_o, n_p, n_{parents}, Iterations$ 
2: Generate  $n_p$  initial population of  $\mathbf{P}^j = [\mathbf{P}_{S_p}^j : (\mathbf{P}_{R_i}^{\mathcal{M}_5})^j]$ , with
3:  $0 \leq \sum_v^{M_{S_p}} (P_{S_p}^j)^v + \sum_u^{M_{R_i}} (P_{R_i}^j)^u \leq P_T, \forall j = 1, \dots, n_p$ 
4: Count=1
5:  $R_{max} = 0$ 
6: while (Count  $\leq$  Iterations, or stopping condition hold), do
7:   for  $m = 1 : n_p$  do
8:     if Constrains in (4.32) are satisfied then
9:        $R_m = R_{S_p, D_p} \left( \mathbf{P}_{S_p}^j, (\mathbf{P}_{R_i}^{\mathcal{M}_5})^j \right) + R_{R_i, U_1}^{(\mathcal{M}_5)} \left( \mathbf{P}_{S_p}^j, (\mathbf{P}_{R_i}^{\mathcal{M}_5})^j \right)$ 
10:       $+ R_{R_i, U_2}^{(\mathcal{M}_5)} \left( \mathbf{P}_{S_p}^j, (\mathbf{P}_{R_i}^{\mathcal{M}_5})^j \right)$ 
11:     else
12:        $R_m = 0$ 
13:     end if
14:   end for
15:    $R_{max} = \max_m R_m$ 
16:   Take the best  $n_{parents}$  vectors of  $\mathbf{P}^j$  and use crossover and mutation go
   generate  $(n_p - n_{parents})$  next population vectors.
17: end while
```

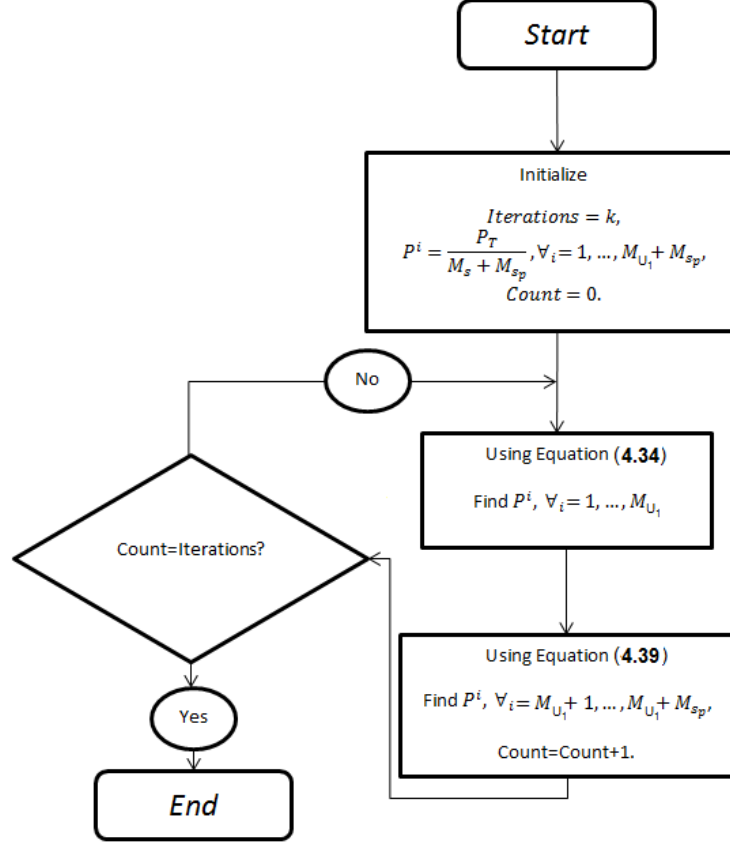


Figure 4.6: Proposed antenna transmission power allocation scheme applied for maximizing $R_{U_1, R_i} + R_{S_p, D_p}$ when the \mathcal{M}_1 mode is selected.

4.4 Simulation Results

In this section, we provide some numerical simulation results for the proposed cognitive MIMO-based relay selection and power allocation strategies. We also compare our results with those of the optimal relay selection and antenna transmission power allocation strategies implemented using ES. Monte-Carlo simulation program is run for 1,000,000 iterations. To decrease simulation complexity, we assume that all receiving nodes are subjected to constant noise power spectral density N_o .

4.4.1 Unidirectional Relaying

In this section, we assume that all transmitting and receiving nodes are equipped with the same number of antennas, that is $M_S = M_R = M_D = M_{S_p} = M_{D_p} = M$.

Figure 4.7 shows the achievable primary and secondary average normalized rates for the optimally simulated solution, proposed sub-optimal solution, and for separate optimal simulation with $I_{th} = 10$ dB, $M = 4$, $N = 4$ and $k = 5$, where k is the number of iterations in the proposed power optimization algorithm. The sepa-

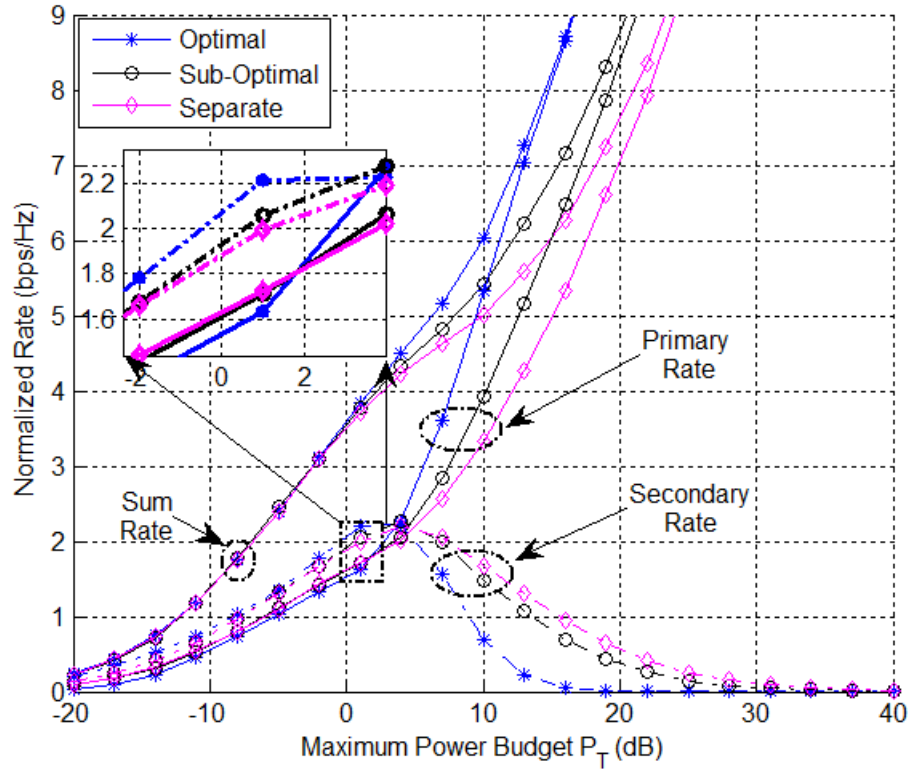


Figure 4.7: Achievable primary and secondary average normalized rate for the optimal simulated solution, proposed sub-optimal solution, and separate optimal simulation with $I_{th} = 10$ dB, $M = 4$, $N = 4$, $L = 10$ and $k = 5$.

rate power allocation scheme divides maximum power budget P_T equally between PNs and SNs and then optimizes the rate of each network separately using the

optimal derived expressions and considering the interference transmission powers to be equally divided among antennas, i.e. $P_{Interference} = \frac{P_T}{M}$. As can be noticed from this figure, the proposed sub-optimal relay selection and antenna transmission power allocation scheme introduces a performance level that lies between the optimal solution and the separate allocation schemes. For example, it can be noticed that at $P_T = 10$ dB, the proposed scheme achieves a gain of 1.5 bps/Hz in the PN rate compared to the equal power allocation scheme. It can be also noticed that using the optimal solution, the secondary rate decays drastically to zero after passing I_{th} . However, the proposed scheme maintains a fair power assignment to SN that is closer to the separate allocation scheme. This is due to the fact that for the optimal scenario where the total sum rate is optimized, the PN gets most of the available power budget due to the interference constraints in the SN transmission power, especially at high P_T .

To investigate the effect buffer size on the performance, Figure 4.8 shows the achievable normalized rate values versus different maximum buffer sizes. It can be seen from this figure that an increment of around 0.8 bps/Hz is achieved in the SN rate when adding a buffer of size $L = 100$ at $P_T = 4$ dB. Additionally, it can be noticed from this figure that physical layer buffering in the SN relay nodes decreases the normalized rate of the PN. This is due to the fact that buffering guarantees better channel gains are achieved for SN links and since power allocation follows water-falling strategy this means more power is invested in these higher gain links. Accordingly, the interference in PN that is caused by SN trans-

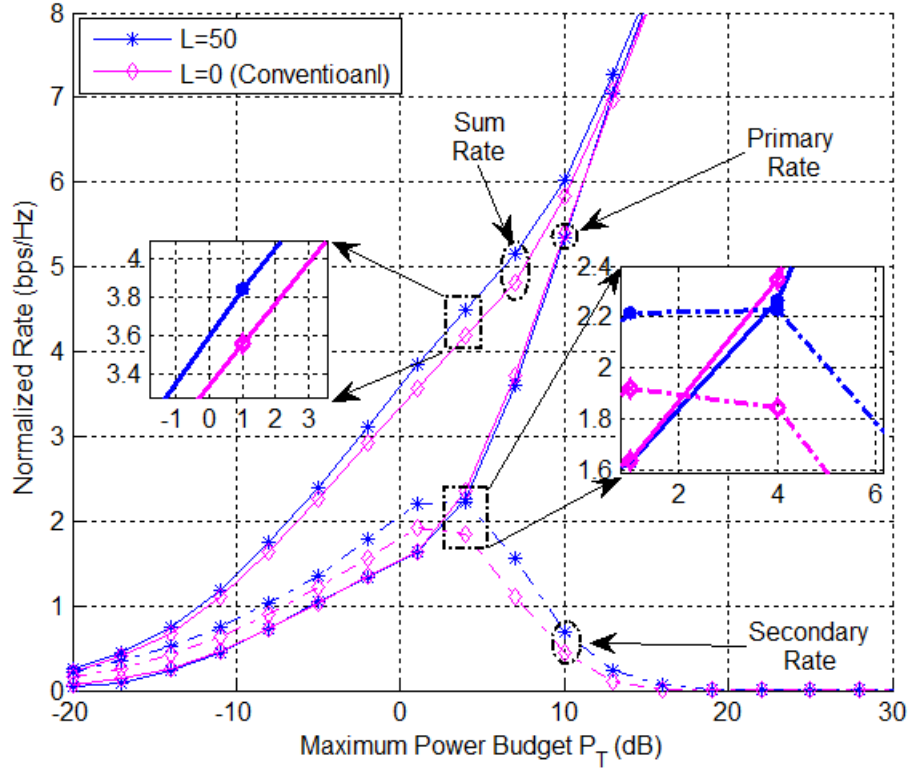


Figure 4.8: Achievable normalized rate versus different values of maximum buffer size L with $I_{th} = 10$, $M = 4$, and $k = 5$.

mission power increases. However, it is clear that the overall sum rate is enhanced by the buffering process in SN.

Figure 4.9 shows the effect of increasing number of antennas M on the overall network performance. It can be noticed from this figure that the overall sum rate of PN and SN enhances significantly with increasing the number of antennas in the network.

In Figure 4.10, the achievable normalized rates of the PN, and the SN along with their overall sum rate is plotted for two different interference threshold values $I_{th} = 10$ dB and $I_{th} = 20$ dB.

It can be noticed from this figure that for higher interference threshold, the

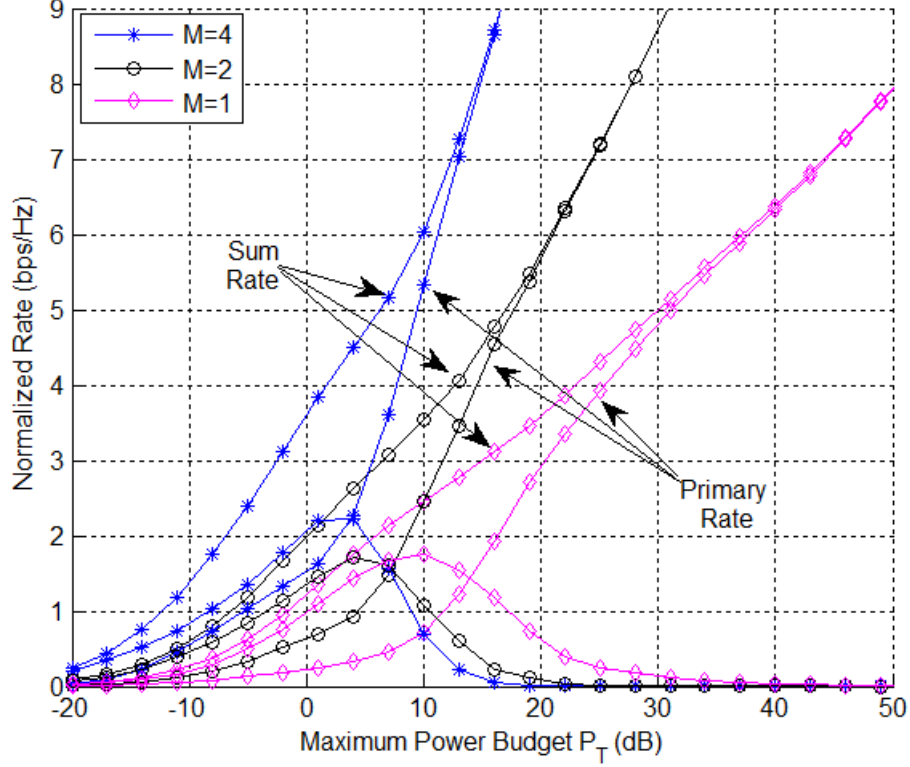


Figure 4.9: Achievable normalized rate versus different values of antennas M with $I_{th} = 10$, $L = 10$, $k = 5$, and $N = 4$.

SN rate decays in much slower than that when the interference threshold is less. Another thing to notice about this figure is that the overall sum rate achieves a performance enhancement of 1 bps/Hz at $P_T = 10$ dB when the interference threshold increases from $I_{th} = 20$ dB to $I_{th} = 20$ dB.

4.4.2 Bidirectional

In this section, we assume that all transmitting and receiving nodes are equipped with the same number of antennas, that is $M_{U_1} = M_R = M_{U_2} = M_{S_p} = M_{D_p} = M$.

Figure 4.11 shows the achievable PN and SN normalized rates versus different number of antennas.

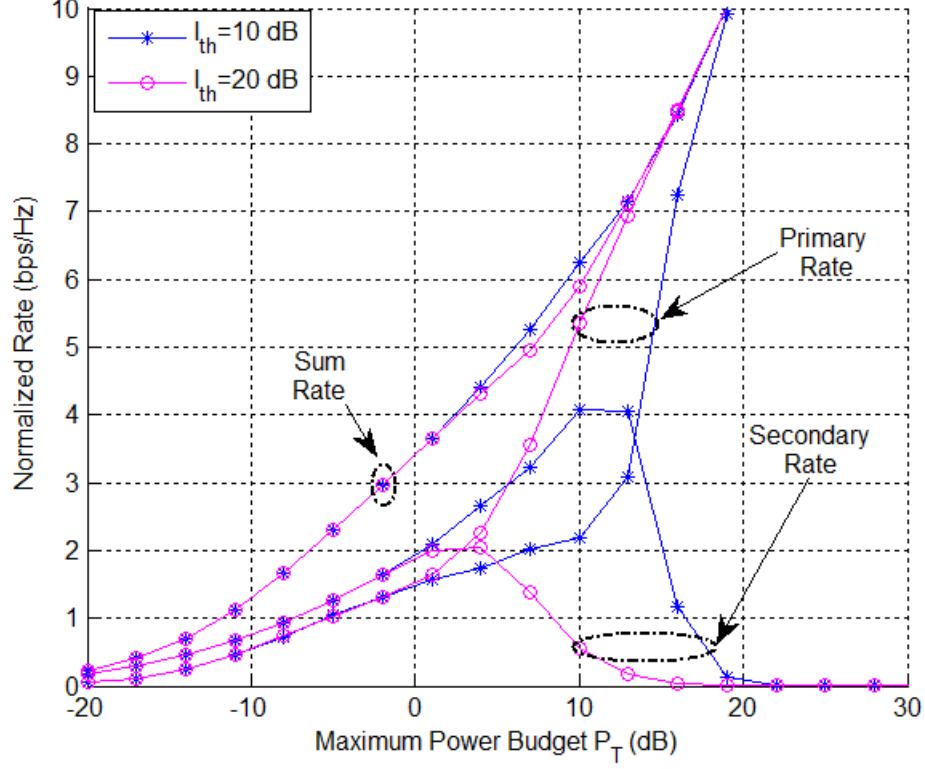


Figure 4.10: Achievable normalized rate versus different values of interference thresholds $I_{th} = 10$ dB and $I_{th} = 20$ with $L = 10$, $M = 4$, and $N = 4$.

It can be noticed from this figure that increasing the number of antennas in the SN does not enhance the network performance significantly. This is due to the fact that higher order MIMO scheme that achieves a multiplexing gain is fully utilized by pumping more power to the transmitting antennas which is not the case on the SN due to the interference constraints. However, it can also be noticed from the figure that the PN performance is enhanced significantly as the number of antennas increases. Additionally, it can be noticed from this figure that the decay in the SN rate is faster for higher number of antennas since interference on the PN becomes higher for higher number of antennas.

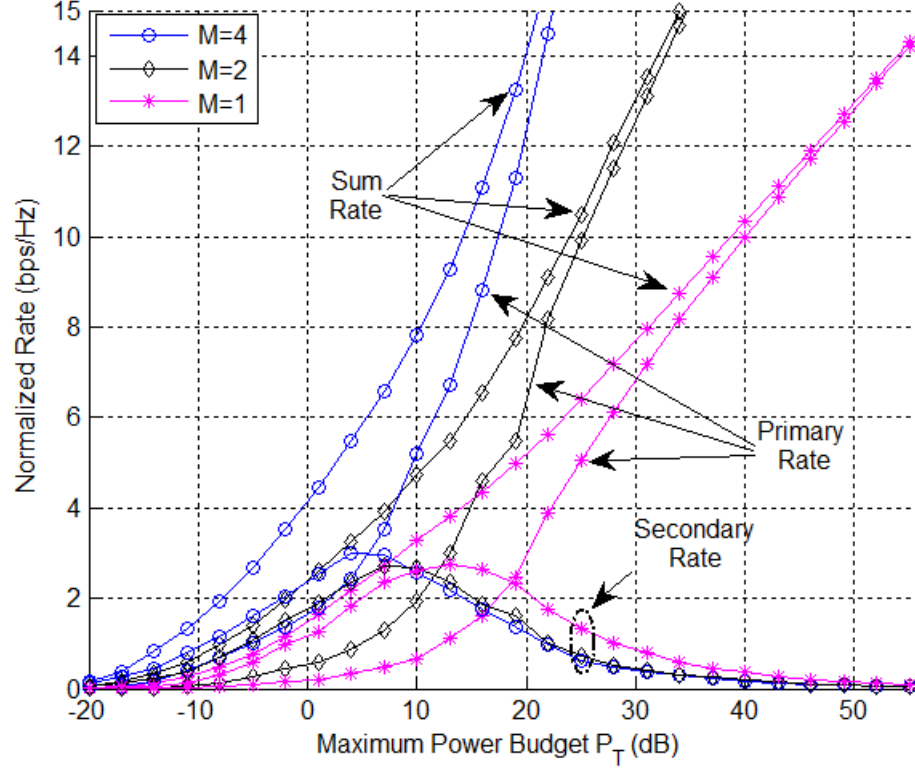


Figure 4.11: Achievable normalized rate versus different values of antennas with $L = 50$, $I_{th} = 10$ dB, and $N = 4$.

4.5 Conclusions

In this chapter, we proposed a low complexity MIMO-based relay selection and sub-optimal antenna transmission power allocation schemes for cognitive MIMO buffer-aided DF relaying network. Convex optimization theory was used to derive closed-form expressions for optimal transmission power that maximizes primary and secondary rates individually. The derived expressions were then used in an iterative algorithm that globally allocates maximum power budget among all transmitting antennas of the network nodes. The analysis was done for both unidirectional and bidirectional relaying schemes. The proposed scheme is found to have a performance level that is close to optimal solution scheme and significantly

better than the separate allocation scheme. It was also found that physical layer buffering on relay network significantly enhances the secondary network performance compared to the case of conventional relaying scheme where no buffers are used.

CHAPTER 5

CONCLUSION AND FUTURE WORK

In this chapter, we conclude our thesis work presented in the previous four chapters including outage behavior of cooperative relay networks, single-antenna design and analysis, multiple-antennas analyses and design, and the delay effect of different buffer-aided relaying schemes. We also propose some interesting topics in the field of buffer-aided relaying networks to be considered in our future researches.

5.1 Introduction

Compared to the conventional relaying, the buffer-aided relaying is found to be outperforming the conventional relaying scheme since it adds some kind of time diversity to the network. This is achieved by selecting the best mode of transmission that is related to the best channel gain for instantaneous data transmission while postponing the transmission of a certain data that is related to weaker links

until better channel conditions are met. A significant enhancement on the system performance occurs by equipping the relay with a buffer that is capable of storing one data packet. However, the enhancement acquired when increasing buffer size will not be as large as that was gained when moving from the conventional relaying into the buffer-aided relaying schemes.

5.2 Outage Behavior of Cognitive Relay Networks

In the analysis of the outage behavior of conventional unbuffered relaying networks, it was found that the network performance is enhanced by increasing the number of relays within the SN. Regarding the SN, it was also found that the outage probability of the PN is not affected by the relay selection mechanism, and it is affected by the interference from the SN wither it was caused by the secondary source or secondary relay. When the relays are equipped with buffers, it was found that the buffer-aided relaying adds significant amount of coding gain to the SN system performance compared to the conventional unbuffered relaying. Furthermore, results showed that the diversity gain of the system is enhanced significantly as the maximum buffer size increases and it reaches a certain level at which any further increment of the buffer size does not add any significant gain.

5.3 Single-Antenna Relaying Scheme

In the analysis of a single-antenna cognitive buffer-aided relay network, optimal/sub-optimal antenna transmission power allocation schemes were proposed and analysed. Additionally, a low complexity bidirectional relaying protocol that achieves a two-way data transmission on buffer-aided relaying network was proposed and analyzed as well. It was found that applying buffering at SN relays enhances the SN performance significantly while degrading the PN performance slightly. Additionally, with a higher delay bound, sum rate was shown to be enhanced with the cost of increasing the information packet delay in the SN.

5.4 Multiple-Antenna Relaying Scheme

In the analysis of multiple-antenna cognitive buffer-aided relay network, a low complexity MIMO-based relay selection scheme was proposed and evaluated. Additionally, a maximum power budget was optimally/sub-optimally allocated between all the PN and SN transmitting antennas for unidirectional and bidirectional scenarios. The proposed transmission power allocation scheme was found to have a performance level that is close to the optimal solution scheme and is significantly better than the separate power allocation scheme. It was also found that the physical layer buffering in relay network significantly enhances the secondary network performance compared to the case of conventional relaying scheme.

5.5 Future Work

There are many open research problems in buffer-aided relaying field that need to be investigated and evaluated under different system parameters and new designs have to be proposed. Here we are enumerating some of these areas of research as follows:

- Deriving of optimal buffer-aided relaying protocols for more complex networks: the optimal buffer-aided relaying protocol has been only derived in this work for simple relay networks such as the one-way and two-way three-node relay networks without a source-destination link. Therefore, the optimal buffer-aided relaying protocols for more complex networks are unknown.
- Performance loss due to non-perfect CSI: buffer-aided relaying protocols require processing the CSI of the transmitting and receiving links. So far, only the case of perfect CSI has been considered and the degradation due to imperfect CSI needs more investigation.
- Optimal delay limited buffer-aided protocol: the optimal buffer-aided relaying protocol introduces an unbounded delay. An optimal delay limited buffer-aided protocol even for the simplest networks is not known. Currently, bounding the delay is done by heuristically modifying the optimal buffer-aided relaying protocol for unbounded delay. However, the heuristic delay-limited buffer-aided protocols are typically applicable only for slot-by-slot uncorrelated fading.

REFERENCES

- [1] A. Goldsmith, S. Jafar, I. Maric, and S. Srinivasa, “Breaking spectrum gridlock with cognitive radios: An information theoretic perspective,” *Proc. IEEE*, vol. 97, no. 5, pp. 894–914, May 2009.
- [2] I. F. Akyildiz, W.-Y. Lee, M. C. Vuran, and S. Mohanty, “Next generation/dynamic spectrum access/cognitive radio wireless networks: A survey,” *Comp. Netwo.*, vol. 50, no. 13, pp. 2127 – 2159, 2006.
- [3] A. Goldsmith, *Wireless Communications*. New York, NY, USA: Cambridge University Press, 2005.
- [4] N. Zlatanov, A. Ikhlef, T. Islam, and R. Schober, “Buffer-aided cooperative communications: opportunities and challenges,” *IEEE Magazine in Commun.*, vol. 52, no. 4, pp. 146–153, April 2014.
- [5] B. Xia, Y. Fan, J. Thompson, and H. Poor, “Buffering in a three-node relay network,” *IEEE Trans. Commun.*, vol. 7, no. 11, pp. 4492–4496, November 2008.

- [6] A. Alsharoa, H. Ghazzai, and M.-S. Alouini, “Efficient multiple antennarelay selection algorithms for mimo unidirectionalbidirectional cognitive relay networks,” *Trans. on Emerging Telec. Tech.*, pp. n/a–n/a, 2014.
- [7] N. Zlatanov, A. Ikhlef, T. Islam, and R. Schober, “Buffer-aided cooperative communications: opportunities and challenges,” *IEEE Magazine in Commun.*, vol. 52, no. 4, pp. 146–153, April 2014.
- [8] I. Psaras and L. Mamatras, “On demand connectivity sharing: Queuing management and load balancing for user-provided networks,” *Comput. Netw.*, vol. 55, no. 2, pp. 399 – 414, 2011, wireless for the Future Internet.
- [9] S. Haykin, “Cognitive radio: brain-empowered wireless communications,” *IEEE Journal Selected Areas in Commun.*, vol. 23, no. 2, pp. 201–220, Feb 2005.
- [10] I. F. Akyildiz, W.-Y. Lee, M. C. Vuran, and S. Mohanty, “Next generation/dynamic spectrum access/cognitive radio wireless networks: A survey,” *Comput. Netw.*, vol. 50, no. 13, pp. 2127–2159, sep 2006.
- [11] A. Holder, Ed., *Mathematical Programming Glossary*. INFORMS Computing Society, 2006–14, originally authored by Harvey J. Greenberg, 1999-2006.
- [12] S. Boyd and L. Vandenberghe, *Convex Optimization*. Cambridge University Press, 2004.
- [13] M. Ren, C. Wang, and X. Zhang, “Power allocation for decode-and-forward relay system employing space-time codes based on genetic algorithm,” in

Conf. of Wireless Commun., Networking and Mobile Computing (WiCOM),
Oct 2008, pp. 1–4.

- [14] S. Menon and R. Gupta, “Assigning cells to switches in cellular networks by incorporating a pricing mechanism into simulated annealing,” *IEEE Trans. Sys., Man, and Cybernetics, Part B: Cybernetics*, vol. 34, no. 1, pp. 558–565, Feb 2004.
- [15] J. R. Koza, “Survey of genetic algorithms and genetic programming,” in *WESCON/’95. Conf. record. ’Microelectronics Communications Technology Producing Quality Products Mobile and Portable Power Emerging Technologies’*, Nov 1995, pp. 589–.
- [16] X. Liang, S. Jin, W. Wang, X. Gao, and K.-K. Wong, “Outage probability of amplify-and-forward two-way relay interference-limited systems,” *IEEE Trans. Veh. Tech.*, vol. 61, no. 7, pp. 3038–3049, Sept 2012.
- [17] G. Chen, O. Alnatouh, and J. Chambers, “Outage probability analysis for a cognitive amplify-and-forward relay network with single and multi-relay selection,” *IET Commun.*, vol. 7, no. 17, pp. 1974–1981, Nov 2013.
- [18] C.-L. Wang, T.-N. Cho, and K.-J. Yang, “On power allocation and relay selection for a two-way amplify-and-forward relaying system,” *IEEE Trans. Commun.*, vol. 61, no. 8, pp. 3146–3155, August 2013.
- [19] L. Yang, K. Qaraqe, E. Serpedin, and M.-S. Alouini, “Performance analysis of amplify-and-forward two-way relaying with co-channel interference and

- channel estimation error,” *IEEE Trans. Commun.*, vol. 61, no. 6, pp. 2221–2231, June 2013.
- [20] A. Afana, V. Asghari, A. Ghayeb, and S. Affes, “On the performance of cooperative relaying spectrum-sharing systems with collaborative distributed beamforming,” pp. 1–15, 2014.
- [21] K. Xie, J.-N. Cao, and J.-G. Wen, “Optimal relay assignment and power allocation for cooperative communications,” *Journal of Computer Science and Technology*, vol. 28, no. 2, pp. 343–356, 2013.
- [22] P. Ubaidulla and S. Aissa, “Optimal relay selection and power allocation for cognitive two-way relaying networks,” *IEEE Lett. Wireless Commun.*, vol. 1, no. 3, pp. 225–228, June 2012.
- [23] Q. Li, R. Hu, Y. Qian, and G. Wu, “Cooperative communications for wireless networks: techniques and applications in lte-advanced systems,” *IEEE Wireless Commun.*, vol. 19, no. 2, April 2012.
- [24] M. Naeem, A. Anpalagan, M. Jaseemuddin, and D. Lee, “Resource allocation techniques in cooperative cognitive radio networks,” *IEEE Commun. Surveys Tutorials*, vol. 16, no. 2, pp. 729–744, Second 2014.
- [25] J. Liu, N. Shroff, and H. Sherali, “Optimal power allocation in multi-relay mimo cooperative networks: Theory and algorithms,” *IEEE Journal Selected Areas in Commun.*, vol. 30, no. 2, pp. 331–340, February 2012.

- [26] I. Krikidis, J. Thompson, S. McLaughlin, and N. Goertz, “Max-min relay selection for legacy amplify-and-forward systems with interference,” *IEEE Trans. Wireless Commun.*, vol. 8, no. 6, pp. 3016–3027, June 2009.
- [27] A. Alsharoa, H. Ghazzai, and M.-S. Alouini, “Efficient multiple antennarelay selection algorithms for mimo unidirectionalbidirectional cognitive relay networks,” *Trans. Emerging Telecommun. Tech.*, pp. n/a–n/a, 2014.
- [28] P. Clarke and R. de Lamare, “Transmit diversity and relay selection algorithms for multirelay cooperative mimo systems,” *IEEE Trans. Veh. Tech.*, vol. 61, no. 3, pp. 1084–1098, March 2012.
- [29] S. Silva, G. Amarasuriya, C. Tellambura, and M. Ardakani, “Relay selection strategies for mimo two-way relay networks with spatial multiplexing,” *IEEE Trans. Commun.*, vol. PP, no. 99, pp. 1–1, 2015.
- [30] A. Ikhlef, D. Michalopoulos, and R. Schober, “Max-max relay selection for relays with buffers,” *IEEE Trans. Commun.*, vol. 11, no. 3, pp. 1124–1135, March 2012.
- [31] N. Zlatanov, R. Schober, and P. Popovski, “Buffer-aided relaying with adaptive link selection,” *Selected Areas in Communications, IEEE Journal on*, vol. 31, no. 8, pp. 1530–1542, August 2013.
- [32] Y. Wu, P. A. Chou, and S.-Y. Kung, “Information exchange in wireless networks with network coding and physical-layer broadcast,” in *Conf. Inf. Sciences and Systems*, March 2005.

- [33] B. Rankov and A. Wittneben, "Spectral efficient signaling for half-duplex relay channels," in *Signals, Systems and Computers, 2005. Conf. Record of the Thirty-Ninth Asilomar Conf.*, October 2005, pp. 1066–1071.
- [34] Z. Tian, G. Chen, Y. Gong, Z. Chen, and J. Chambers, "Buffer-aided max-link relay selection in amplify-and-forward cooperative networks," *IEEE Trans. Veh. Tech.*, vol. 64, no. 2, pp. 553–565, Feb 2015.
- [35] N. Zlatanov, A. Ikhlef, T. Islam, and R. Schober, "Buffer-aided cooperative communications: opportunities and challenges," *IEEE Magazine Commun.*, vol. 52, no. 4, pp. 146–153, April 2014.
- [36] V. Jamali, N. Zlatanov, A. Ikhlef, and R. Schober, "Achievable rate region of the bidirectional buffer-aided relay channel with block fading," *IEEE Trans. Inf. Theory*, vol. 60, no. 11, pp. 7090–7111, Nov 2014.
- [37] H. Liu, P. Popovski, E. De Carvalho, and Y. Zhao, "Sum-rate optimization in a two-way relay network with buffering," *IEEE Let. Commun.*, vol. 17, no. 1, pp. 95–98, January 2013.
- [38] V. Jamali, N. Zlatanov, A. Ikhlef, and R. Schober, "Adaptive mode selection in bidirectional buffer-aided relay networks with fixed transmit powers," in *Proc. Signal Processing Conf. (EUSIPCO)*, Sept 2013, pp. 1–5.
- [39] V. Jamali, N. Zlatanov, A. Ikhlef, and R. Schobert, "Adaptive mode selection and power allocation in bidirectional buffer-aided relay networks," in *IEEE Global Commun. Conf. (GLOBECOM)*, Dec 2013, pp. 1933–1938.

- [40] V. Jamali, N. Zlatanov, and R. Schober, “Bidirectional buffer-aided relay networks with fixed rate transmission – part ii: Delay-constrained case,” *IEEE Trans. Commun.*, vol. PP, no. 99, pp. 1–1, 2014.
- [41] A. Host-Madsen and J. Zhang, “Capacity bounds and power allocation for wireless relay channels,” *IEEE Trans. Inf. Theory*, vol. 51, no. 6, pp. 2020–2040, June 2005.
- [42] N. Ahmed, M. Khojastepour, A. Sabharwal, and B. Aazhang, “Outage minimization with limited feedback for the fading relay channel,” *IEEE Trans. Commun.*, vol. 54, no. 4, pp. 659–669, April 2006.
- [43] Z. Jingmei, S. Chunju, W. Ying, and Z. Ping, “Optimal power allocation for multiple-input-multiple-output relaying system,” in *IEEE Conf. Veh. Tech.*, vol. 2, Sept 2004, pp. 1405–1409 Vol. 2.
- [44] F. Vitiello, T. Riihonen, J. Hamalainen, and S. Redana, “On buffering at the relay node in lte-advanced,” in *IEEE Conf. Veh. Tech.*, Sept 2011, pp. 1–5.
- [45] A. Bletsas, A. Khisti, D. Reed, and A. Lippman, “A simple cooperative diversity method based on network path selection,” *IEEE Journal Selected Areas in Commun.*, vol. 24, no. 3, pp. 659–672, 2006.
- [46] X. Kang, Y.-C. Liang, A. Nallanathan, H. Garg, and R. Zhang, “Optimal power allocation for fading channels in cognitive radio networks: Ergodic capacity and outage capacity,” *IEEE Trans. Commun.*, vol. 8, no. 2, pp. 940–950, Feb 2009.

- [47] J.-B. Kim and D. Kim, “Exact and closed-form outage probability of opportunistic decode-and-forward relaying with unequal-power interferers,” *IEEE Trans. Commun.*, vol. 9, no. 12, pp. 3601–3606, 2010.
- [48] —, “Outage probability of opportunistic decode-and-forward relaying with co-channel interferences,” in *Int’l Conf. Advanced Commun. Tech (ICACT)*, vol. 02, Feb 2009, pp. 919–922.
- [49] I. Krikidis, T. Charalambous, and J. Thompson, “Buffer-aided relay selection for cooperative diversity systems without delay constraints,” *IEEE Trans. Commun.*, vol. 11, no. 5, pp. 1957–1967, May 2012.
- [50] W. Yu and R. Lui, “Dual methods for nonconvex spectrum optimization of multicarrier systems,” *IEEE Trans. Wireless Commun.*, vol. 54, no. 7, pp. 1310–1322, July 2006.
- [51] S. Boyd and L. Vandenberghe, *Convex Optimization*. New York, NY, USA: Cambridge University Press, 2004.
- [52] J. D. C. Little, “A proof for the queuing formula: $L = w$,” *Operations Research*, vol. 9, no. 3, pp. 383–387, 1961.

Vitae

- **Name:** Yasser Fadhl Ali Al-Eryani
- **Nationality:** Yemeni
- **Date of Birth:** 17/06/1987
- **Email:** *eryani1987@gmail.com*
- **Permanent Address:** Sanaa, Yemen
- **MSc.** Degree in Telecommunication Engineering, KFUPM, Dhahran, KSA, 2015.
- **BACHELOR'S DEGREE** in Electrical and Electronics Engineering (Communication Sector), IBB UNIVERSITY, Ibb, Yemen, 2012.
- **Research Field of Interest:** Wireless Communications, Cooperative Networks, Cognitive Radio, Massive MIMO and Error Control and Coding.
- **Publications:**
 - Yasser Al-Eryani, Anas Salhab, Salam Zummo, “A Low Complexity Relay Selection & Power Allocation Schemes for Cognitive MIMO Buffer-Aided DF Relay Networks”, *IEEE Conf. Wireless Commun. and Netwo. (WCNC)*, 2016.